12-13-2003

Design, Assembly, and Assessment of an Experimental Apparatus to Measure Fouling of Condenser Tubes

Gregory J. Zdaniuk

DESIGN, ASSEMBLY, AND ASSESSMENT OF AN EXPERIMENTAL APPARATUS TO MEASURE FOULING OF CONDENSER TUBES

By

Gregory Zdaniuk

A Thesis
Submitted to the Faculty of
Mississippi State University
in Partial Fulfillment of the Requirements
for the Degree of Master of Science
in Mechanical Engineering
in the Department of Mechanical Engineering

Mississippi State, Mississippi

December 2003

DESIGN, ASSEMBLY, AND ASSESSMENT OF AN EXPERIMENTAL APPARATUS TO MEASURE FOULING OF CONDENSER TUBES

By

Gregory Zdaniuk

Approved:

Louay M. Chamra Associate Professor of Mechanical Engineering (Major Professor)	B. Keith Hodge Professor of Mechanical Engineering (Committee Member)
Carl James Assistant Research Professor of Mechanical Engineering (Committee Member)	Rogelio Luck Associate Professor and Graduate Coordinator of Department of Mechanical Engineering
A. Wayne Bennett Dean of the College of Engineering	

Name: Gregory Zdaniuk

Date of Degree: December 13, 2003

Institution: Mississippi State University

Major Field: Mechanical Engineering

Major Professor: Dr. Louay M. Chamra

Title of Study: DESIGN, ASSEMBLY, AND ASSESSMENT OF AN EXPERIMENTAL APPARATUS TO MEASURE FOULING OF CONDENSER TUBES

Pages in Study: 125

Candidate for Degree of Master in Science

This thesis discusses the design, construction, and debugging of an experimental apparatus to measure fouling in smooth and/or augmented copper alloy condenser tubes. In addition, guidelines and recommendations are made for construction of similar devices. Specification sheets of the system components, detailed design calculations, and photographs of the apparatus are included in the appendices.

ACKNOWLEDGEMENTS

I would like to express my sincere gratitude to my family members who have provided continuous support for my education. I would like to express my deepest appreciation to my major professor, Dr. Louay Chamra, for his valuable help and guidance in my research and education. I would also like to thank my graduate committee members, Dr. B. Keith Hodge and Dr. Carl James, for their advice and assistance in the preparation of this thesis. I furthermore want to recognize the help of Mr. Reese Yontz in implementing the LabVIEW program. He spent a lot of his valuable time setting up and explaining LabVIEW and SCXI systems to me. Finally, I would like to thank the Mississippi State University Department of Mechanical Engineering and its staff (especially Mr. Luke Nason, Mr. Victor Latham, and Mr. Seth Myers) for their dedication and outstanding service to the university and students.

TABLE OF CONTENTS

CHAPTER Page

LIST OF TABLES

TABLE Page

LIST OF FIGURES

FIGURE Page

NOMENCLATURE

A_i	Internal surface area based on the nominal diameter (m^2)
B	Constant
$c_{p,w}$	Specific heat of water at constant pressure (J/kg–K)
ID	Inside diameter (m)
OD	Outside diameter (m)
LMTD	Log Mean Temperature Difference (K)
L	Length of the tube (m)
$\dot{m}_w$	Mass flow rate of water (kg/s)
$\dot{Q}$	Heat transfer rate (W)
R_f	Fouling resistance ($K*m^2/W$)
R_f*	Asymptotic fouling resistance ($K*m^2/W$)
t	Time (s)
t_o	Initial time (s)
$T_{w,in}$	Water inlet temperature (K)
$T_{w,out}$	Water outlet temperature (K)
T_{ref}	Temperature of the refrigerant (K)
U_c	Overall heat transfer coefficient of clean tubes (W/m^2–K)

U_f	Overall heat transfer coefficient of fouled tubes (W/m^2–K)
U_i	Overall heat transfer coefficient based on the tube ID (W/m^2–K)

CHAPTER I

INTRODUCTION

I.A Fouling – A Brief Definition

Fouling is defined as the accumulation of deposits on heat transfer surfaces. These deposits represent an additional resistance layer, which deteriorates the heat exchanger's performance. Engineers are concerned with fouling because it leads to increases in design, manufacturing, and operating costs.

In order to study the causes and effects of fouling, an understanding of how fouling takes place is important. There are six modes of fouling:

1. Scaling: Precipitation of material dissolved in a fluid due to a change in the fluid's temperature.
2. Particulate fouling: Deposition of particles suspended in a fluid on a heat transfer surface.
3. Corrosion fouling: Accumulation of deposits that result from an electro-chemical reaction in which the heat transfer surface takes part.
4. Chemical reaction fouling: The deposition of particles that come from a reaction in which the fluid takes part.
5. Biological fouling: Growth of micro- or macro-organisms on heat transfer surfaces.

6. Freezing fouling: Solidification of a fluid on a heat transfer surface below the fluid freezing point.

Fouling is a time-dependent phenomenon and is usually preceded by a nucleation period. Once fouling starts, it can follow three functional forms. Figure 1 presents the three types of behavior of fouling resistance with respect to time. A linear fouling rate means that the fouling resistance grows at a constant rate. A falling rate means that the rate at which the fouling layer grows decreases with time. Finally, an asymptotic fouling rate is the case where the fouling resistance approaches a limiting value over time.

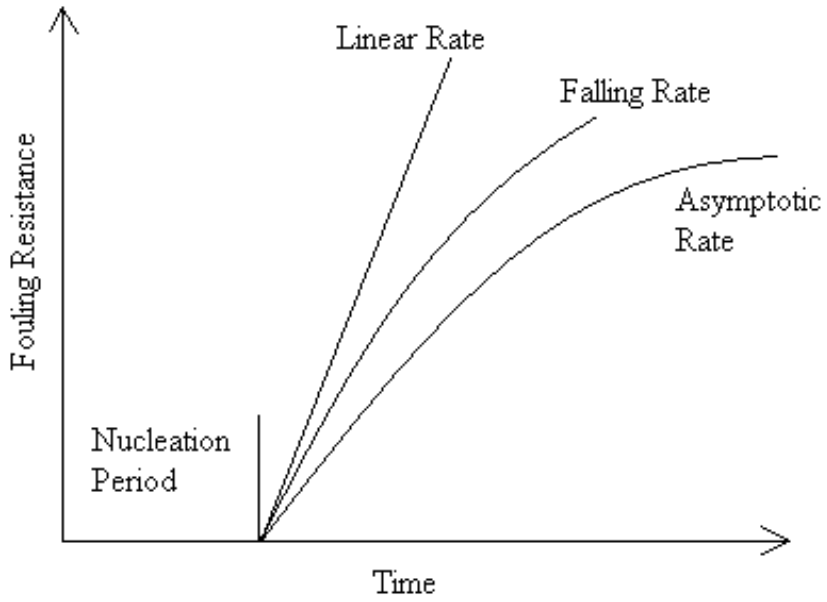

Figure 1. Fouling-rate Types.

I.B Introduction to Cooling Towers and Enhanced Tubes

Because of its natural abundance, non-harmful chemical composition, and suitable thermal properties, water is a frequently used fluid in heat exchangers. A cooling

tower is a common component of a building HVAC system. Figure 2 presents a schematic of a cooling tower. A cooling tower uses several steps (loops) to reject heat to the atmosphere. From a fouling perspective, the most critical loop is the "open recirculating loop" (see Figure 2) in which cooling tower water is exposed to the atmospheric air, and then circulated through a set of condenser tubes to be heated by a condensing refrigerant.

Cooling tower water is a complex solution that contains many dissolved constituents. In addition, cooling tower water picks up particles (dust, for example) while in contact with the atmospheric air. These solutes and particles are the primary cause of fouling in condenser tubes.

Because cooling tower water is treated with corrosion inhibitors and biocides, corrosion and biological fouling do not occur in the open recirculating loop. Moreover, no chemical reaction or freezing takes place in the condenser tube, so the only two fouling modes that are of concern in condenser tubes are particulate fouling and scaling (precipitation fouling).

Another factor that affects fouling in the condenser tubes is the internal geometry of the tube. In recent years, the use of enhanced tube geometries has become widespread. Enhanced geometries can drastically improve the heat transfer properties of the condenser tube. One of the most common enhancement geometry encountered today is the helical fin. Figure 3 shows an example of helically-finned and axially-finned tubes. Several terms are used in the nomenclature of enhanced heat transfer to describe a helically-finned tube. These terms are the helix angle, the fin height, and the number of starts. The helix angle is the angle that the edge of the fin forms with the axis of the tube.

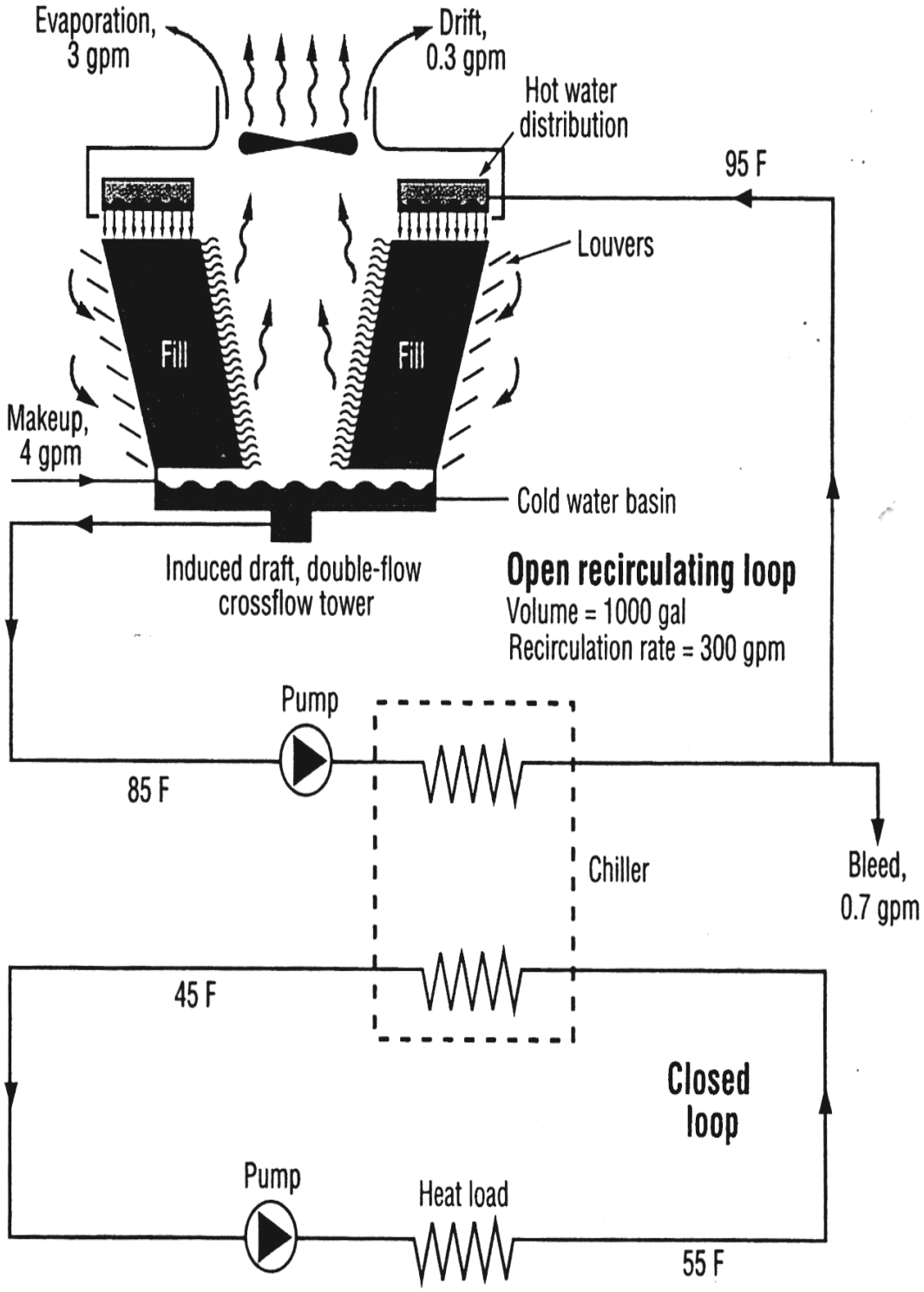

Figure 2. Schematic of a Cooling Tower (Meitz, 1999).

The fin height is the distance measured from the internal wall of the tube to the top of the fin. The number of starts refers to how many fins one can count around the circumference of the test tube. For example, the axially-finned tube of Figure 3 has eight starts.

Figure 3. Axially-finned and Helically-finned Tubes.

The current practice to account for tube fouling during the design of heat exchangers is to use a fouling resistance in the calculations for the overall heat transfer coefficient. The problem is that the existing fouling resistance factors are based on smooth-tube data (Somerscales, 1990), since the factors were obtained before the enhanced tube geometries were used. Recent studies (Webb and Kim, 1989, Webb and Li, 2000) suggest that the enhancements in the tube geometry may actually promote fouling to the point where the additional thermal resistance caused by fouling overwhelms the enhancement-resulting gain in the tube's heat transfer performance. The reason could be that enhancement geometry creates additional surface area where the deposits can attach. Deposits can also fill in the space between fins (see Figure 3).

I.C TRP-1205

TRP-1205 is a project sponsored by the American Society of Heating, Refrigerating, and Air Conditioning Engineers (ASHRAE). The full title of the project is

"Water-Side Fouling Inside Smooth and Augmented Copper Alloy Condenser Tubes in Cooling Tower Water Applications." This project has three objectives:

1. Develop a water quality database for cooling tower water applications.
2. Correlate fouling data with water quality.
3. Experimentally determine the fouling of smooth and augmented tubes by directly using or simulating cooling tower water.

These objectives are to be accomplished in three phases:

Phase I: Perform a literature survey of the topic.

Phase II: Collect and analyze cooling tower water samples to compile a database.

Phase III: Perform a precipitation and particulate fouling experiment to determine the influence of tube geometry, water velocity, and water chemistry on fouling resistance.

Phases I and II were performed by Tubman (Tubman, 2002) during his graduate work at Mississippi State University. This thesis focuses on Phase III, and more specifically, on the design of the experimental apparatus needed for Phase III.

In order to fully satisfy the objectives of Phase III of the project, the experimental apparatus has to simulate, as closely as possible, the condenser of a cooling tower system chiller. To achieve this, a shell-and-tube (or double-pipe) heat exchanger must be used with water flowing in the inner tube and refrigerant condensing in the annulus. The simplest simulation of this arrangement is a double-pipe counterflow heat exchanger.

I.D Phase III of TRP-1205 – Objectives

The three objectives of Phase III are to experimentally determine the influence of (1) tube geometry, (2) water velocity, and (3) water chemistry on the water-side fouling of condenser tubes. Previous research (Li and Webb, 2000) demonstrated that the fin geometry (fin height, helix angle, and number of fin starts) affects fouling of condenser tubes. In order to study the influence of tube geometry on the fouling resistance (the first objective of Phase III), tubes with different internal fin geometries have to be tested at similar water-velocity and water-chemistry conditions. This can only be achieved if tubes with different fin geometries are placed in parallel. With this in mind, nine tube geometries to be tested were selected by the research team and approved by the Project Monitoring Subcommittee. Table 1 delineates tube geometries of the nine tubes. Each tube has the same outside fin geometry and outside diameter so that the outside heat transfer coefficient is equal for each test tube. The length of each tube is 10 ft. For installation purposes, six inches from both ends of the tube are unfinned.

Table 1. Recommended Tube Geometries.

Tube #	OD (inch)	ID (inch)	Fin Height (inch)	Helix Angle (°)	Number Of Starts
1	0.75	0.612	0.015	25	10
2	0.75	0.612	0.015	25	30
3	0.75	0.612	0.015	48	30
4	0.75	0.612	0.015	25	45
5	0.75	0.612	0.012	35	45
6	0.75	0.612	0.015	35	45
7	0.75	0.612	0.020	35	45
8	0.75	0.612	0.015	48	45
9	0.75	0.612	-	-	-

Table 2 presents the dimensions of the tubes that were manufactured by Wieland-Werke AG for Phase III of TRP-1205.

Table 2. Manufactured Tube Geometries.

Tube #	External Structure			Root Wall	Internal Structure			
	OD	fin pitch	fin height	thickness	fin height	number of starts	helix angle	ID
	(inch)	(fins/inch)	(inch)	(inch)	(inch)	-	(°)	(inch)
1	0.741	40	0.0372	0.0254	0.0150	10	25	0.616
2	0.741	40	0.0364	0.0268	0.0148	30	25	0.615
3	0.743	40	0.0370	0.0268	0.0150	30	48	0.615
4	0.740	40	0.0364	0.0270	0.0150	45	25	0.613
5	0.741	40	0.0354	0.0280	0.0122	45	35	0.614
6	0.740	40	0.0366	0.0268	0.0150	45	35	0.613
7	0.741	40	0.0368	0.0268	0.0201	45	35	0.614
8	0.739	40	0.0364	0.0264	0.0150	45	48	0.613
9	0.742	40	0.0366	0.0264	0.0000	-	-	0.616

The second and third objectives of Phase III are to determine the influences of water velocity and water quality on the fouling characteristics of condenser tubes. To satisfy the second objective, the Project Monitoring Subcommittee required the research team to perform tests with water velocities at 2 ft/s, 5 ft/s, and 8 ft/s, with the stipulation that the water velocity in each test tube must remain constant during a single test. An increase in the water velocity might increase the removal rate of the fouling deposits because of increased wall shear stress. To study the effects of water quality on fouling resistance in condenser tubes (third objective), the water chemistry of the simulated cooling tower water was mandated to vary between low, average, and high fouling-potential conditions.

The test parameters described above require nine conditions (three water qualities at three different velocities) per tube. Thus, nine test runs are required. The concentrations of different constituents for the three water qualities to be tested have not

yet been determined, but will come from the conclusions, now being discussed with the Project Monitoring Subcommittee, of Phase II of the project.

I.E Measuring Fouling in Heat Exchangers

Consider how fouling is measured. Somerscales (1990) presents the history of fouling research from its first appearance in the literature in 1756 to the "International Conference on the Fouling of Heat Transfer Equipment" in 1979. He portrays the origins of the fouling factor as a means of accounting for the fouling resistance in the design of heat exchangers. In 1941, the Tubular Exchanger Manufacturers Association (TEMA) first published a table of fouling factors for different fluids in a multitude of applications (Chenoweth, 1990).

The fouling factor, R_f, is defined as

$$R_f = \frac{1}{U_f} - \frac{1}{U_c} \qquad (1)$$

where U_f and U_c are the overall heat transfer coefficients for the clean and fouled conditions, respectively. Equation (1), the data reduction equation of the experiment of Phase III, requires two overall heat transfer coefficients to be measured. Therefore, the apparatus is first run at clean conditions (clean tube, distilled water) to determine the clean-tube overall heat transfer coefficient. Solutes are then added to the water to induce fouling and to determine the fouled-tube overall heat transfer coefficient. A key point is to maintain the same operating conditions (water velocity, chemistry, and heat supplied to the refrigerant) while a foulant layer is being built up.

The rate of heat transfer by a heat exchanger is

$$\dot{Q} = U_i A_i \times LMTD \tag{2}$$

where A_i is the inside surface area, U_i is the overall heat transfer coefficient based on the inside surface area, and LMTD is the log mean temperature difference. For comparison purposes, the inside surface area is based on the nominal tube diameter ($A_i = \pi * ID * L$). The log mean temperature difference for a double-pipe counterflow heat exchanger with refrigerant at constant temperature (condensing) and water as the cold fluid is

$$LMTD = \frac{T_{w,in} - T_{w,out}}{\ln \frac{T_{ref} - T_{w,out}}{T_{ref} - T_{w,in}}} \tag{3}$$

From equation (2)

$$U_i = \frac{\dot{Q}}{A_i * LMTD} \tag{4}$$

With the tube geometry and fluid temperatures known, the only missing information for finding U_i is the heat transfer rate, which can be found using an energy balance on the water flowing through the test tube:

$$\dot{Q} = \dot{m}_w c_{p,w} (T_{w,out} - T_{w,in}) \tag{5}$$

Thus, the fouling factor can be estimated with the following measurements:

1. Water inlet temperature
2. Water outlet temperature
3. Refrigerant temperature
4. Mass flow rate of the water

The experimentally-obtained fouling factor may possess an asymptotic behavior as illustrated in Figure 1. In such case, an exponential regression can be performed to the following equation:

$$R_f = R_f^*(1 - e^{-Bt}) \tag{6}$$

where t is the time, R_f^* is the asymptotic fouling resistance, and B is a constant. Evaluating the time derivative of equation (6) at t = 0 yields the initial fouling rate

$$\frac{dR}{dt_o} = BR_f^* \tag{7}$$

CHAPTER II

EXPERIMENTAL APPARATUS DESIGN

II.A Preliminary Data

Each test will start with new tubes in clean condition. The alternative was to clean the tubes after each test with steel brushes. This alternative was rejected because there was no assurance that the cleaning would not affect the fouling rate of the cleaned tube.

Design requirements for the experimental facility include:

1. The apparatus must accommodate nine 10-foot-long tubes in parallel.
2. The design must be versatile so that tubes can be changed easily.
3. The water in the tubes must be able to flow at 2 ft/s, 5 ft/s, and 8 ft/s.
4. There must be an annulus side around each test tube with condensing refrigerant.

II.B Detailed Mechanical Design

II.B.1 System Overview

The design of the experimental apparatus started by utilizing the software AutoCAD 2000 to place the system components on a virtual lab floor. The system components are: nine test sections with refrigerant loops, water pump, water tank, draining valves, control panel, and water-cooling heat exchangers. The purpose of the

cooling heat exchangers is to reject the heat added to the test water in the condenser tubes. Because of space, the refrigerant loops are located underneath each test section.

Figure 4 illustrates a preliminary system schematic drawn to scale. The schematic shows nine test sections placed in parallel (numbers 1 through 9) between two manifolds. According to the flow direction, the two manifolds are defined as the inlet and outlet manifold. Each test section is surrounded by a shell where the refrigerant condenses. From the mixing tank, the test water goes through the water pump into the cooling heat exchangers, and then through the inlet manifold, the test sections, the outlet manifold, and the return line back into the tank.

The idea for the operation of the refrigerant loop is to use buoyancy forces to raise the refrigerant vapors into the annulus of the test section and to use gravity to drain the liquid out. Such a design requires no refrigerant pump or compressor. Figure 5 shows a preliminary schematic of the test section with the refrigerant loop. Refrigerant R-134a is stored in liquid form in a tank and is then evaporated with electric heaters so that vapors rise into the annulus. The vapor condenses on the outside of the test tube and flows back into the tank through a return pipe. The next sections describe each system component in detail.

II.B.2 Piping

Because the condenser tubes to be tested are made of copper, copper was selected as the material for all of the piping. The original design water velocity was less than 10 ft/s for each segment of the apparatus. However, this constrain resulted in large tube

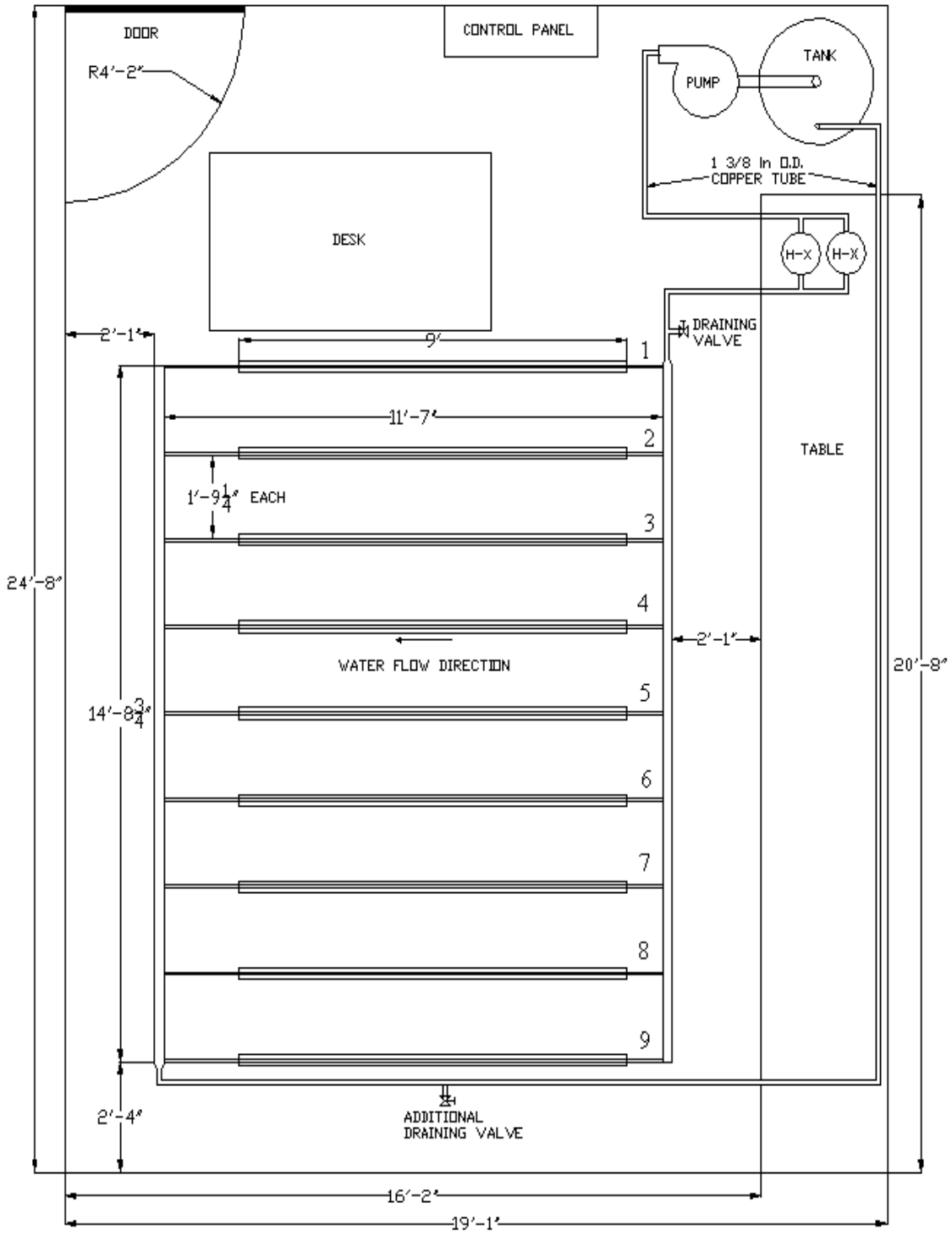

Figure 4. System Schematic.

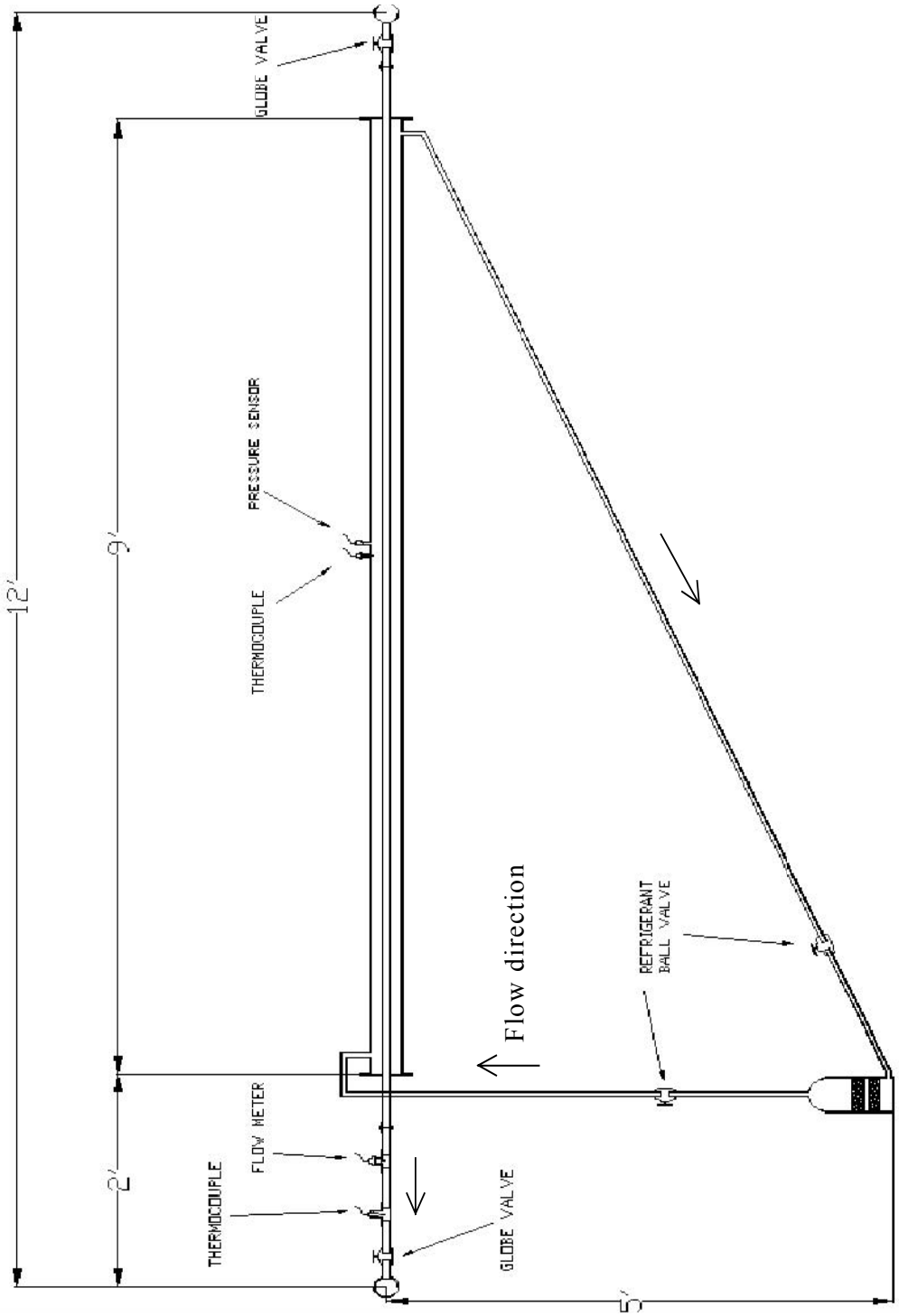

Figure 5. Test Section Diagram.

diameters, which meant higher cost and difficulties with soldering and installation. Based on cost and availability, a 1⅜-inch diameter tube was chosen to be the basis of the design.

The shell side of the test section has to be relatively large to ensure a uniform vapor distribution around a test tube and to accommodate the temperature and pressure sensors. For these reasons, a 3-inch diameter tube was selected for the shell. In the same manner, the inlet and outlet manifolds need to be large enough to be able to host the test sections. The manifolds were chosen to be 2⅝-inch in diameter.

A ⅞-inch tube was selected to connect the test tube to the manifolds. This diameter matches the copper fittings that host the flow meter and the thermocouple. Reducing compression fittings are used to install a ¾-inch test tube in the test section.

The pipes used in the refrigerant loop were chosen to be ⅞-inch diameter for the vapor supply line and ⅝-inch diameter for the liquid return line. Using a larger size for the vapor line promotes the proper circulation of the refrigerant. To further assure vapor circulation, the vapor line connects to the side of the shell to prevent the condensates to enter the vapor line. The liquid return line connects to the bottom of the shell to guarantee proper draining. These connections guarantee a counterflow arrangement. Except for the 3-inch diameter shell, all of the copper tubing selected was type ACR (Air Conditioning and Refrigeration).

II.B.3 Test Section Shell Design

Since the experimental matrix (described in Section I.D) includes nine tests of nine tube geometries (a total of 81 tubes to be tested), the design of the test section shell has to be sufficiently flexible to allow frequent and rapid changing of the test tubes. For

this reason, the original plan was to use 3-inch ground-joint fittings (unions) on both sides of the test section shell, as shown in Figure 6. When a test tube would be changed, one end of the shell would be unsoldered from the tube, and the union at the other end would be opened. Due to leaks, this design was changed and unions were eliminated. A more detailed description of the new arrangement is given in Section IV.B.

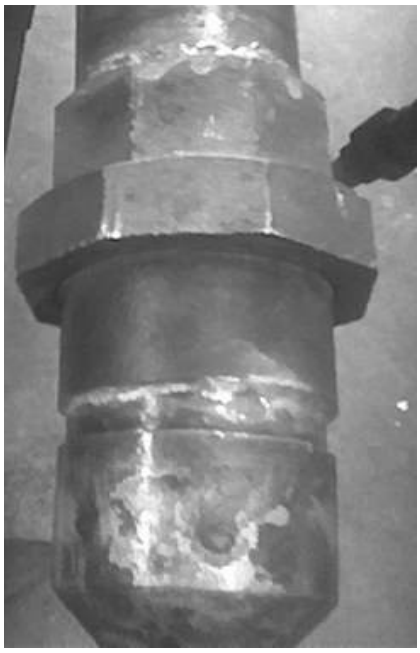

Figure 6. Shell Union.

II.B.4 Valves

The apparatus has two drain valves. The first one is located upstream of the inlet manifold, and the second one on the return line. The drain valves are installed to obtain water samples during the test and to be able to drain the system after a test is performed.

The water-side of the test section contains one valve at the inlet and one at the outlet of a test tube, which allows for control of the water flow or isolation of a test

section from the system to change a test tube. The test tube water velocity of 2 ft/s, 5 ft/s, or 8 ft/s is achieved by manipulating either the pump discharge valve or both of the test section valves.

The design of each refrigerant loop includes refrigerant ball valves on the vapor supply and the liquid return lines. Closing these valves isolates the shell from the refrigerant tank during the replacement of a test tube.

II.B.5 Mixing Tank

The test water solution is prepared and monitored in the mixing tank. The size of the tank has to be greater than the total volume of the system so that a solution can be prepared in the tank first and then circulated through the system. The volume of the system was found by adding the volumes of the individual pipe segments. The diameter of each segment was known and the lengths were estimated from Figure 4. The total volume of the system was estimated to be 18 gallons.

Diverse Plastic Tanks, Inc recommended a 65-gallon conical bottom tank with a steel stand. The tank has a conical bottom to prevent possible settlement of particles, which could affect the fouling potential of the test water. A drawing of the tank is included in Appendix A.

II.B.6 Water-cooling Heat Exchangers

The purpose of the water-cooling heat exchangers is to remove the heat added to the test water by the refrigerant condensing in the test sections. The first idea was to connect the hot test water to a 10-ton condenser that was available from the Two-Phase

Flow Lab (Patterson 100-E) and to run city water through the condenser's cold line. The maximum water flow-rate rating of the 10-ton condenser is 32 gal/min. The maximum volumetric flow rate of the test water was calculated (see Pressure Drop Calculations in Appendix B) to be 66 gal/min, which corresponds to a water velocity of 8 ft/s in the test tubes. A second 10-ton condenser was purchased and connected in parallel to reduce the water flow rate to an acceptable level of 33 gal/min through each condenser. Both 10-ton condensers are models S-10-I from Edwards Engineering Corp. Refer to Appendix A for a specification sheet of the S-10-I.

II.B.7 Pressure Drop and Pump Selection

The pressure drop and the flow rate determined the size of the water pump needed for the experiment. Appendix B presents detailed calculations of the pressure drop through the system. Pressure drop through each test section was calculated by Tubman (2002) and was based on experimentally-determined friction characteristics equations for internal helical-rib roughness (Webb, Narayanamurthy, and Thors, 2000). Calculations were made for all three water velocities. Loss coefficients for the valves were taken at half-closed condition for more conservative calculations. Pressure drop through the water-loop heat exchangers was modeled as flow through parallel pipes with the appropriate loss coefficients for bent tubing and was compared with the manufacturer's specifications (see Appendix A). The pressure drop values agreed closely.

The head at the highest test water velocity (8 ft/s in test tubes, 66 gal/min total volumetric flow rate) was determined to be 218.5 ft. Tencarva Machinery Co. was contacted to get a quote for a pump that meets the calculated head and flow rate

specifications. Tencarva suggested using the Goulds Pumps Model 3756 1X2-7. This is a close-coupled, bronze-fitted pump powered by a 3-phase, 2-pole, 3500-RPM, 10-hp motor. The manufacturer's specification sheet and pump curves are included in Appendix A.

II.B.7.a Vibration Isolators

Vibration isolators are rubber dampers that are installed under the pump to limit the noise and vibration of the piping and pump assembly. The design includes four Karman Rubber type-A cylindrical isolators 1 9/16-inch-diameter and 1-inch high. A catalog page showing the vibration isolators is included in Appendix A.

II.B.8 Refrigerant Tanks

The selection of the refrigerant tanks was problematic because none of the ones available on the market met the project's requirements. As described in Section II.B.1, the refrigerant tanks hold R-134a at boiling conditions. Vapors rise into the test section by means of buoyancy and return in liquid form due to gravity. In order to achieve this circulation, the tank has to have an outlet at the top and an inlet at the bottom, and electric ring heaters placed above the inlet.

Suction accumulators were first examined. In a regular air conditioning system, the suction accumulator has an internal U-tube to help separate vapors from liquid before the refrigerant is fed to the compressor. Several manufacturers were contacted to see if the design could be modified by removing the internal U-tube. Refrigeration Research, Inc., bid a modified steel accumulator rated for a burst pressure of 450 psi. Refrigeration

Research also agreed to install copper stubs on the steel nipples in order to facilitate the soldering of the test section copper piping. Appendix A includes a detailed drawing of the modified suction accumulator (refrigerant tank).

II.B.9 Rupture Discs

The rupture discs were incorporated into the design for mechanical safety. The discs are installed in the refrigerant tanks. The function of the rupture discs is to burst in case the pressure in the tank exceeds 200 psig. Figure 7 is a drawing of a rupture disc. The discs are made of graphite and are placed between two rubber gaskets and ANSI steel flanges. The flanges are secured with four bolts tightened to 10 ft*lb of torque. The rupture discs were special-ordered from Graphilor Carbone of America. A specification sheet for the rupture discs is included in Appendix A.

Figure 7. Rupture Disc.

II.B.10 Refrigerant Heaters

The purpose of the refrigerant heaters was to supply the heat needed to evaporate the refrigerant. The heaters are sized according to a calculation performed on the water-

side of the test section (see Calculations of Refrigerant Heat Loads in Appendix B). The increase of the water temperature across the test section was assumed to be at least 3°F in order for the data to be relevant. Using the first law of thermodynamics and assuming no heat losses to the surroundings, 3250 W of power need to be supplied to the refrigerant tank to increase the temperature of the test water (flowing at 8 ft/s) by 3°F.

II.B.10.a Ring Heaters

The design of the ring heaters has to be such that the heaters can be installed around a refrigerant tank. Two smaller heaters, instead of one large one, were selected in order to be able to supply less heat for the tests at lower water velocities. Two 2250-W ring heaters made by Omegalux were chosen as the best alternative. They are 8½-inch diameter, 2½-inch thick, and can be powered by a 240- or 480-V AC. A ring heater specification sheet is provided in Appendix A.

II.B.10.b Tape Heaters

A wrap-around tape heater is installed on each shell-side inlet tube to provide the energy required to feed superheated refrigerant into the test section. The selected tape heater is a 1-inch wide, 6-ft long strip connected to a 240-V outlet through a percentage controller, having a maximum output power of 432 W. The tape heater was also purchased from Omegalux. A specification sheet of the tape heater is attached in Appendix A.

II.B.11 Insulation

Several parts of the apparatus are insulated for safety reasons and in order to limit losses of heat assuring more accurate temperature readings. Half-inch thick elastomeric pipe insulation was purchased from Manhattan Supply Co. for the inlet manifold, and the test section water tubing and shell. Air duct insulation was purchased for the refrigerant tanks and heaters. Appendix A includes pipe insulation specifications.

II.C Data Acquisition System

II.C.1 Transducers

As described in Section I.E, the following variables have to be measured during the experiment: test tube water inlet temperature, water outlet temperature, water flow rate, refrigerant temperature, and refrigerant pressure. The following subsections describe in more detail each transducer used in the apparatus.

II.C.1.a Thermocouples

Because of its simplicity, the thermocouple was chosen to measure the water and refrigerant temperatures. Instead of using nine separate thermocouples to measure the water temperature at the inlet of every test section, one thermocouple measures the temperature of the water inside the water inlet manifold. The temperature of the water in the inlet manifold is taken as the water inlet temperature for every test section, consequently reducing the number of thermocouples needed. From the Omega catalog, the Type-T thermocouple was determined to be the best-suited type for the experiment. A Type-T thermocouple with a 3-inch long, ¼-inch NPT pipe plug probe and 30 feet of

thermocouple wire was special-ordered from Omega. The thermocouple specification sheet is provided in Appendix A.

II.C.1.b Flow Meters

To measure the water flow rates, the FP-5300 paddle wheel flow sensor from Omega Engineering was chosen. This flow meter has a velocity range of 1 to 20 ft/s and works on a simple principle. Four permanent magnets, mounted in the rotor blades, spin past a coil in the sensor body. As the fluid flow causes the rotor to move, a sine-wave signal is produced, directly proportional in amplitude and frequency to the flow rate. An FP-5300 flow sensor specification sheet is attached in Appendix A. In addition to the flow meter, a special copper installation fitting, namely the FP-5307CU, was purchased. A catalog page with the FP-5307CU fitting can be found in Appendix A.

II.C.1.c Pressure Transducers

For more accurate pressure readings, an absolute pressure transducer was initially considered. The highest range available on an absolute pressure transducer was 300 psia. A higher range was desired so that the pressure sensor could be used in the future for other projects. Therefore, a 500-psig model with a ¼-inch NPT connection was purchased from Omega Engineering. Appendix A contains a specification sheet for the PX302-500GV pressure transducer.

II.C.2 Transducer Calibration

The flow meter was calibrated by placing it in the same assembly as the one used in the real apparatus and connecting the assembly to a water hose. The flow meter leads were connected to an oscilloscope. The water coming out of the flow meter assembly was captured in a tub, which was placed on a balance. The time it took the tub to fill and the weight of the water in the tub were recorded. At the same time, the frequency of the output signal was recorded. The resulting calibration curve of the mass flow rate versus frequency is shown in Appendix B.

The pressure transducer was calibrated with a calibrating device from Amthor Testing Instrument Co., Inc. This device uses an oil chamber connected to a cylinder with a 1-square-inch piston. The pressure of the oil in the chamber is varied by placing weights on the piston. The pressure transducer to be calibrated is connected to the calibrating device to read the pressure of the oil. The calibration of the pressure transducer was performed by adding weights on the piston in increments of 5 lbs and recording the output voltage of the transducer to obtain a calibration curve attached in Appendix B.

The thermocouples were not calibrated since accurate calibration plots for a Type-T thermocouple are commonly available.

II.C.3 SCXI Modular System

SCXI stands for Signal Conditioning eXtensions for Instrumentation. It is a signal conditioning system marketed by National Instruments of Austin, Texas. Any SCXI data acquisition system is composed of the following items:

1. Chassis. The chassis provides power to the SCXI modules, and handles all signal routing between the SCXI system and the DAQ card.
2. Modules. Modules connect to the chassis, and condition analog and digital signals.
3. Terminal Blocks. Terminal blocks connect the I/O signals (e.g. transducers) to SCXI modules.
4. Cable Assemblies. Cable assemblies connect the SCXI chassis to the digitizer (DAQ card). For a single-chassis system, only one cable is needed.
5. Measurement/Control Device. This device acquires conditioned signals from the SCXI system and controls the SCXI system. This device is typically a DAQ card.
6. Optional Accessories. These are items such as batteries for portable applications and rack-mounting kits.

The SCXI system used in Phase III is composed of an SCXI-1000 chassis, an SCXI-1102C module with an SCXI-1303 terminal block, an SCXI-1100 module with an SCXI-1303 terminal block, and an SCXI-1163R module with an SCXI-1326 terminal block. The SCXI-1102C module handles temperature readings, the SCXI-1100 handles pressure and flow-rate readings, and the SCXI-1163R is a safety switch that turns the system off in case prescribed conditions occur (see Section II.D). The SCXI chassis is connected to a DELL Pentium 4 personal computer and is controlled by a National Instruments DAQCard-AI-16XE-50 data acquisition card. Appendix A includes detailed information about the SCXI chassis and modules.

II.C.4 Data Acquisition Program

The program that controls the SCXI system and records transducer measurements is written in LabVIEW 6.1 from National Instruments. The purpose of this program is to determine and display water temperatures and flow rates, refrigerant pressures and temperatures, overall heat-transfer coefficients and fouling resistances of the test tubes. Current readings, plots, and user-input information are viewed and modified through a control panel, shown in Figure 8. The control panel displays numeric values of the current measurements and graphs past readings. The graphs are helpful in determining the time behavior of each variable. The following variables must be specified to start the program: tube dimensions, number of past measurements to display on the plots, clean-tube overall heat-transfer coefficients, time between consecutive scans, the units system, and whether or not each tube is connected. Except for the number of past measurements to display on the plots and the units system, every input variable can be changed while the program is running.

Every time a reading is taken, 600 measurements are acquired from each transducer at a rate of 300 scans per second. The measurements are then averaged to give a single value for a single-time. Since flow meters output an AC signal, the program counts the number of peaks and valleys for each flow meter, and divides that number by two to obtain the number of cycles. Then, this number is divided by two seconds (the time it takes to scan a single flow meter channel) to obtain the signal frequency. The method in which the frequency of the signal is determined contributes to the uncertainty of the mass flow rate (see uncertainty analysis calculations in Appendix B).

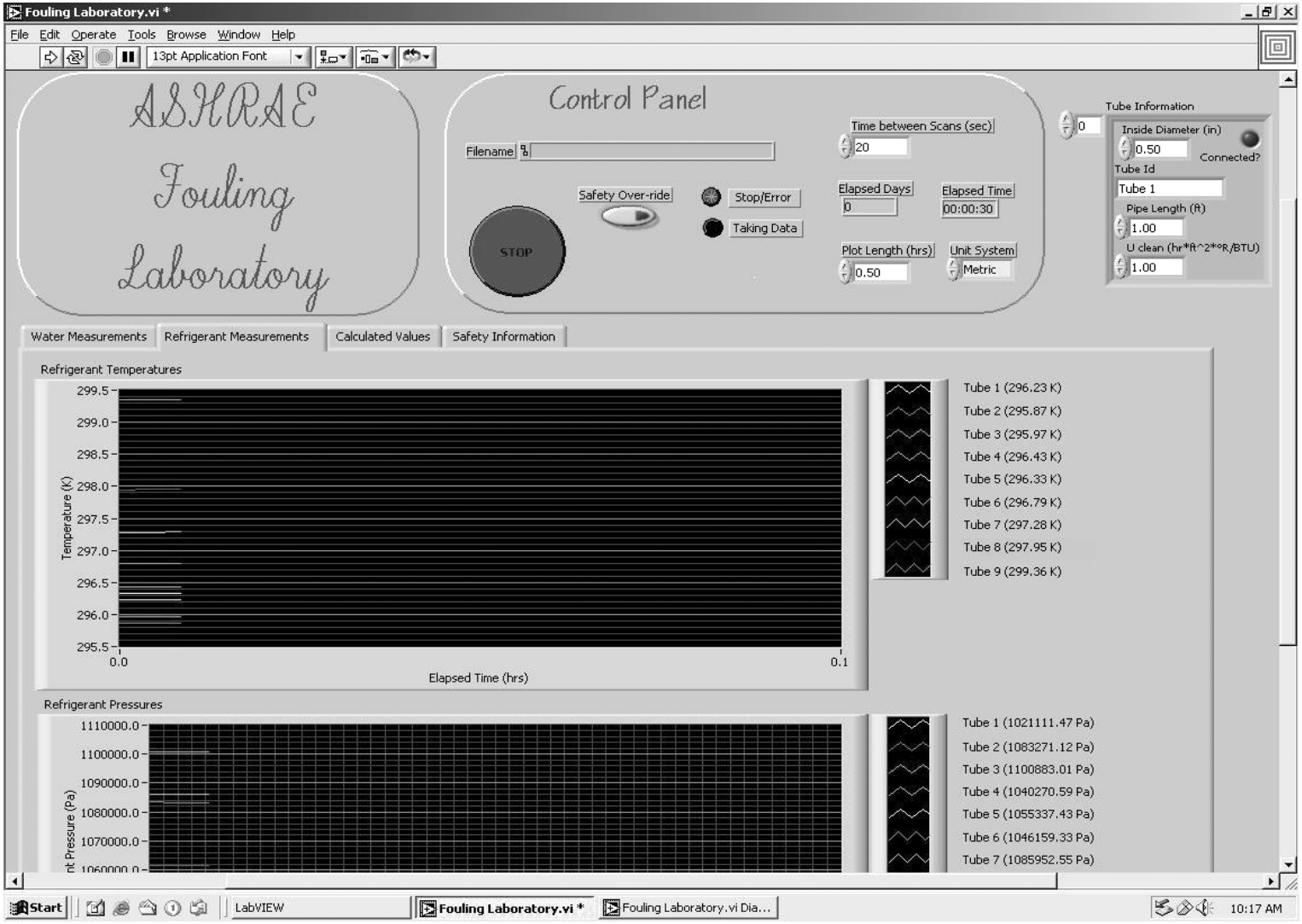

Figure 8. LabVIEW Control Panel.

The readings are saved to a spreadsheet file every ten minutes. The user can copy the file while the program is running and look at the data recorded from the beginning of the test up to the point when the file was copied. These data can be further processed or plotted within the spreadsheet.

II.D Safety

Because of hot tanks containing pressurized refrigerant, several safety precautions are incorporated in the design. The safeties consist of a relay (controlled by the LabVIEW program) capable of shutting the whole system down, one rupture disc in each tank, and a mechanical stop button placed on the electrical control panel. The relay will turn everything off if one of the following conditions below is encountered:

1. Refrigerant temperature reaches or exceeds 120 °F in any of the test sections.
2. Refrigerant pressure reaches or exceeds 186 psia in any of the test sections.
3. Water velocity drops below 0.7 ft/s in any of the connected test tubes.
4. The user-interface stop button is pushed.

These safety limits were thought to be adequate because of the expected refrigerant operating conditions (a boiling temperature of approximately 100°F). The 186 psia safety condition is the boiling pressure of R-134a at 120°F. The water velocity constraint is set to prevent any of the tubes from becoming completely clogged due to excessive fouling or in case there is a large leak and the pump starts running dry. If a test section is disconnected from the system while the test is running, a “tube connected?” toggle switch

is turned off in the control panel so that the LabVIEW program does not apply the water velocity condition to the unused test section. Nevertheless, the refrigerant and pressure safety conditions apply even to the disconnected test section. All of the LabVIEW safety constraints can be modified before each test.

CHAPTER III

EXPERIMENTAL APPARATUS ASSEMBLY

III.A Supporting Structure

The construction of the experimental apparatus began with the assembly of the supporting structure (shown in Appendix C). The structure was made out of aluminum beams that could be bolted to each other at any location. Using bolted aluminum beams made the structure light, flexible, and easy to assemble.

III.B Apparatus Assembly

The assembly of the piping began by laying out the test sections, the inlet, and outlet manifolds on the floor next to a measuring tape. This allowed for the piping to be cut into correct lengths so the pieces would fit together precisely. The pieces were joined together with high-melting-temperature silver solder. To facilitate the changing of the test tubes, low-melting-temperature soft solder was used to install the test tube in the annulus. Appendix C contains several photographs of the apparatus assembly process, including photographs of the test section construction and an assembled outlet manifold.

Once the test sections and manifolds were assembled, they were placed on the supporting structure so that the transducers could be installed. The test sections were then connected to the water manifolds. Next, the inlet and outlet manifolds were connected to

the water supply and return lines, respectively. Subsequently, the entire system was connected to the refrigerant tanks, the water pump, the mixing tank, and the water-cooling heat exchangers. Finally, the rupture discs and the ring and tape heaters were placed on the refrigerant tanks. Appendix C shows photographs of the progressive assembly of the system (installed test sections, mixing tank and pump, water-loop heat exchangers, rupture discs, and completed experimental apparatus). The last step was to insulate the inlet manifold, the test sections, and the refrigerant tanks.

III.C Power

In order to overcome the electric limitations of the existing electrical wiring, one 480-V, 100-A service was added to the laboratory. This power service feeds all system components via appropriate transformers and a control panel. The control panel holds all of the fuses and switches. The switches include a main ON/OFF switch, a pump ON/OFF switch, a stop button, LabVIEW-controlled safety relays, and an ON/OFF switch for every band heater (18 total). However, as a safety precaution, the ring heaters cannot be turned on unless the pump is running. Appendix C contains a photograph of the control panel.

CHAPTER IV

SYSTEM QUALIFICATION AND MODIFICATIONS

IV.A Supporting Structure

During the construction of the experimental apparatus, the previously-assembled supporting structure was under too much stress and was not stable with the center beams bowing. Aluminum beams were used to reinforce the structure. As shown in Figure 9, two additional legs were installed in the center of the assembly. Furthermore, as pictured in Figure 10, extra beams were added in the corners. The reinforcements made the supporting structure stiffer and stronger.

IV.B Shell Design Modification

After the test sections were assembled, they were charged with pressurized air in order to find any leaks. To detect leaks, the shells were sprayed with soapy water since air leaks would create bubbles. Nearly all of the shells leaked around the threaded ground-joint fittings (shown in Figure 6). Several sealants were applied to try to stop the leaks but nothing worked. The design had to be modified to reduce or eliminate the large threaded areas.

The ground-joint fittings were removed and smaller concentric reducers were installed and sealed with soft solder to make it easier to change the test tubes. Figure 11

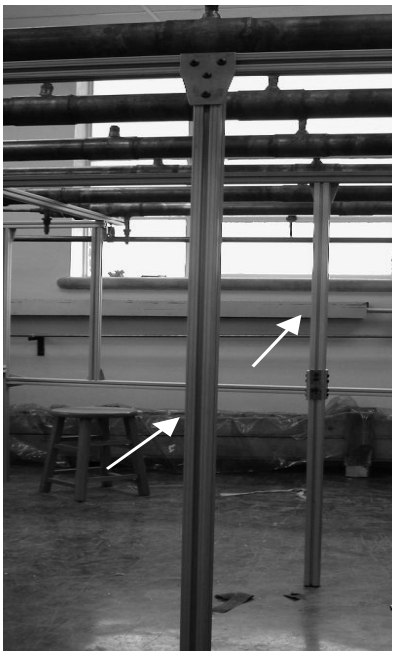

Figure 9. Additional Center Legs.

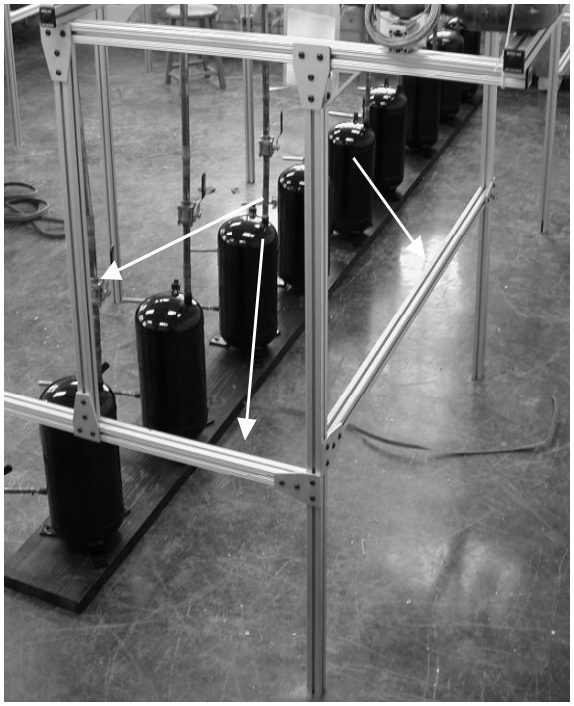

Figure 10. Corner Supports.

shows a leaking union, and Figure 12 pictures the new design with a silver-soldered small concentric reducer. This shell modification solved the leak problem. Figure 13 is a detailed schematic of the new test section.

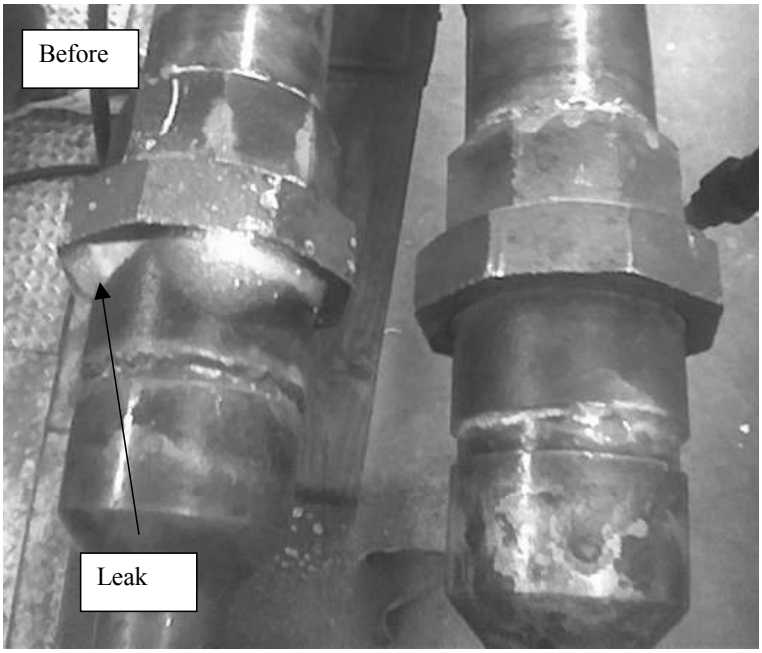

Figure 11. Leaking Unions.

Figure 12. Shell Modification.

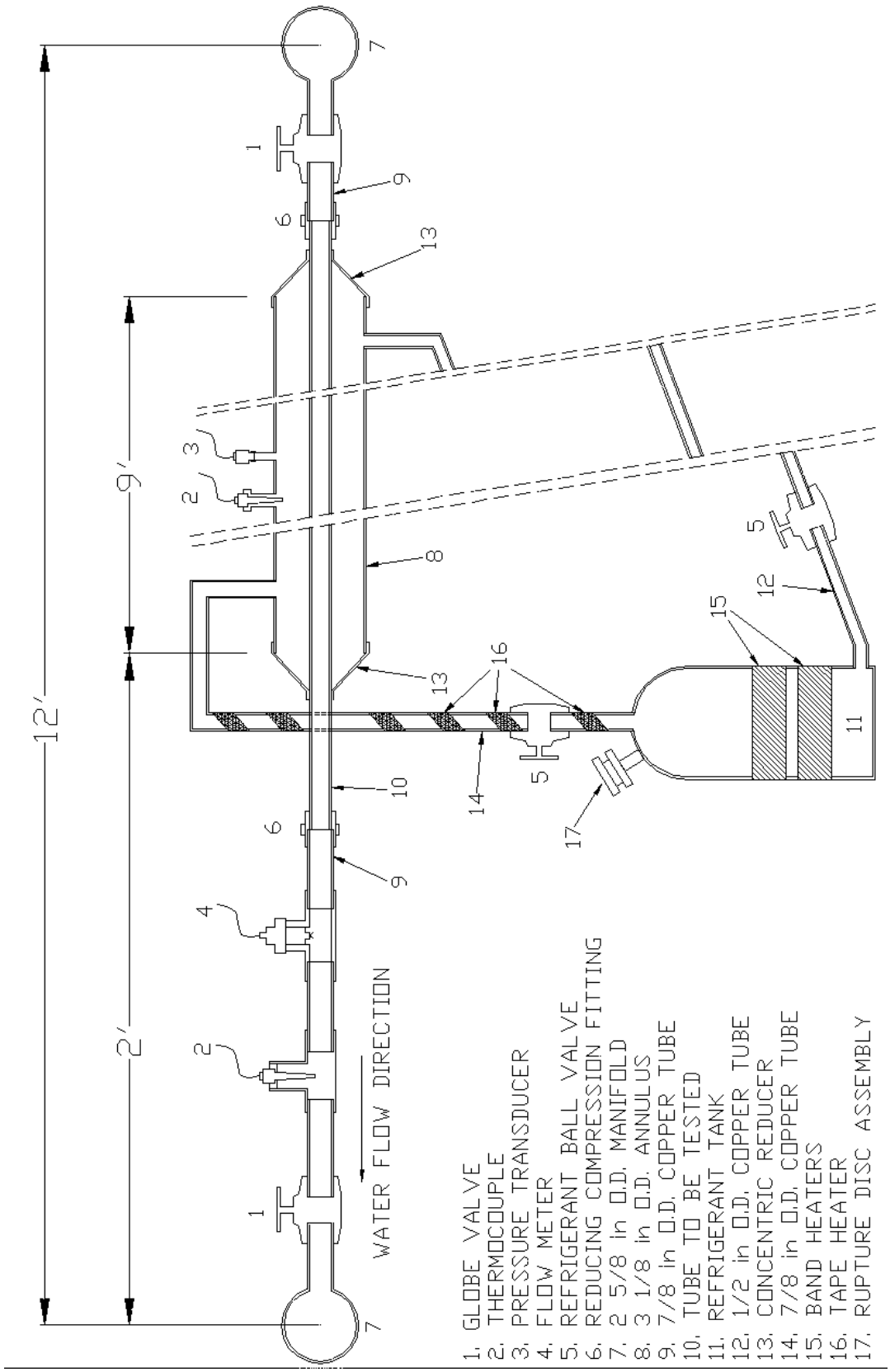

Figure 13. Detailed Test Section Diagram.

IV.C Insulation

Regular duct insulation was installed around the tank and the ring heaters. The purpose of the insulation around the ring heaters was to prevent heat losses and to protect personnel from the high voltage heater wiring. When both heaters were turned on, the insulation started smoking due to excessive temperature. The purchase of high-temperature insulation was investigated but the price was too high. Thus, the insulation was removed from the tanks and fiberglass protections were installed around the wiring of each tank heater (as shown in Figure 14).

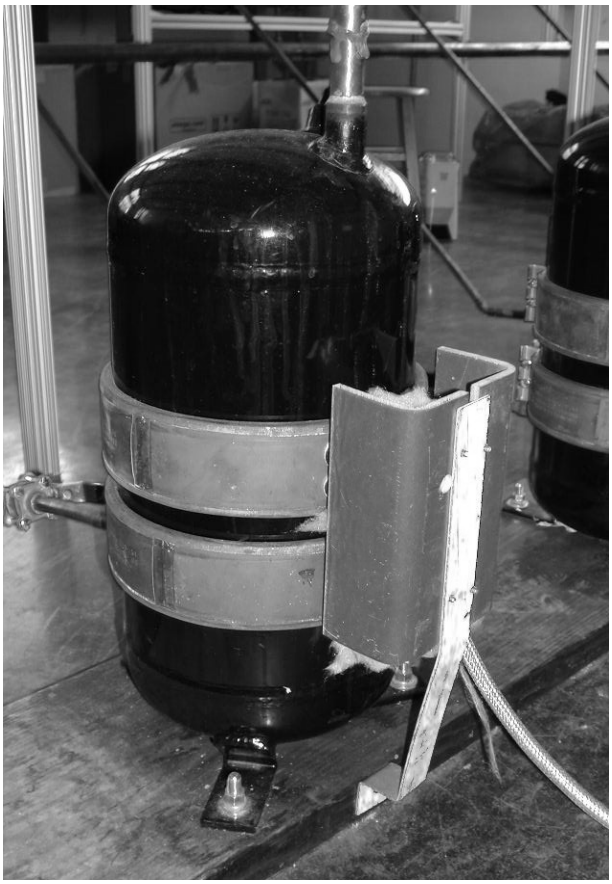

Figure 14. Ring Heater Protection.

IV.D Mixing Tank

When the pump was turned on, the water in the mixing tank was very agitated and many air bubbles were present. These bubbles could be dangerous if they traveled down to the pump (cavitation). In order to decrease the turbulence of the water in the mixing tank, a system of baffles that can be installed and removed from that tank within minutes was constructed. The baffles were made out of an old PVC pipe. The baffles have not been tested.

IV.E Data Acquisition System

Once the leaks in the system were fixed, the data acquisition system was tested. The first problem encountered was the signal noise associated with the flow meters. Because of their design (refer to Section II.C.1.b), the flow meters had very low input impedance. This caused a current leak within the module from one flow meter to the next one in the scanning sequence. An increase in the inter-channel delay, to let the noise die out before scanning the next flow meter, could not be done. Instead, each flow meter channel in the SCXI-1100 module was isolated with one empty channel. The empty channels were set to read zero Volts by placing a jumper wire across their positive and negative connectors. With this set up in place, only odd channels were read by the data acquisition program and the noise was eliminated.

Another problem encountered was the memory used by LabVIEW. When left running, the data acquisition program would stop after 20 hours of operation and list an "out of memory" error. After many hours of research, some commands in LabVIEW were found to cause memory leaks. The subroutine that was causing the memory leak

was the “delete from array” command, which was used to clear the graphs’ history. To solve the problem, the “delete from array” command was removed and the program was set to use “charts” instead of “graphs.” Charts clear their history automatically so the memory leak problem did not occur.

IV.F Water-loop Heat Exchangers

A test run of the apparatus was performed. Each refrigerant tank was charged with 20 lbs of R134a. One band heater (2250 W) was turned on around each refrigerant tank. The city water flowing through the cold lines of the two water-cooling heat exchangers was turned to full flow. The water velocity in the test sections varied between 6 ft/s and 7 ft/s. Once steady-state conditions were obtained, the refrigerant saturation temperature reached about 105°F, and the average test water inlet temperature was about 98.5°F. The average water outlet temperature was about 100°F, which means that temperature rise across each test section was only 1.5°F. To solve this problem, the inlet temperature of the test water can be lowered by running chilled water in the cold lines of the water-cooling heat exchangers. This idea is currently being investigated by the research team.

IV.G Uncertainty Analysis

The data obtained from the test run allowed the research team to get an idea of the uncertainty associated with the measured fouling resistance. Before performing an uncertainty analysis of the data reduction equation, the uncertainty of the mass flow rate calibration curve had to be obtained. Whenever dealing with calibration plots, the uncertainty of the Y-value depends on the position on the X-axis (Coleman and Steele,

1999). In the case of the mass flow-rate calibration curve, X is the frequency measured and Y is the mass flow rate obtained from the calibration curve equation. The uncertainty is the smallest in the middle of the plot and highest at the ends of the plot.

Appendix B presents a detailed Mathcad worksheet used to obtain the uncertainty of the mass flow rate calibration plot. The uncertainty was calculated for the range of frequencies obtained in the calibration process. The mass flow-rate uncertainty values were plotted and a quadratic least squares regression was performed to obtain an equation for the uncertainty of the mass flow rate.

Once the uncertainty of the mass flow rate was known, the next step was to use it in the fouling resistance uncertainty propagation equation. The detailed calculations are shown in the Mathcad worksheet in Appendix B. For the measurements obtained during the test run, the calculated uncertainty is 48% of the resulting fouling resistance.

The relative uncertainty in the fouling resistance obtained from the test run is high. At this point of the project, the uncertainty can be reduced by tuning the log mean temperature difference. The first option is to vary the test sections water inlet temperature, which can be achieved by manipulating the flow rate through the cold lines of the water-cooling heat exchangers. The second option is to vary the saturation temperature of the refrigerant. This alternative can be achieved by switching on both ring heaters around each refrigerant tank, or by manipulating the percentage controller of the tape heater. Table 3 shows the influence of the variation of the water inlet temperature on the relative uncertainty in the fouling resistance. Table 4 shows the influence of the variation of the refrigerant saturation temperature on the relative uncertainty in the fouling resistance. Both tables were generated by taking the measurements obtained

during the test run and varying only the inlet water temperature for Table 3, and only the refrigerant saturation temperature for Table 4. The values of the remaining variables were held constant. Both tables show that there is a point of minimum uncertainty in the fouling factor.

Table 3. Water Inlet Temperature Parametric Study.

Water Inlet Temperature Variation (K)	Clean Tube LMTD (K)	Fouled Tube LMTD (K)	Relative Uncertainty in R_f (%)
+0.5	2.553	1.897	58.5
0	2.763	2.099	48.7
-0.5	2.965	2.292	41.8
-1	3.160	2.477	38.0
-1.5	**3.349**	**2.655**	**36.7**
-2	3.533	2.828	36.8
-2.5	3.712	2.996	37.8
-3	3.888	3.161	39.5
-3.5	4.060	3.322	41.4
-4	4.228	3.479	43.6
-4.5	4.394	3.634	45.8
-5	4.557	3.787	48.1

Table 4. Refrigerant Saturation Temperature Parametric Study.

Refrigerant Saturation-Temperature Variation (K)	Clean Tube LMTD (K)	Fouled Tube LMTD (K)	Relative Uncertainty in R_f (%)
-0.5	2.244	1.566	49.9
0	2.763	2.099	48.7
+0.5	3.277	2.619	45.9
+1	3.787	3.132	42.3
+1.5	4.294	3.642	38.2
+2	4.800	4.149	34.2
+2.5	5.305	4.654	30.9
+3	**5.809**	**5.159**	**29.3**
+3.5	6.312	5.662	30.9
+4	6.815	6.165	36.7
+4.5	7.317	6.668	46.8
+5	7.819	7.170	61.2

CHAPTER V

RECOMMENDATIONS

Several conclusions can be drawn from the design, assembly, and modifications of the experimental apparatus. The following is a list of ten recommendations for building a similar apparatus.

1. Use a large mixing tank.
2. Have the necessary equipment to guarantee adequate cooling of the test water.
3. Limit the use of threaded surfaces to avoid water or refrigerant leaks.
4. Be conservative in the evaluation of the water pressure drop through the apparatus.
5. Make sure the supporting structure is sturdy.
6. Check in advance the power capabilities of the laboratory.
7. Be very familiar with LabVIEW, and run the data acquisition program on a stable computer system.
8. Ensure the safety of the laboratory and its users by implementing electronic and mechanical safety systems.
9. Perform a general uncertainty analysis prior to the experiment to identify the variables that contribute the most to the overall uncertainty

in the fouling factor. Use the results to select optimal transducers and measurement methods.

10. Avoid using low impedance transducers that output an AC signal.

CHAPTER VI

FUTURE WORK

VI.A Water Chemistry

Before Phase III of the project can begin, the Project Monitoring Subcommittee must approve the three chemistry conditions of the test water (low, average, and high fouling potential). This decision will be based on the results of Phase II (Tubman, 2002) as well as additional information found in the literature (Li et al., 2001). The test water preparation procedure has already been devised with the help of the Mississippi State Chemical Laboratory. Only the constituents and concentrations have to be specified to start testing.

VI.B Experimental Apparatus

The immediate task is to test the influence of the tank baffles on the formation of air bubbles in the test water. The next possible undertaking is to install the chilled water line in the laboratory and to connect it to the cold line of the water-loop heat exchangers. Finally, if time and money allow, high temperature insulation needs to be installed around the refrigerant tanks. These tasks and modifications are not necessary to perform any of the tests.

VI.C Experimental Procedure

An experimental procedure, already devised, will be discussed with the Project Monitoring Subcommittee. The mixing tank and the apparatus will be filled with distilled water. The pump will be turned on, and the valves will be adjusted so that the water velocity in each test tube reaches the desired value. The ring heaters will be turned on around each tank, and the tape heaters will be adjusted to give the required superheat. Once steady-state conditions are reached, the clean-condition overall heat-transfer coefficient will be obtained for each test tube.

On the same day, the employees of the Mississippi State Chemical Laboratory will add the foulants to the distilled water. Appropriate amounts of the reagents will be dissolved in five gallons of distilled water for dilution to the desired values in 75 gallons (approximate volume of the system) upon introduction into the system. Once the spiking solution is added and the container holding the solution rinsed three times, the system will be allowed to run several minutes before taking a sample for pH measurement. Concentrated HCl will be added until the pH reaches approximately 9 by checking with pH paper. At that point, a water sample will be taken as a baseline ($t = 0$) to be used for comparisons of chemical quality over time. The test water will run continuously during the addition of the chemicals and the entire course of the experiment. Water samples will be taken every week to ensure a constant water quality.

Once the tests are performed and the data are available, a least squares fit to the fouling resistance factors will be performed. The acquired data will also be used in attempt to obtain a model predicting the fouling resistance in helically-finned tubes. If

possible, the relationship between long-term fouling data and short-term results will also be investigated.

BIBLIOGRAPHY

Chamra, L.M., and Webb, R.L., "Effect of Particle Size and Size Distribution on Particulate Fouling in Enhanced Tubes," Enhanced Heat Transfer, Vol. 1, no. 1, 1993, 65-75.

Chamra, L.M., and Webb, R.L., "Modeling Liquid-Side Particulate Fouling in Enhanced Tubes," International Journal of Heat and Mass Transfer, Vol. 37, no. 4, 1994, 571-579.

Chenoweth, J., "Final Report of the HTRI/TEMA Joint Committee to Review the Fouling Section of the TEMA Standards," Heat Transfer Engineering, Vol. 11, no. 1, 1990, 73-107.

Coates, K.E., and Knudsen, J.G., "Calcium Carbonate Scaling Characteristics of Cooling Tower Water," ASHRAE Transactions, Vol. 86, no. 2, 1980, 68-91.

Coleman, H.W., and Steele, W.G., Experimentation and Uncertainty Analysis for Engineers, 2nd edition, John Wiley & Sons, New York, 1999.

Dreytser, G.A., Gomon, V.I., and Arnoz, I.Z., "Comparison of Fouling in Tubes with Annular Turbulence Promoters and in Smooth Tubes of Shell-and-Tube Heat Exchangers," Heat Transfer-Soviet Research, Vol. 15, No. 1, January-February 1983, 87-93.

Epstein, N., "Fouling in Heat Exchangers," Fouling of Heat Transfer Equipment, E.F.C. Somerscales and J.G. Knudsen, eds., Hemisphere, New York, 1981, 701-734.

Epstein, N. "Fouling: Technical Aspects," presented at the 1st International Conference on the Fouling of Heat Exchangers, August 1979, Troy, New York.

Haider, S.I., Webb, R.L., and Meitz, A.K., "A Survey of Water Quality and Its Effect on Fouling in Flooded Water Chiller Evaporators," ASHRAE Transactions, Vol. 97, no. 1, 1991, 55-67.

Haider, S.I., Webb, R.L., and Meitz, A.K., "An Experimental Study of Tube-side Fouling Resistance in Water-chiller-flooded Evaporators," ASHRAE Transactions, Vol. 98, no. 2, 1992, 86-103.

Hasson, D., "Precipitation Fouling," Fouling of Heat Transfer Equipment, E.F.C. Somerscales and J.G. Knudsen, eds., Hemisphere, New York, 1981, 527-568.

Hasson, D., Avriel, M., Resnick, W., Rozenman, T., and Windreich, S., "Mechanism of Calcium Carbonate Scale Deposition on Heat-Transfer Surfaces," I&EC Fundamentals, Vol.7, no. 1, February 1968, 59-65.

Hasson, D., Sherman, H., and Biton, M., "Prediction of Calcium Carbonate Scaling Rates," National Safety News, No. 2, 1978, 193-199.

Hodge, B.K., and Taylor, R.P., Analysis and Design of Energy Systems, 3rd edition, Prentice Hall, Upper Saddle River, 1999.

Knudsen, J.G., "Cooling Water Fouling – A Brief Review," Transactions of the ASME: Journal of Heat Transfer, Vol. 17, 1981, 29-38

Knudsen, J.G., Santoso, E., Breske, T.C., Donohue, J.M., and Chenoweth, J. M., "Fouling Characteristics of Cooling Tower Water Containing Phosphate Corrosion Inhibitors," Proceedings of the 1987 ASME-JSME Thermal Engineering Joint Conference, Vol. 3, 1987, 10.

Knudsen, J.G., and Story, M., "The Effect of Heat Transfer Surface Temperature on the Scaling Behavior of Simulated Cooling Tower Water," AIChE Symposium, Series, Vol. 74, no. 174, 1978, 25-30.

Lahm, Jr., L., and Knusden, J.G., "Precipitation of Cooling Water," Heat Transfer Sourcebook, J.W. Palen, ed., Hemisphere Publishing, Washington, 1986.

Lee, S.H., and Knudsen, J.G., "Scaling Characteristics of Cooling Tower Water," ASHRAE Transactions, Vol. 85, no. 1, 1979, 281-289.

Li, W., "The Performances of Internal Helical-Rib Roughness Tubes Under Fouling Conditions: Practical Cooling Tower Water Fouling and Accelerated Particulate Fouling," Transactions of the ASME: Journal of Heat Transfer, Vol. 125, August 2003, 746-748.

Li, W. and Webb, R.L. "Fouling in Enhanced Tubes Using Cooling Tower Water Part II: Combined Particulate and Precipitation Fouling," International Journal of Heat and Mass Transfer, Vol. 43, 2000, 3579-3588.

Li, W., Webb, R.L., and Bergles, A.E., "Particulate Fouling of Water in Internal Helical-Rib Roughness Tubes," Proc. Of the 12th International Conference of Heat Transfer at Grenoble, France, 2002, editor: Jean Taine, Société Française des Thermiciens (SFT), Elsevier, Paris.

Li, W., Webb, R.L., and Scherer, L., "Tube Side Fouling in Enhanced Tubes in Water Chiller-flooded Condenser," EPRI Reports, December 2001.

Meitz, A., "Water Treatment for Cooling Towers," Heating, Piping, Air Conditioning, January 1999, 125-134.

Morse, R.W., and Knudsen, J.G, "Effects of Alkalinity of Simulated Cooling Tower Water," The Canadian Journal of Chemical Engineering, Vol. 55, June 1977, 272-278.

National Instruments, The Measurement and Automation Catalog, Austin, 2002.

Rabas, T.J., Panchal, C.B., Sasscer, D.S., and Schaefer, R., "Comparison of Power-plant Condenser Cooling-water Fouling Rates for Spirally-indented and Plain Tubes," HTD-Vol. 164, Fouling and Enhancement Interactions, ASME, 1991, 29-36.

Sheikholeslami, R., and Watkinson, A.P., "Scaling of Plain and Externally Finned Heat Exchanger Tubes," Transactions of the ASME: Journal of Heat Transfer, Vol. 108, February 1986, 147-152

Socorro de Almeida, L.F., de Matos Beleza, V., and Bras Pereira, I., "Contribution of Air Pollution to the Fouling of Heat Exchangers in Cooling Water Circuits," Experimental Thermal and Fluid Science. Vol. 14, 1997, 438-441.

Somerscales, E.F.C., "Fouling of Heat Transfer Surfaces: An Historical Review," Heat Transfer Engineering, Vol. 11 no. 1 1990, 19-36

Somerscales, E.F.C., Ponteduro, A.F., and Bergles, A.E., "Particulate Fouling of Heat Transfer Tubes Enhanced on Their Inner Surface," HTD, Vol. 164, Fouling and Enhancement Interactions, ASME, 1991, 17-26.

Suitor, J.W., Marner W.J., and Ritter, R.B., "The History and Status of Research In Fouling of Heat Exchangers in Cooling Water Service," The Canadian Journal of Chemical Engineering, Vol. 55, August 1977, 374-380.

Taborek, J., Aoki, T., Ritter, R.B., Palen, J.W., and Knudsen, J.G., "Fouling – The Major Unresolved Problem in Heat Transfer, Part I," Chemical Engineering Progress, Vol. 88, no. 2, 1972, 59-67.

Taborek, J., Aoki, T., Ritter, R.B., Palen, J.W., and Knudsen, J.G., "Fouling – The Major Unresolved Problem in Heat Transfer, Part II," Chemical Engineering Progress, Vol. 88, no. 7, 1972, 69-78.

Tubman, I., An Analysis of Water-Side Fouling Potential Inside Smooth and Augmented Copper Alloy Condenser Tubes in Cooling Tower Water Applications, M.Sc. Thesis, Mechanical Engineering Department, Mississippi State University, Mississippi State, December 2002.

Watkinson, A.P., "Water Quality Effects on Fouling from Hard Water," Heat Transfer Sourcebook, J.W. Palen, ed., Hemisphere Publishing, Washington, 1986.

Watkinson, A.P., and Epstein, N., "Particulate Fouling of Sensible Heat Exchangers," Proc. of the 4th International Heat Transfer Conference, Paper No. HE 1.6.

Watkinson, A.P., Louis, L., and Brent, R., "Scaling of Enhanced Heat Exchanger Tubes," The Canadian Journal of Chemical Engineering, Vol. 52, October 1974, 558-562.

Watkinson, A.P., and Martinez, O., "Scaling of Spirally Indented Heat Exchanger Tubes," Transactions of the ASME: Journal of Heat Transfer, August 1975, 490-492

Webb, R.L., Principles of Enhanced Heat Transfer, John Wiley & Sons, Inc., New York, 1994.

Webb, R.L., and Kim, N-H., "Particulate Fouling in Enhanced Tubes," Heat Transfer Equipment Fundamentals, Design, Applications and Operating Problems, HTD, Vol 108, ASME, 1989, 315-324.

Webb, R.L. and Li, W. "Fouling in Enhanced Tubes Using Cooling Tower Water Part I: Long-term Fouling Data," International Journal of Heat and Mass Transfer, Vol. 43, 2000, 3567-3578.

Webb, R.L., Narayanamurthy R., and Thors, P., "Heat Transfer and Friction Characteristics of Internal Helical-Rib Roughness," Transactions of the ASME: Journal of Heat Transfer, Vol. 122, February 2000, 134-142.

APPENDIX A

SYSTEM COMPONENTS

A1. Mixing Tank

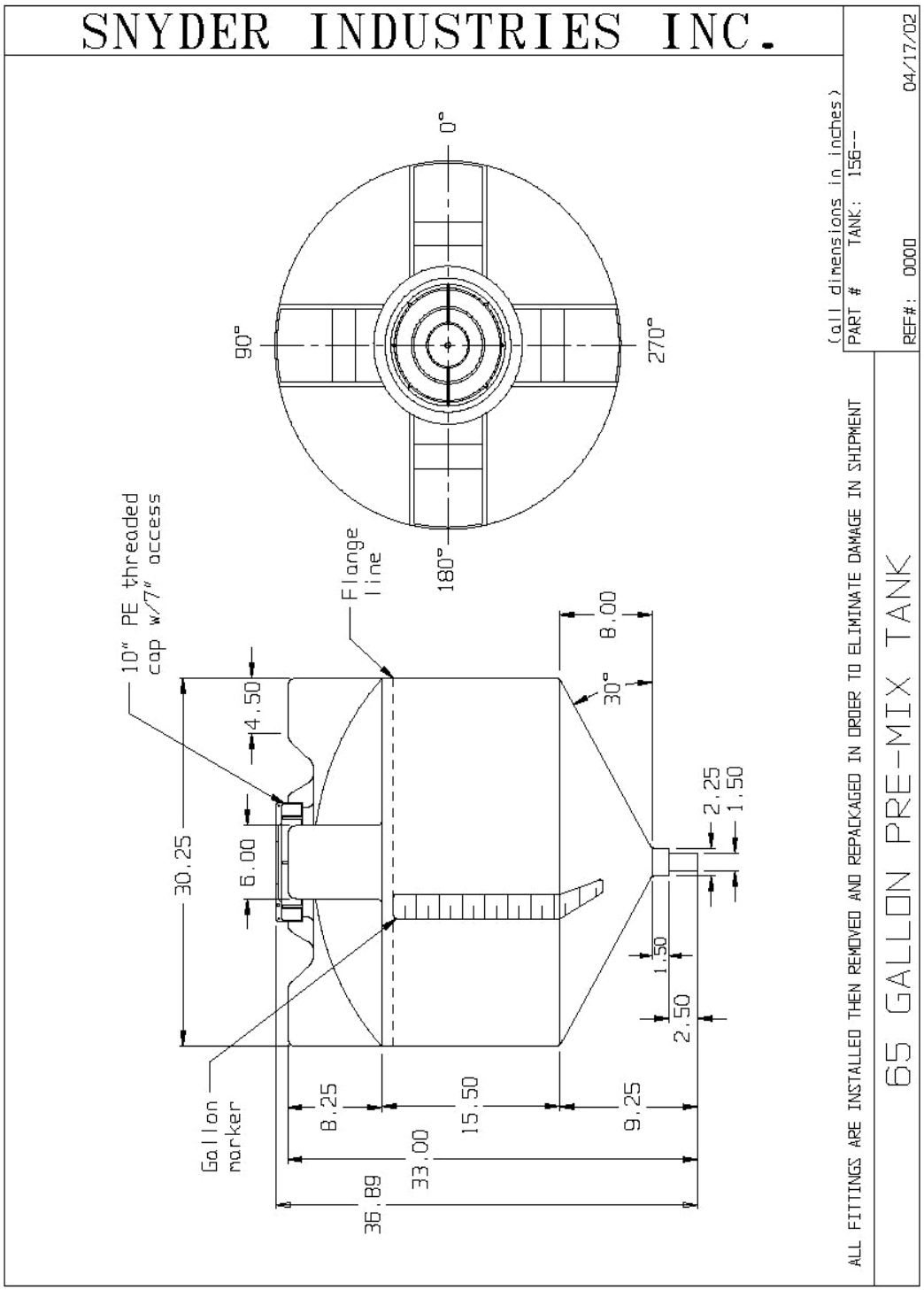

A2. S-10-I Condenser Specification Sheet

WATER COOLED CONDENSERS

20° Temperature Difference — ARI-450 Group 2

MODEL	Water Flow Rate - GPM									MAX GPM
	1	2	3	4	5	6	8	10	12	
	BTUH PD	BTUH PD	BTUH PD	BTUH PD	BTUH PD	BTUH PD	BTUH PD	BTUH PD	BTUH PD	
S-1-1	7.6 0.3	11.4 0.9	14.5 2.0	18.1 3.3	20.1 5.0	21.9 7.0				6
S-1.5-I	8.9 0.4	14.0 1.2	17.8 2.6	22.4 4.5	25.1 6.7	27.1 9.4				6
S-2-I		14.1 0.4	17.9 0.8	21.0 1.4	23.9 2.1	26.5 3.0	32.5 5.1	36.5 7.7		10
S-2.5-I		16.2 0.5	20.9 1.1	24.7 1.8	28.2 2.7	31.5 3.8	38.9 6.5	43.7 9.8		10
S-3-I			20.7 0.4	24.5 0.7	27.8 1.0	30.5 1.5	35.9 2.5	43.3 3.8	47.7 5.3	12
S-3.5-I			23.6 0.5	28.2 0.9	32.2 1.3	35.7 1.8	42.0 3.1	50.8 4.7	56.1 6.6	12
	8	10	12	14	16	20	24	28	32	
S-4-I	42.0 1.4	47.2 2.1	52.3 3.0	60.1 4.0	64.2 5.0	72.1 7.6				20
S-5-I	48.8 1.7	55.3 2.6	61.4 3.7	70.6 4.9	75.7 6.3	85.5 9.5				20
S-6-I	49.0 0.9	55.6 1.2	61.0 1.7	66.6 2.1	71.8 2.7	86.6 4.0	95.4 5.5			24
S-7-I	56.4 1.1	64.5 1.5	71.4 2.0	77.8 2.6	84.4 3.3	101.6 4.9	112.2 6.8			24
S-8-I				78.4 1.3	84.0 1.6	94.4 2.3	104.6 3.1	120.2 4.1	128.4 5.2	32
S-10-I				90.8 1.6	97.6 1.9	110.6 2.8	122.8 3.9	141.6 5.1	151.4 6.5	32

PD = Water pressure drop, lbs/sq inch.

25° Temperature Difference

MODEL	Water Flow Rate - GPM									MAX GPM
	1	2	3	4	5	6	8	10	12	
	BTUH PD	BTUH PD	BTUH PD	BTUH PD	BTUH PD	BTUH PD	BTUH PD	BTUH PD	BTUH PD	
S-1-I	9.6 0.3	14.7 0.9	18.5 2.0	22.2 3.3	25.8 5.0	28.3 7.0				6
S-1.5-I	11.3 0.4	17.8 1.2	22.8 2.6	28.7 4.5	32.2 6.7	35.5 9.4				6
S-2-I		17.9 0.4	22.8 0.8	26.9 1.4	30.5 2.1	34.0 3.0	41.7 5.1	46.4 7.7		8
S-2.5-I		20.6 0.5	26.6 1.1	31.6 1.8	36.1 2.7	40.4 3.8	49.8 6.5	55.8 9.8		8
S-3-I			26.4 0.4	31.2 0.7	35.5 1.0	39.2 1.5	46.1 2.5	55.5 3.8	61.1 5.3	12
S-3.5-I			30.0 0.5	35.8 0.9	41.0 1.3	45.5 1.8	54.0 3.1	65.0 4.7	72.0 6.6	12
	8	10	12	14	16	20	24	28	32	
S-4-I	53.7 1.4	60.5 2.1	67.0 3.0	77.0 4.0	82.5 5.0	92.7 7.6				20
S-5-I	62.2 1.7	70.6 2.6	78.4 3.7	90.2 4.9	96.9 6.3	109.3 9.5				20
S-6-I	62.4 0.9	71.0 1.2	78.4 1.7	85.4 2.1	93.2 2.7	111.0 4.0	122.2 5.5			24
S-7-I	71.0 1.1	82.0 1.5	91.0 2.0	99.4 2.6	108.0 3.3	130.0 4.9	144.0 6.8			24
S-8-I				100.2 1.3	107.4 1.6	121.0 2.3	134.0 3.1	154.0 4.1	165.0 5.2	32
S-10-I				115.4 1.6	124.4 1.9	141.2 2.8	156.8 3.9	180.4 5.1	193.8 6.5	32

The charts on this page are for our Advanced Fin Surface Design (AFSD) condensers

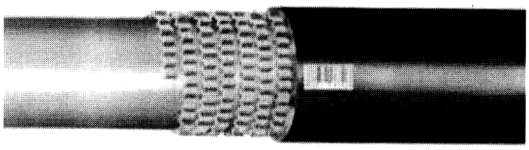

A3. Model 3656 Water Pump Specification Sheets

3656/3756 S-Group Numbering System For All Units Built After June 1, 1998

Sistema de numeración del Grupo S, modelos 3656/3756, para todas las unidades fabricadas luego del 1° de junio de 1998

The various versions of the 3656 and 3756 S-Group are identified by a product code number on the pump label. This number is also the catalog number for the pump. The meaning of each digit in the product code number is shown below.

Not all combinations of motor, impeller and seal options are available for every pump model. Please check with Goulds on non-cataloged numbers.

Not recommended for operation beyond printed H-Q curve. For critical application conditions consult factory.

Las diferentes versiones de los modelos 3656 y 3756 del Grupo S se identifican con un número de código de producto en la etiqueta de la bomba. Este número es también el número de catálogo de la bomba. A continuación se ilustra el significado de cada dígito en el código del producto.

No todas las combinaciones de motor, impulsor y sellos están disponibles para cada modelo. Consulte a Goulds sobre números que no aparecen en el catálogo.

No se recomienda la operación más allá de la curva impresa de H-Q (carga-capacidad). Para aplicaciones bajo condiciones críticas, consulte con la fábrica.

Example Product Code, *Ejemplo del código de producto*

9 BF 1 H 2 G 0 H

High Head Impeller (1½ x 2 – 6H Only), *Impulsor de carga alta (1½ x 2 – 6H únicamente)*

Mechanical Seal and O-ring, *Sello mecánico y anillo en O*

Seal Code *Código del sello*	Rotary *Rotativo*	Stationary *Estacionario*	Elastomers *Elastómeros*	Metal Parts *Partes metálicas*	Part Numbers *Número de pieza*
0	Carbon, *Carbono*	Ceramic, *Cerámica*	BUNA-N	Type 316 SS *Acero inoxidable tipo 316*	10K13
1	Carbon, *Carbono*	Ni-Resist	EPR		10K19
2	Carbon, *Carbono*	Ceramic, *Cerámica*	Viton, *Viton*		10K25
3	Carbon, *Carbono*	Sil-Carbide, *Carburo de silicio*	Viton, *Viton*		10K27
4	Sil-Carbide, *Carburo de silicio*	Sil-Carbide, *Carburo de silicio*	Viton, *Viton*		10K64
9	Packed Box Design with BUNA O-ring, *Diseño con empaque y anillo en O BUNA*				15K3

Impeller Option Code, *Código de opción de impulsor*

Impeller Code, *Código del impulsor*	22BF	9BF	3BF		5BF	4BF	6BF
	1 x 2 – 7	1 x 2 – 8	1½ x 2 – 6	1½ x 2 – 6H	1½ x 2 – 8	2½ x 3 – 7	3 x 4 – 7
	Dia.	Dia.	Dia.	Dia.	Dia.	Dia.	Dia.
A	6¾"	8 1/16"	5 15/16"	5 15/16"	8 1/16"	7 1/16"	7 1/16"
B	6 7/16	7 5/8	5 3/8	5 3/8	7 5/8	6 3/4	6 3/8
C	6	7 5/16	5 1/4		6 3/4	6 3/8	5 1/2
D	5 3/4	7	4 3/4		5 3/4	5 1/8	4 11/16
E	5 1/2	6 1/2			7 3/4	5 3/8	5 1/8
F	5 1/16	6 3/16			7	5 1/16	6
G	4 13/16	5 3/8			6 1/4	5 1/4	
H	4 9/16	5 1/16			6 1/8	4 15/16	
J	4 3/8					4 3/4	
K	4 1/16					4 1/8	
L	3 13/16						

Driver, *Elemento motor*

1 = 1 PH, ODP
2 = 3 PH, ODP
3 = 575 V, ODP
4 = 1PH, TEFC
5 = 3 PH, TEFC
6 = 575 V, TEFC
7 = 3 PH, XP
8 = 575 V, XP
9 = 3 PH, TEFC, PREFF
0 = 1 PH, XP

1 PH = Monofásico, 3 PH = Trifásico

HP Rating, *Potencia nominal, HP*

C = ½ HP
D = ¾ HP
E = 1 HP
F = 1½ HP
G = 2 HP
H = 3 HP
J = 5 HP
K = 7½ HP
L = 10 HP
M = 15 HP
N = 20 HP

Driver: Hertz/Pole/RPM, *Elemento motor: Hertz/Polos/RPM*

1 = 60 Hz, 2 pole, 3500 RPM
2 = 60 Hz, 4 pole, 1750 RPM
3 = 60 Hz, 6 pole, 1150 RPM
4 = 50 Hz, 2 pole, 2900 RPM
5 = 50 Hz, 4 pole, 1450 RPM

For frame mounted version, substitute the letters "FRM" in these positions.

Para las versiones de montaje en bastidor, reemplazar las letras en esta ubicación con "FRM".

Material, *Material*

BF = Bronze fitted, *Accesorios de bronce*
AI = All iron, *Todo hierro*
AB = All bronze, *Todo bronce*

Pump Size, *Tamaño de bomba*

3 = 1½ x 2 – 6(H)
4 = 2½ x 3 – 7
5 = 1½ x 2 – 8
6 = 3 x 4 – 7
9 = 1 x 2 – 8
22 = 1 x 2 – 7

The 1 x 2 – 8 and 1 x 2 – 7 are only available in Bronze Fitted.
Los tamaños 1 x 2 – 8 y 1 x 2 – 7 están disponibles con accesorios de bronce únicamente.

3656 S-Group Materials of Construction
Materiales de construcción - Grupo S, modelo 3756

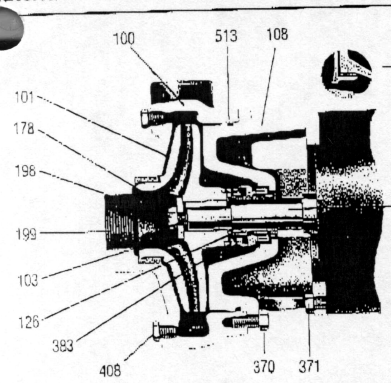

Back wearing ring on S-Group (2½ x 3 – 7) only
Anillo de desgaste posterior en el Grupo S (2½ x 3 – 7) únicamente.

AISI 1045 steel motor shaft extension (typical)
Extensión del eje del motor de acero AISI 1045 (típico)

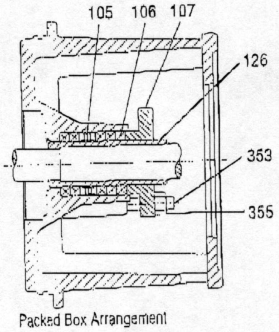

Packed Box Arrangement
Caja prensaestopas

Item No. *No. ítem*	Description *Descripción*	Materials, *Materiales*		
		All Iron *Todo hierro*	Bronze Fitted *Accesorios de bronce*	All Bronze *Todo bronce*
100	Casing, *Carcasa*	1001	1001	1101
101	Impeller, *Impulsor*		1101	
103	Casing wear ring, *Anillo de desgaste de la carcasa*		1618	1618
108	Adapter, *Adaptador*		1001	1001
184	Seal housing, *Cubierta del sello* ①	One piece with adapter, *Una pieza con adaptador* 1101		
126	Shaft sleeve, *Camisa del eje*	AISI Type 300 series stainless steel *Acero inoxidable serie AISI tipo 300*		
178	Impeller key, *Chaveta del impulsor*			
198	Impeller bolt, *Perno del impulsor*			
199	Impeller washer, *Arandela del impulsor*			
370	Hex head cap screw (adapter to case), *Tornillo de cabeza hexagonal (del adaptador a la cubierta)*	Steel SAE 1200 Grade 5 *Acero SAE 1200 grado 5*		
371	Hex head cap screw (adapter to motor), *Tornillo de cabeza hexagonal (del adaptador al motor)*			

	Mechanical Seal *Sello mecánico*	Part No. *Pieza No.*	Service *Servicio*	Rotary *Rotativo*	Stationary *Estacionario*	Elastomers *Elastómeros*	Metal Parts *Partes metálicas*
383	Standard, *Estándar*	10K13	General, *General*	Carbon *Carbono*	Ceramic, *Cerámica*	BUNA	Type 316 SS *Acero inoxidable tipo 316*
	Optional, *Optativo*	10K19	Hi-Temp, *Alta temp.*		Ni-Resist	EPR	
	Optional, *Optativo*	10K25	Chem. Duty *Sustancias químicas*		Ceramic, *Cerámica*	Viton *Vitón*	

408	Pipe plug ¼" or ⅜", *Tapón de tubos de ¼ de pulgada ó ⅜ de pulgada*	Steel, *Acero* Bronze, *Bronce*
513	O-ring, *Anillo en O*	BUNA-N, *BUNA-N*

Material Code, *Código de material*	Engineering Standard, *Norma de ingeniería*
1001	Cast iron ASTM A48 CL20, *Hierro fundido ASTM A48 CL20*
1101	Silicon bronze ASTM B584, C87500, *Silicíuro de bronce ASTM B584, C87500*
1618	Bizmuth brass, *Latón al bismuto*

Packed Box Arrangement, *Caja prensaestopas*

Item No. *No. ítem*	Description *Descripción*	Materials *Materiales*
105	Lantern ring, *Aro de linterna*	Teflon™
106	Packing, 5 rings; *Empaquetadura, 5 aros*	Teflon Impregnated, *Impregnado de Teflon*
107	Gland, *Casquillo*	AISI 316SS
126	Shaft sleeve, *Camisa del eje*	AISI Type 300 Series Stainless Steel *Acero inoxidable serie AISI tipo 300*
353	Gland stud, *Perno del casquillo*	
355	Gland nut, *Tuerca del casquillo*	

① For separate seal housing and adapter construction, all bronze material only, see repair parts page.

Para la construcción separada del compartimiento del sello y el adaptador, materiales de bronce únicamente, consulte la página de piezas de repuesto.

NOTE:
Pumps will be shipped with top-vertical discharge position as standard. For other orientations, remove casing bolts – rotate discharge to desired position – replace and tighten bolts to 25 ft./lbs. Note that discharge may extend below motor mounting surface in bottom-horizontal position; adequate clearance must be provided.

NOTA:
Las bombas salen de la fábrica con la descarga orientada en posición vertical superior de manera estándar. Para modificar la orientación, retirar los pernos de la carcasa, hacer girar la descarga hasta la posición deseada y volver a colocar los pernos, ajustándolos a una torsión de 25 pies/libras. Se ha de notar que la descarga se puede extender por debajo de la superficie de montaje del motor en la posición horizontal inferior; por lo tanto, debe proveerse suficiente espacio.

3656 S-Group Dimensions and Weights
Grupo S, modelo 3656 - Peso y dimensiones

Mechanical Seal
Sello mecánico

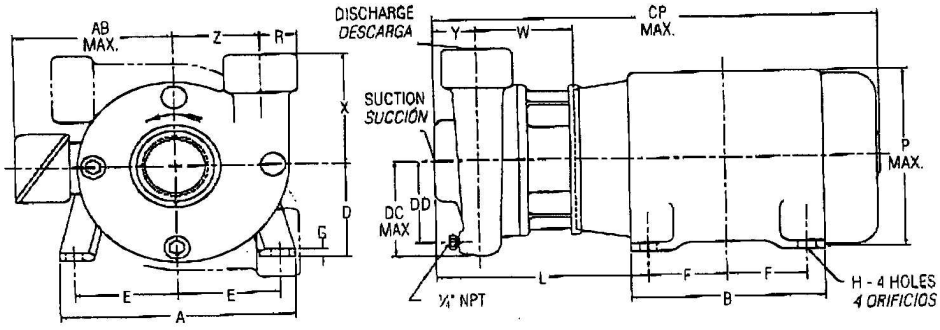

Pump Dimensions and Weights (Dimension "L" determined by Pump and Motor)
Peso y dimensiones de la bomba *(la dimensión "L" está determinada por la bomba y el motor)*

Pump *Bomba*	Suction *Succión*	Discharge *Descarga*	CP Max.	DC Max.	DD	R	W	X	Y	Z	Wt. (lbs.) *Pesos (libras)*	Motor Frame Size, *Bastidor* 140	180	210	250
												L			
1 x 2 – 7	2	1	27	4¼	3½	1 1/16	4⅛	5½	3	4	52	10	10¾	—	—
1 x 2 – 8					4		3 15/16	5¾	3 1/16	4¼	52			—	—
1½ x 2 – 6		1½	23¾		3½	1¼	4¼	4½	2⅛	3½	34	9¾	10½	—	—
1½ x 2 – 8			27⅛	5⅛	4⅝			5		4¼	54			11⅜	11⅜
2½ x 3 – 7	3	2½	25⅝	5¼	4½	1 3/16		6	3	4	49	10¼	10¾	11¾	—
3 x 4 – 7	4"	3"	25¼	5¾	5⅛	3¾	4⅜		2½	4½	82	9¾	10⅞	11¾	—

Motor Dimensions and Weights (may vary with manufacturer)*
Peso y dimensiones del motor *(pueden variar de acuerdo al fabricante) **

Frame Size JM *Tamaño del bastidor JM*	A	AB (Max.)	B	D	E	F	G	H	P (Max.)	Weight (lbs.) *Pesos (libras)*
143	6½	5¼	6	3½	2¾	2	1/4	1 1/32	6¾	41
145						2½				57
182	8½	5¼	6½	4½	3¾	2¼	3/16	1 3/32	7⅛	77
184						2¾				97
213	9½	7¼	8	5¼	4¼	2¾	1/32	1 5/32	9⅝	122
215						3½				155
254 TCZ	11¼	9	9½	6¼	5	4¼	1/4	1 7/32	11½	265
256 TCZ			11¾			5				320

NOTE:
All pumps shipped in vertical discharge position. May be rotated in 90° increments. Tighten casing bolts to 25 ft./lbs. torque.

NOTA:
Todas las bombas se embarcan con la descarga en posición vertical. Esta posición puede rotarse en incrementos de 90°. Ajustar los pernos de la carcasa a una torsión de 25 pies/libras.

Motor Frames and Horsepower
Bastidores del motor y potencia en HP

Motor Frame *Bastidor del motor*	3500 RPM 1 Phase ODP	3500 RPM 1 Phase TEFC	3500 RPM 3 Phase ODP	3500 RPM 3 Phase TEFC	1750 RPM 1 Phase ODP	1750 RPM 1 Phase TEFC	1750 RPM 3 Phase ODP	1750 RPM 3 Phase TEFC
143 JP	—	¾,1,1½	¾,1,1½	¾,1,1½	—	½,¾	½,¾,1	½,¾,1
145 JP	—	2	2,3	2,3	—	1,1½	1½,2	1½,2
182 JP	3	3	5	5	3	2,3	3	3
184 JP	5	3,5	7½	5	—	—	5	5
213 TCZ	7½	—	10	7½	5	—	7½	7½
215 TCZ	10	—	15	10,15	—	—	—	—
254TCZ	—	—	20	—	—	—	—	—
256TCZ	—	—	25	20,25	—	—	—	—

All dimensions in inches and weights in lbs. Do not use for construction purposes.
Todas las dimensiones están en pulgadas, el peso en libras. No utilizar para fines de construcción.

A4. Model 3656 Water Pump Curves

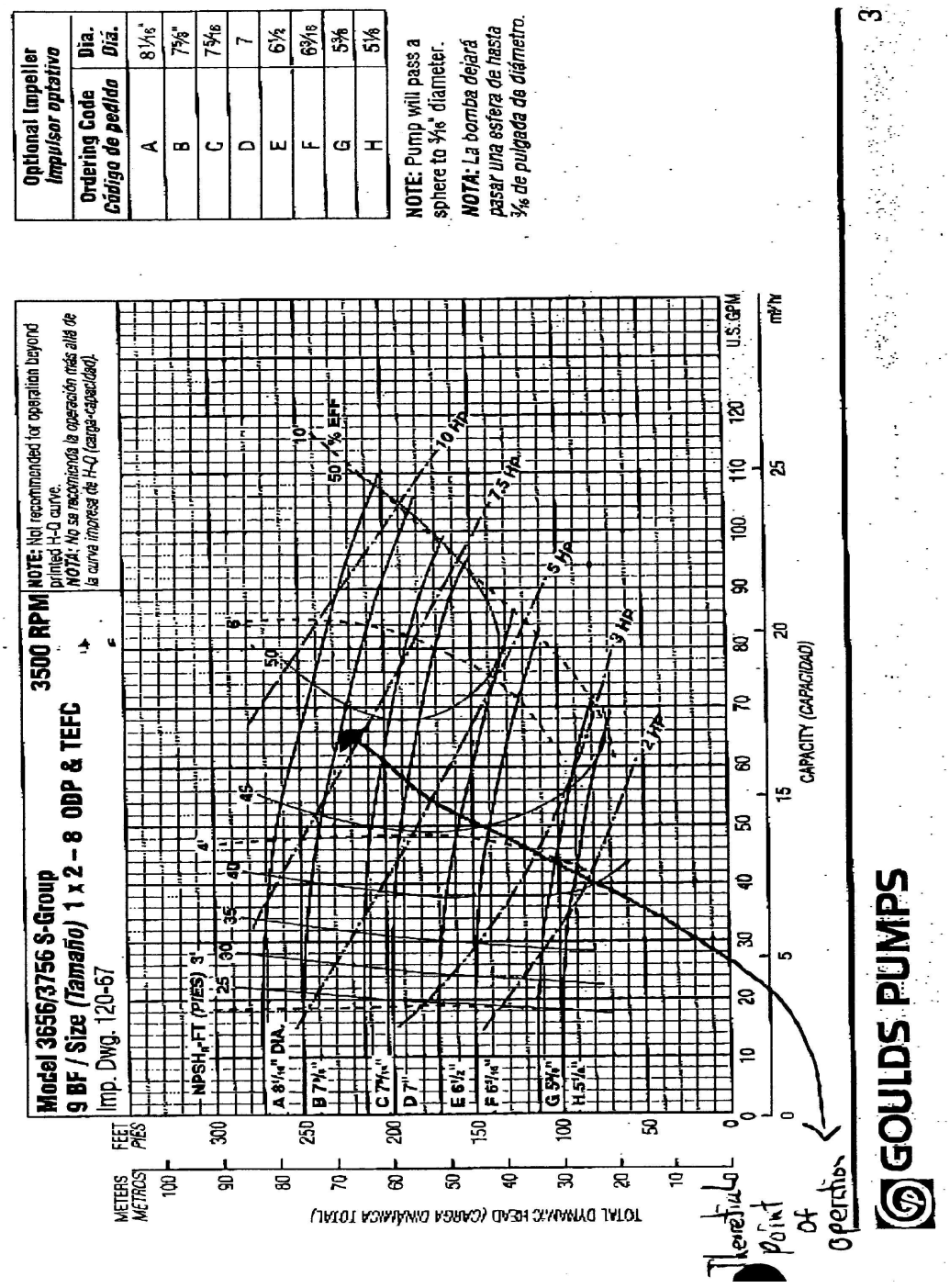

Optional Impeller *Impulsor optativo*	
Ordering Code *Código de pedido*	**Dia.** *Dia.*
A	8 1/16"
B	7 5/8"
C	7 5/16
D	7
E	6 1/2
F	6 1/16
G	5 5/8
H	5 1/8

NOTE: Pump will pass a sphere to 1/16" diameter.

NOTA: *La bomba dejará pasar una esfera de hasta 1/16 de pulgada de diámetro.*

A5. Cylindrical Vibration Isolator

Item Details

Product Category: Material Handling > Mounts and Vibration Control > Cylindrical Vibration Isolators

Description
Cylindrical Vibration Isolator, Maximum Load Downward Compression 125 Pounds, Maximum Load Sideways Shear 20 Pounds, Thread Size 3/8-16 Inch, Dimension A 1 9/16 Inches, Dimension B 1 Inch, Dimension C 5/8 Inch

Grainger Item: 3CC06
Price (ea) : $2.87
Manufacturer: KARMAN RUBBER
Mfg. Model#: K37

Ship Qty : 1
Sell Qty (Will-Call) : 1
Usually Ships : Today
Catalog 394 Page: 2065

Select Qty.

Add to Personal List >> ADD TO ORDER >>

Price shown may not reflect your price. *Log-in* above, or click here to register.

NOTES & RESTRICTIONS
See Catalog 394 Page for application and/or safety information.

ALTERNATE PRODUCTS
Description
Cylindrical Vibration Isolator, Maximum Load Downward Compression 165 Pounds, Maximum Load Sideways Shear 55 Pounds, Thread Size 3/8-16 Inch, Dimension

Price (ea): $4.25
Grainger Item#: 3CC08

Usually Ships : Today

Select Qty.

Add to Personal List >> ADD TO ORDER >>

TECHNICAL SPECIFICATIONS
Dimensions (Inches) A: 1 9/16
Dimensions C (Inches): 5/8
Maximum Load Downward Compression (Pounds): 125
Maximum Load Sideways Shear (Pounds): 20
Thread Size: 3/8-16
Dimensions B: 1

A6. Modified Suction Accumulator (Refrigerant Tank)

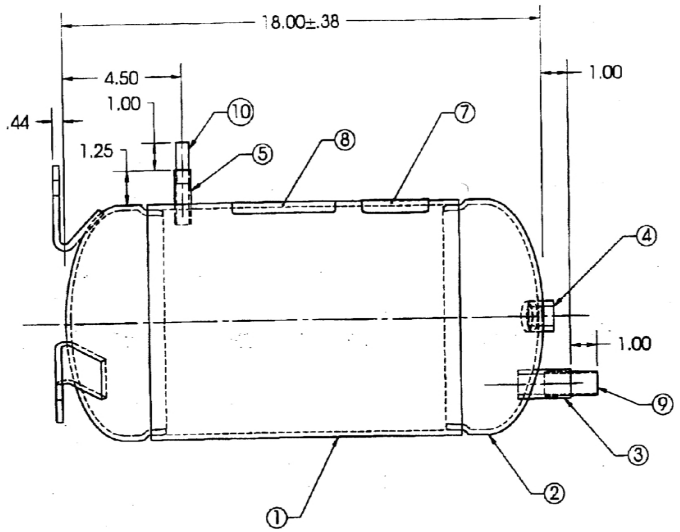

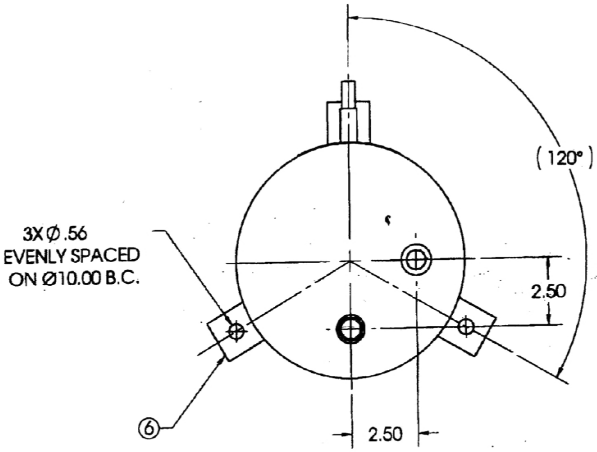

ITEM NO.	QTY.	PART NO.	DESCRIPTION
1	1	shell	8.625 O.D. X .188 WALL
2	2	8060	Ø8.625 ASME HEAD
3	1	6578-3	.875 I.D. NIPPLE
4	1	7495	1/2 - 14 NPTF FEM. FITTING
5	1	X9396-1	.500 I.D. NIPPLE
6	3	1186	MOUNTING BRACKET
7	1	7028	ASME TAG
8	1	7108-3	PART LABEL
9	1	CU. STUB	.875 O.D. X .049 CU. STUB
10	1	CU. STUB	.500 O.D. X .035 CU.

ARC WELD CONSTRUCTION SEE DETAIL 3639-W

SEAL 6578-3 NIPPLE W/ PB988 PLUG & J0943 COVER
SEAL 9361-3 NIPPLE W/ PLUG & COVER
SEAL 7495 FEM PIPE FITT. W/ 444746

PNEUMATIC TEST AT 275 psig

POWDER PAINT BLACK

TOLERANCES NOT SPECIFIED
FRACTIONS ± 1/16
DECIMALS ± .0625
ANGLES ± 2.5°

REFRIGERATION RESEARCH
BRIGHTON, MICHIGAN

POINTING THE WAY

NO.	DATE	CH'D	APP'D	REVISIONS
1	12/06/02	JBN	JBN	ADDED CU. STUB
2	01/13/03	JBN	JBN	ADDED CU.STUB FOR .500 NIPPLE

MATERIAL: SA 53 GRADE B TYPE E

NAME: ACCUMULATOR

DRAWN BY: MJH | SCALE: 1 : 4 | DRAWING NO.: X8828
CH'D: JBN | DATE: 12/03/02
CUT L [illegible] | APP'D [illegible]

A7. Rupture Disc Data Sheet

GRAPHILOR®

CARBONE OF AMERICA

SINGLE PIECE DISC INSTRUCTIONS
(SERIES 3)

TYPICAL INSTALLATION

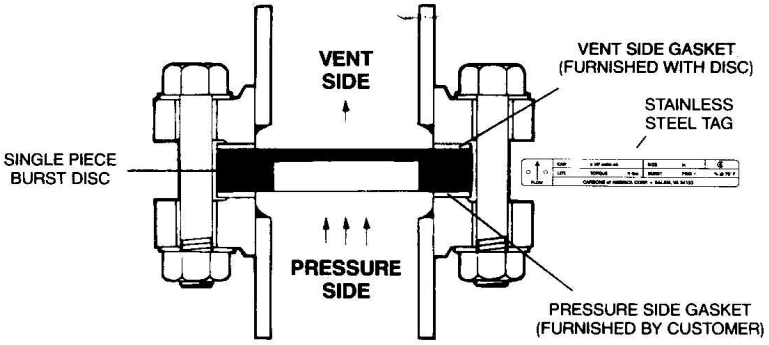

IMPORTANT NOTES:

1. All Graphilor® single piece burst discs have a stainless steel label, as shown below, affixed to the outer circumference.

FLOW	CAP. 2.92 x 10^3 scfm-air	SIZE 1 in.
	LOT. 3663 TORQUE 10 ft-lbs	BURST 200 PSIG ± 5 % @ 70° F
	CARBONE of AMERICA CORP. • SALEM, VA 24153	

   Make sure the disc information agrees with the intended application.

2. Discs are designed to fit within the bolt circle of 150# or 300# ANSI flanges. Make sure disc is properly centered between flanges during installation.

3. It is important to install the disc in the correct flow direction. This is noted by an arrow on the label.

4. Flange faces should be parallel to each other in order to eliminate excessive bolting forces when installing disc.

5. The vent side gasket is furnished with the disc because the gasket material and inside diameter are critical to the burst disc accuracy.

6. The process (or pressure) side gasket, furnished by customer, must be compatible with the process fluid and therefore the preferred type is a standard 150# ANSI TFE envelope gasket with a soft ⅛" thick filler. Do not us a gasket having a metal insert.

7. Burst pressure shown on label has been established at ambient temperature. Elevated temperatures may cause a reduction in the actual burst pressure of the disc.

A8. Ring Heater Specification Sheet

ONE-PIECE BAND HEATERS

1½"(4cm) & 2½"(6cm) Wide DB & DBW Series

- **Rugged, Reliable, Heavy Duty**
- **5"(13cm) to 12½"(32cm) Barrel Diameter**
- **Barrel Temperatures up to 900°F**

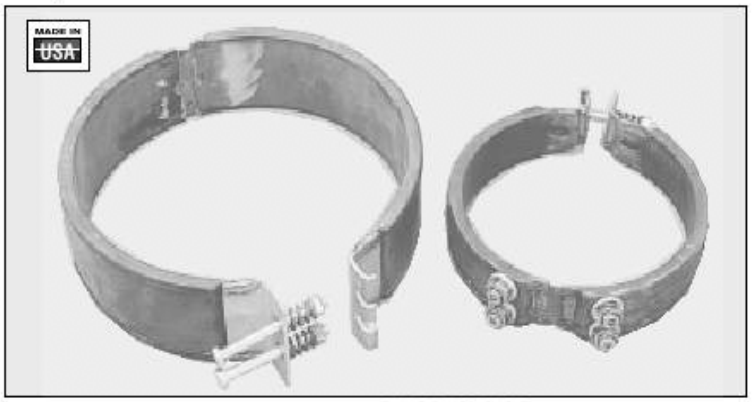

APPLICATIONS

- Heating barrels of plastic injection molding machines and extruders
- Die and die holder heating of plastic extruders and blow molding machines
- Autoclaves
- Burn-out ovens
- Heated kettles
- Fluidized beds
- Heat treating pipes
- Any application requiring heat applied to a cylindrical surface

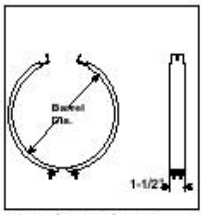

DB Dimensions

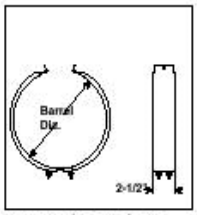

DBW Dimensions

To Order *(Specify Model No.)*

MOST POPULAR MODELS HIGHLIGHTED!

Watts	W/In²	Barrel Dia. In. (cm)	Model No.	Price	Wt. lbs. (kg)
DB-1¼ inches (4cm), 240/480 volts**					
770	33	5 (13)	**DB-050772**	**$56**	1.5 (.7)
1000	42	5⅛ (14)	**DB-054102**	**59**	1.75 (.8)
750	27	6 (15)	**DB-060752**	**61**	2 (.9)
1000	33	6⅛ (17)	**DB-064102**	**63**	2 (.9)
1000	30	7 (18)	**DB-070102**	**66**	2 (.9)
1250	35	7⅛ (19)	**DB-074122**	**68**	2 (.9)
1200	32	8 (20)	**DB-080122**	**70**	2 (.9)
1600	40	8⅛ (22)	**DB-084162**	**73**	2.5 (1.1)
1500	35	9 (23)	**DB-090152**	**75**	2.5 (1.1)
1700	38	9⅛ (24)	**DB-094172**	**78**	3 (1.4)
1200	25	10 (25)	**DB-100182**	**81**	3 (1.4)
1200	24	10⅛ (27)	**DB-104122**	**84**	3 (1.4)
2100	39	11⅛ (29)	**DB-114212**	**94**	3 (1.4)
1500	25	12⅛ (32)	**DB-124152**	**108**	3 (1.4)
DB-2¼ inches (6cm), 240/480 volts**					
1525	30	6⅛ (17)	**DBW-064152**	**86**	3.75 (1.7)
1800	31	7⅛ (19)	**DBW-074182**	**95**	3.75 (1.7)
2000	35	8 (20)	**DBW-080202**	**100**	3.75 (1.7)
2250	34	8⅛ (22)	**DBW-084222**	**104**	3.75 (1.7)
2500	35	9 (23)	**DBW-090252**	**109**	3.75 (1.7)
2800	36	10 (25)	**DBW-100282**	**118**	3.75 (1.7)
2950	36	10⅛ (27)	**DBW-104292**	**127**	3.75 (1.7)
3250	36	11⅛ (29)	**DBW-114322**	**132**	4 (1.8)

*** The two 240V strip heating elements must be wired in series for 480V*
NOTE: Watt densities are based on heated area of contact surface only.

FEATURES

Ten times the life–only slightly higher cost. This economical long life heavy duty band heater has a ¾ inch thick chrome steel (stainless) sheath, which offers ten times the life of a mica band heater at only a slightly higher cost than mica, and considerably lower than ceramic band and aluminum shoe designs.

Flexible one-piece construction for easy installation and removal. The unheated section between heated halves functions as a hinge and permits repeated opening and closing for moving heaters from one application to another. The heavy duty spring loaded clamping bolt pulls the heater tight to the work and maintains tightness by compensating for expansion.

Heavy duty – uses a pair of formed 240V OMEGALUX® PT series strip heaters.

Spring loaded – for tight fit with Inconel-x spring and nickel-plated clamping bolts and nuts—maintains tightness.

Uniform high temperature capability. Highly compacted refractory insulation assures efficient heat transfer, therefore lower resistance wire temperatures.

SPECIFICATIONS

Power: 240/480V**
Wattage: 750 to 3250 watts.
Sheath Material: Chrome Steel
Maximum Sheath Temperature: 1200°F

A9. Tape Heater Specification Sheet

HEATING TAPE WITH PERCENTAGE CONTROLLER

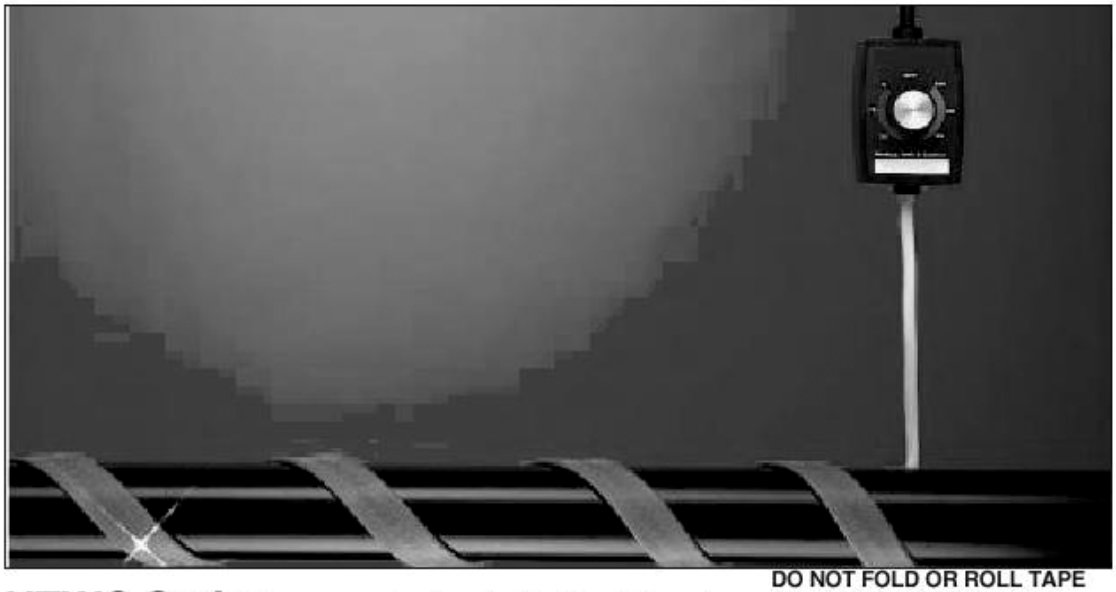

HTWC Series

- Reliable
- Integral Percentage Controller
- Silicone Rubber Encapsulated Heating Tape
- High Temperature Rating of 500°F

The tape consists of a flexible heating strip 1" wide and of varying lengths with a permanently incorporated temperature controller. Standard tapes are available for either 120 or 240 volt operation and develop 72 watts per lineal foot. These tapes are completely safe when operated according to directions, and with reasonable care, will give long service.

This economical semi-automatically controlled heating tape has been developed by OMEGALUX® for use in small scale heating applications.

DO NOT FOLD OR ROLL TAPE WHEN IT IS BEING HEATED.

APPLICATIONS

Heat Tracing for Temperature maintenance or heat loss.

Plastic Sheet Bending.

SPECIFICATIONS

Power: 120 or 240V.

Wattage: 72 watts/lineal foot.

Heating Element : Fine gage stranded resistance wires insulated with fiberglass yarn and completely enclosed in a silicone rubber extrusion.

Controller: Rugged and dependable percentage controller. Includes power cord and 2 prong plug.

To Order ***(Specify Model Number) MOST POPULAR HIGHLIGHTED!***

Watts	Volts	Size	Model Number	Price
144	120	1" x 2'	**HTWC101-002**	**$97**
288	120	1" x 4'	**HTWC101-004**	**105**
432	120	1" x 6'	**HTWC101-006**	**115**
576	120	1" x 8'	**HTWC101-008**	**123**
720	120	1" x 10'	**HTWC101-010**	**132**
144	240	1" x 2'	**HTWC102-002**	**97**
288	240	1" x 4'	**HTWC102-004**	**105**
432	240	1" x 6'	**HTWC102-006**	**115**
576	240	1" x 8'	**HTWC102-008**	**123**
720	240	1" x 10'	**HTWC102-010**	**132**

CAUTION AND WARNING!

Fire and electrical shock may result if products are used improperly or installed or used by non-qualified personnel. See inside back cover for additional warnings.

A10. Pipe Insulation Data Sheet

Elastomeric Pipe Insulation & Accessories

Temperature Range: -40° F To 220° F

A flexible elastomeric thermal insulation used to retard heat gain and prevent condensation or frost formation on cold water plumbing, chilled-water and refrigerant lines. Also retards heat flow for hot water plumbing, liquid heating, dual temperature piping and many solar systems. The expanded closed cell structure makes it an efficient insulation and an effective vapor barrier. Commonly used to insulate pre-charged line sets for leading o.e.m.'s and distributors of air conditioners and heat pumps.
Pipe insulation slides easily over pipe or tubing. A factory applied coating of talc on the smooth inner surface speeds application. When applied to existing lines, tubing is slit lengthwise and snapped into place. Slitting can be done on the job with a razor or sharp knife. All seams and butt joints are to be sealed with contact adhesive.

Accessories:

Desc.	Thickness (In.)	W. (In.)	Length (In.)	Order #	Price Ea.
Flat Sheet	½	36	48	37030798	**$22.38**
Flat Sheet	¾	36	48	37030806	**34.00**
Flat Sheet	1	36	48	37030814	**34.93**
1 Pint Adhesive				[1]37030822	**8.26**
1 Quart Adhesive				[1]37030830	**13.52**
1 Gallon Finish				37030848	**18.13**

[1]DOT REGULATED. May require special handling.

If Used Outdoors, It Should Be Coated With Exterior Acrylic Latex Paint.

- .277 K Value At +75° F.
- FHC 25/50 Per ASTM E84
- Flexible 6' Black Lengths
- ASTM C534, MIL-P-15280

Pipe Insulation Size ID (In.)	Pipe/Tube OD (In.)	⅜" Thick [1]Lengths (6')/Carton	⅜" Thick Order #	⅜" Thick Price Ea. Piece	⅜" Thick Price Ea. Carton	½" Thick [1]Lengths (6')/Carton	½" Thick Order #	½" Thick Price Ea. Piece	½" Thick Price Ea. Carton	¾" Thick [1]Lengths (6')/Carton	¾" Thick Order #	¾" Thick Price Ea. Piece	¾" Thick Price Ea. Carton
⅜	⅜	147	37030400	**$2.09**	**$1.88**	76	37030491	**$3.17**	**$2.85**	49	37030640	**$4.82**	**$4.34**
½	½	85	37030418	**2.15**	**1.93**	60	37030509	**3.43**	**3.09**	38	37030657	**5.05**	**4.54**
⅝	⅝	71	37030426	**2.46**	**2.21**	60	37030517	**3.63**	**3.27**	35	37030665	**5.84**	**5.26**
¾	¾	63	37030434	**2.59**	**2.33**	50	37030525	**3.69**	**3.32**	30	37030673	**6.33**	**5.70**
⅞	⅞	53	37030442	**2.77**	**2.49**	40	37030533	**4.02**	**3.62**	23	37030681	**6.93**	**6.24**
1⅛	1⅛	46	37030459	**3.13**	**2.82**	33	37030541	**4.67**	**4.20**	19	37030699	**7.79**	**7.01**
1⅜	1⅜	35	37030467	**3.55**	**3.19**	25	37030558	**4.95**	**4.45**	15	37030707	**9.55**	**8.59**
1⅝	1⅝	30	37030475	**4.35**	**3.91**	20	37030566	**5.78**	**5.20**	13	37030715	**12.62**	**11.36**
2	2					19	37030574	**7.02**	**6.32**	11	37030723	**13.90**	**12.51**
2⅛	2⅛	16	37030483	**5.34**	**4.81**	14	37030582	**7.70**	**6.93**	11	37030731	**15.01**	**13.51**
2⅜	2⅜					11	37030590	**9.24**	**8.32**	8	37030749	**15.92**	**14.33**
2⅝	2⅝					10	37030608	**10.04**	**9.04**	8	37030756	**18.59**	**16.73**
2⅞	2⅞					8	37030616	**11.37**	**10.23**	7	37030764	**20.88**	**18.79**
3⅛	3⅛					8	37030624	**11.89**	**10.70**	7	37030772	**21.36**	**19.22**
3⅝	3⅝					8	37030632	**14.85**	**13.36**	5	37030780	**24.63**	**22.17**

[1] Refers to the number of 6 foot lengths contained in each carton

A11. Thermocouple Data Sheet

Pipe Plug Probe

This high pressure thermocouple plug sensor is ideal for vessel applications, pressurized containers and applications requiring mounted NPT security for fixed readings. Its 304SS sheath has a 6.4 mm (0.25") dia. probe that extends ½"** from a ¼" NPT pipe plug, with 1.8 m (6') of 20 AWG fiberglass insulated stranded thermocouple grade wire with sainless steel overbraiding and either stripped leads or a miniature male connector.

For grounded or ungrounded junctions, pressure rating is 2500 PSI. The hex flats are 0.560" on the flats; 16.1 mm (0.635") between points. Hex flats width is 5.8 mm (0.23"). Maximum temp rating: Types J, K, E: 480°C (900˚F); Type T: 370°C (700˚F).

For low pressure applications grounded junctions may be replaced with an exposed junctions for faster response time. Prices are the same for grounded and exposed junctions. Simply replace "**G**" with "**E**" in model number.

TC-K-NPT-U-72, $39
Pipe Plug Probe With Ungrounded Junction, Stripped Wire Leads and Stainless Steel Overbraid Shown

TC-(*)-NPT-G-72
$34
Grounded Junction Stripped Leads

TC-(*)-NPT-U-72
$39
Ungrounded Junction with Stripped Leads

**Specify calibration: J, K, T or E*
" Other lengths available, consult Sales Department
*For exposed junction, replace **G** with **E** in model number, same price*
*For subminiature connector, add suffix **"-SMP"** and $5 to price*
For stainless steel overbraiding

Ordering Example: *TC-K-NPT-G-72 is a grounded pipe plug probe with stripped leads, **$34***

A12. Flow Meter Specification Sheets

THE FLOW SENSOR THAT MAKES SHORT WORK OF YOUR FLOW MEASUREMENTS

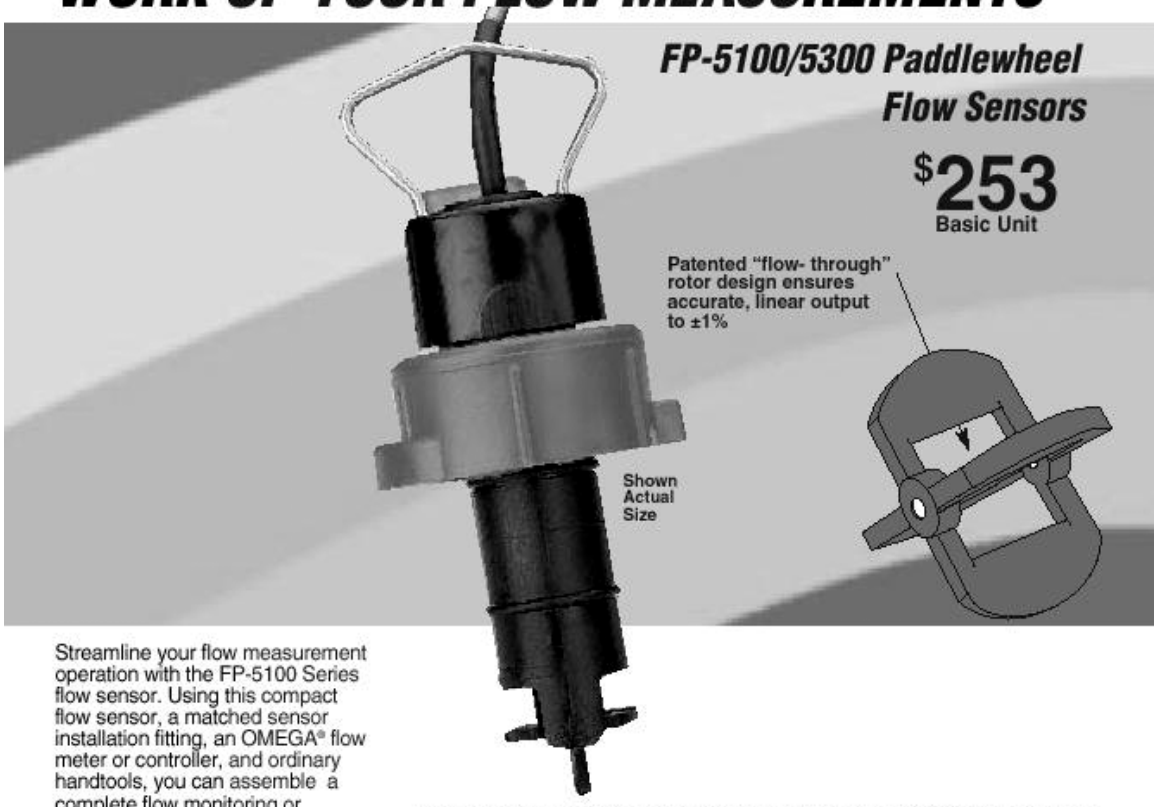

Streamline your flow measurement operation with the FP-5100 Series flow sensor. Using this compact flow sensor, a matched sensor installation fitting, an OMEGA® flow meter or controller, and ordinary handtools, you can assemble a complete flow monitoring or controlling system in minutes. Accurate to ±0.2 fps, with repeatability at ±0.1 fps, this insertion sensor operates on a simple electromechanical principle, proven in thousands of liquid flow applications worldwide. It all adds up to precision, dependability, and convenience–basic advantages that are quickly surpassing its in-line competition.

A TIMESAVER YOU CAN BANK ON

Convert your maintenance hours into minutes with the FP-5300. Should a sensor, rotor, or O-ring need to be replaced, it takes only seconds. Reduce your system downtime substantially with a stand-alone FP-5300 sensor, or simply add a Wet Tap Assembly and eliminate downtime completely. Combined with the FP-5300 during initial installation, the Wet Tap allows sensor removal without system shut-down. Optional local or remote capability lets you place your meter up to 200 feet away without signal amplification, and you can install the FP-5300 in pipe sizes ranging from ½ inch to 36 inches without a lot of additional cost, because the price of the FP-5300 increases only slightly for larger pipe sizes.

RUGGED CONSTRUCTION FOR LONG WEAR

Available in a choice of chemically resistant, non-contaminating housing materials, the FP-5300 stands up to the harshest environments. The glass-filled polypropylene housing version is lightweight but strong, which makes it ideal for handling a wide range of liquids, including corrosive fluids in chemical processing. For processes involving acids and solvents, the PVDF (polyvinylidene fluoride) housing version is a tough fluorocarbon that is highly resistant to more severe fluids. (See page F-25 for more information on OMEGA's all-PVDF flow monitoring systems.)

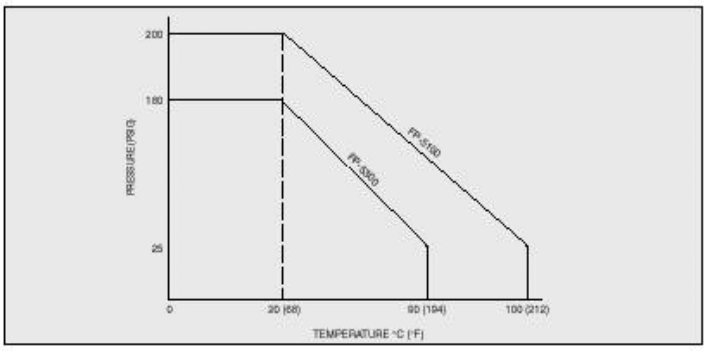

Flow Measurement Simple and Accurate

The sensor works on a simple but precise electromechanical principle based on measuring the rate and volume of flow in your pipe. Four permanent magnets, imbedded in the rotor blades, spin past a coil in the sensor body. As the fluid flow causes the rotor to move, a sine wave signal is produced, directly proportional to the flowrate. The patented "open cell" feature of the rotor ensures a linear, repeatable output, up to 23 fps, with accuracy of ±0.2 fps. The result is minimal head loss and no cavitation.

Replacement rotor/paddlewheel FMK-1538-2, $36.

Replacement titanium rotor pin FMK-1546-1, $7.50.

Replacement PVDF rotor and rotor pin: FMK-51545-1, $46.

Accuracy: 1%Full Scale

SPECIFICATIONS

Accuracy: ±1% full scale
Output Signal: 1 V p-p/fps
Output Frequency: 6 Hz/fps nominal
Flow Rate Range: 1 to 20 fps
Source Impedance: 8 Kohm
Maximum Pressure:
FP-5300 Series: 180 psig max. @ 20°C (68°F)
FP-5100 Series: 200 psig max. @ 20°C (68°F)
Minimum Temperature: 0°C (32°F)
Maximum Temperature:
See page F-24 for complete temperature and pressure rating
Pressure Drop: Equal to 2.5 m (8') of straight pipe
Material: Transducer Housing: glass-filled polypropylene; O-Rings: Viton®; Shaft: Titanium (PVDF opt.); Rotor: PVDF
Maximum % Solids: 1% of fluid volume, non-abrasive, nonmagnetic, <100 micron diameter and length **Standard Cable Length:** 7.5 m (25')
Max. Viscosity: 1 centipoise (water); up to 5 cp above 5 fps velocity

Quick, Easy Conduit Installation

Designed to allow optional conduit installation, the FP-5300 easily lets you comply with local codes requiring conduit protection. For instance, pry off the plug on top of the sensor: underneath, you'll find a ½ inch (F) NPT thread. Using an optional conduit adaptor fitting kit, you can connect your conduit (**FPSP-51589** conduit adaptor kit, **$27**), and an optional instrument back-cover kit will provide everything you need for quick conduit connection to a meter or controller. Additionally, you can adapt to both rigid and flexible liquid-tight conduits, protecting your system hookup from harsh elements and mechanical damage.

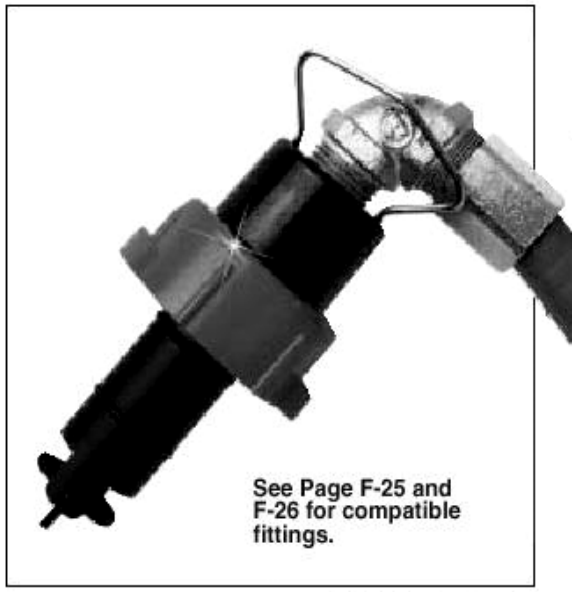

See Page F-25 and F-26 for compatible fittings.

See page F-16 for Flowrates
See pages F-25 and F-26 for Required Fittings

Paddlewheel Flow Sensors ***MOST POPULAR MODELS HIGHLIGHTED!***

To Order *(Specify Model Number)*

Part No.	Housing Material	Shaft Material	Pipe Size (in)	Weight g (oz)	Sensor Length mm (in)	Price	Compatible Meters
FP-5300	Polypro	Titanium	½ to 4	341 (12)	89 (3.50)	**$253**	DPF701, DPF402, DPF70W/ FLSC-AMP, FPM-5500, FPM-5740 FP-85A FPM-9020A
FP-5301	Polypro	Titanium	5 to 8	341 (12)	127 (5.00)	**264**	
FP-5302	Polypro	Titanium	10 or larger	454 (16)	197 (7.75)	**286**	
FP-5100	PVDF	Hastelloy C	½ to 4	341 (12)	89 (3.50)	**453**	
FP-5101	PVDF	Hastelloy C	5 to 8	341 (12)	127 (5.00)	**469**	

*For all-plastic unit with PVDF shaft, add suffix "**-AP**" to **FP-5100** and add **$40** to price. **Ordering Example: FP-5300**, paddlewheel sensor, plus **FP-5310**, 1 inch PVC fitting, $253 + 162 = **$415**. See pages F-25 and F-26 for required fittings.*

Wet Tap Assembly* (see page F-19)

Part No.	Wet Tap Valve Assembly Material	Sensor Housing Material	Shaft Material	Pipe Size (in)	Weight kg (lb)	Sensor Length mm (in)	Price
FP-3193	PVC	Polypro	Titanium	½ to 4	2.4 (5.25)	298 (11.75)	**$764**
FP-3194	PVC	Polypro	Titanium	5 to 8	2.4 (5.25)	330 (13.00)	**800**
FP-3195	PVC	Polypro	Titanium	10 and up	2.4 (5.25)	406 (16.00)	**840**

**Pipe installation fitting not included.*

Wet Tap Max. Operating Temperature/Pressure:
100 psig @ 20°C (68°F); 60°C (140°F) @ 25 psig

A13. Flow Meter Installation Fitting

SENSOR INSTALLATION FITTINGS
For FP-5300, FP-5100, FP8500, FP-5600 and FP-5200 Series

Fittings now supplied without plug. Order part number FMK-31536-1 for polypropylene plug. Price = $42. Order FMK-31536-2 for PVDF plug. Price = $76.

FP-5200 Series Only

☐ ***HIGHLIGHTED MODELS STOCKED FOR FAST DELIVERY!***

Pipe Mat'l	Galvanized Iron		Carbon Steel		Copper/Bronze (Brass)		Metal Sensor	
Pipe Size	Model No.	Price	Model No.	Price	Model No.	Price	Model No.	Price
½"	N/A	–	FP-5305CS	$253	FP-5305CU	$211	FP-5205†	$277
¾"	N/A	–	FP-5307CS	253	FP-5307CU	211	FP-5207†	277
1"	FP-5310GI	$103	FP-5310CS	253	FP-5310CU FP-5310BR	211 108	FP-5210†	277
1¼"	FP-5312GI	103	FP-5312CS	135	FP-5312CU FP-5312BR	108 108	FP-5212	277
1½"	FP-5 315GI	103	FP-5315CS	194	FP-5315CU FP-5315BR	141 130	FP-5215	277
2"	FP-5320GI FP-5320GIS*	103 130	FP-5320CS	248	FP-5320CU FP-5320BR	168 162	FP-5220 FP-5220S*	277 303
2½"	FP-5325GI*	168	FP-5325CS*	130	FP-5325BR*	313	FP-5225 FP-5225S	277 303
3"	FP-5330GI*	168	FP-5330CS*	130	FP-5330BR*	313	FP-5230 FP-5230S*	277 335
4"	FP-5340GI*	168	FP-5340CS*	130	FP-5340BR*	313	FP-5240 FP-5240S*	277 335
5"	FP-5350GI*	226	FP-5350CS*	168	FP-5350BR*	431	FP-5250 FP-5250S*	277 368
6"	FP-5360GI*	238	FP-5360CS*	168	FP-5360BR*	431	FP-5260 FP-5260S*	277 368
8"	FP-5380GI*	248	FP-5380CS*	168	FP-5380BR*	431	FP-5280 FP-5280S*	277 380
10"	FP-5381GI*	469	FP-5381CS*	388	FP-5381BR*	646	FP-5281 FP-5281S*	277 425
12"	FP-5382GI*	469	FP-5382CS*	388	FP-5382BR*	646	FP-5282 FP-5282S*	277 458

**Models with saddle-type fittings (pictured in bottom row)*

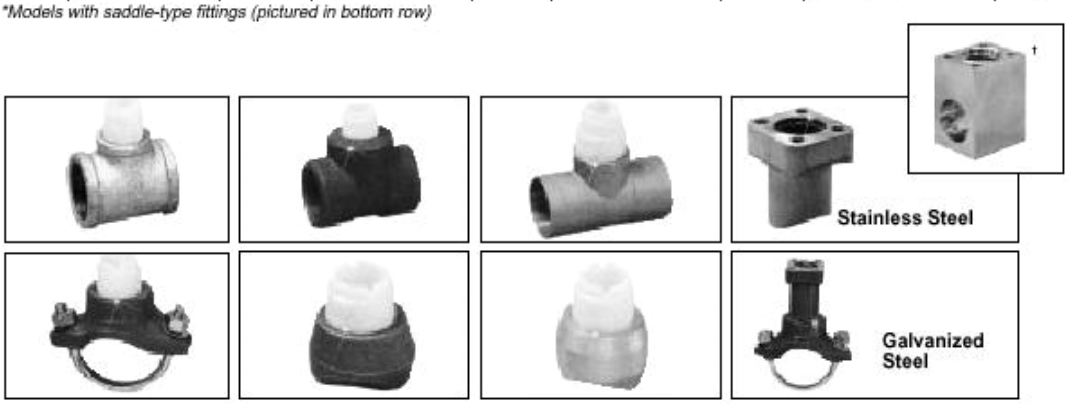

NOTE: All 10" and larger fittings limited to 60°C (140°F) liquid temperature due to PVC Insert.

*All copper fittings **"-CU"** suffix for copper and brass tubing have sweat-on end fittings; brass fittings 2 inches and smaller are NPT threaded tees; above 2 inches, brass fittings are Brazelots.*

*All FP-52XX fittings with suffix **"- S"** are galvanized iron double strap-on; those without suffix **"- S"** are weld-on stainless steel.*

***Note:** Please specify pipe schedule if other than schedule 40 for PVC or iron saddles, and for Weldolets and Brazelots.*

Please contact OMEGA for special fitting requirements not covered in this chart.

A14. Pressure Transducer Specification Sheet

GENERAL PURPOSE 100 MILLIVOLT OUTPUT PRESSURE SENSOR

AVAILABLE IN ABSOLUTE AND GAGE MODELS

PX302 SERIES $180

- Rugged ALL Stainless Steel Construction
- Integral Strain Relief for Cable
- High Sensitivity 10 mV/V Output
- NEMA 3 Enclosure

PX302 Series
0-15 to 0-10,000 psi

Shown with DP41-S Meter and PS-4 Snubber
Meter and Snubber Sold Separately.

SPECIFICATIONS

Excitation: 10 Vdc (5 to 15 Vdc Limits)
Output: 10mV/V 100mV±1mV @ 10V
Accuracy: 0.25% FS (linearity, hysteresis, repeatability)
Zero Balance: ±2 mV
Span Acuracy: ±1%
Long Term Stability: ±0.5% FS
Typical Life: 100 million cycles
Operating Temperature: 0 to 160°F (-18 to 71 °C)
Compensated Temperature: 30 to 160°F (-1 to 71 °C)
Total Thermal Effects: 1% FS max
Proof Pressure: 200%, 13000 PSI max
Input Resistance: 15000Ω maximum
Response Time: 1 msec
Shock: 50 g @ 11msec
Vibration: 15 g 10-2000 Hz
Wetted Parts: 17-4 PH and 300 Series Stainless Steel
Pressure Port: ¼ NPT male
Electrical Conn.: 4 cond, 22 AWG, PVC unshielded, 3 ft pigtail cable
Weight: 4.6 oz (131) to 1000 psi
6.7 oz (190 g) from 1000 psi
Snubbers protect sensors from fluid spikes/hammers!
Dimensions: See previous page

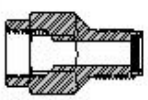

¼ NPT Pressure Snubbers $10
PS-4G = Gas
PS-4E = Lt Oil
PS-4D = Dense Lq

MOST POPULAR MODELS HIGHLIGHTED

To Order *(Specify Model Number)*

RANGE	MODEL NO.	PRICE	COMPATIBLE METERS
GAGE MODELS			
0 to 15 psig	**PX302-015GV**	**$180**	DP41-S, DP2000-S2, DP460-S
0 to 50 psig	**PX302-050GV**	**180**	DP41-S, DP2000-S1, DP460-S
0 to 100 psig	**PX302-100GV**	**180**	DP41-S, DP2000-S2, DP302-S
0 to 200 psig	**PX302-200GV**	**180**	DP41-S, DP2000-S3, DP302-S
0 to 300 psig	**PX302-300GV**	**180**	DP41-S, DP3002-S, DP460-S
0 to 500 psig	**PX302-500GV**	**180**	DP41-S, DP3002-S, DP460-S
0 to 1000 psig	**PX302-1KGV**	**180**	DP41-S, DP2000-S2, DP460-S
0 to 2000 psig	**PX302-2KGV**	**180**	DP41-S, DP2000-S3, DP460-S
0 to 3000 psig	**PX302-3KGV**	**180**	DP41-S, DP3002-S, DP460-S
0 to 5000 psig	**PX302-5KGV**	**180**	DP41-S, DP3002-S, DP460-S
0 to 7500 psig	**PX302-7.5KGV**	**180**	DP41-S, DP3002-S, DP460-S
0 to 10000 psig	**PX302-10KGV**	**180**	DP41-S, DP3002-S, DP460-S
ABSOLUTE MODELS			
0 to 15 psia	**PX302-015AV**	**$180**	DP41-S, DP2000-S2, DP460-S
0 to 50 psia	**PX302-050AV**	**180**	DP41-S, DP302-S1, DP460-S
0 to 100 psia	**PX302-100AV**	**180**	DP41-S, DP2000-S2, DP460-S
0 to 200 psia	**PX302-200AV**	**180**	DP41-S, DP2000-S3, DP460-S
0 to 300 psia	**PX302-300AV**	**180**	DP41-S, DP302-S, DP460-S

Comes with complete operator's manual.

Ordering Example: *PX302-050GV pressure transducer with 50 psig full scale rating and PS-4E pressure snubber for water and light oils, $180 + 10 =* ***$190.***

A15. SCXI-1000 Chassis Data Sheet

SCXI Chassis

SCXI-1000

NI SCXI-1000, NI SCXI-1000DC, NI SCXI-1001

- Shielded enclosures for SCXI modules
- Low-noise environment for signal conditioning
- Rugged, compact chassis
- Forced air cooling
- Optional rack mounting
- NI-DAQ driver software simplifies configuration and measurement
- 3 internal analog buses
- Timing circuitry for high-speed multiplexing
- AC, DC, or battery-power options

Operating Systems
- Windows 2000/NT/XP/Me/9x
- Mac OS

Recommended Software
- LabVIEW
- LabWindows/CVI
- Measurement Studio
- Lookout
- VILogger

Driver Software*
- NI-DAQ
- NI-SWITCH

*included with DAQ device or switch

Overview

National Instruments offers rugged, low-noise SCXI chassis to house, power, and control your SCXI modules and conditioned signals. The unique SCXI chassis architecture includes the SCXIbus, which routes analog and digital signals and acts as the communication conduit between modules. Chassis control circuitry manages this bus, synchronizing the timing between each module and the DAQ device. With this architecture, you can scan input channels from several modules in several chassis at rates up to 333 kS/s for every DAQ device.

The versatility of SCXI lies in its various chassis options and expandability. You can choose from a number of different standard AC or DC power options. You can control the system by connecting directly to an E Series or basic multifunction DAQ device. You can even daisy-chain up to eight chassis for control by a single DAQ device. Regardless of your configuration, programming the system does not change. You use the same function calls you use with a DAQ device by itself. NI-DAQ or NI-SWITCH driver software handles all low-level programming.

The SCXIbus

The SCXIbus is a guarded analog and digital bus located in the backplane of the SCXI chassis. Modules inserted into the chassis connect to this backplane automatically. This bus acts as a conduit for signal routing, transferring data, programming modules, and passing timing signals.

Chassis Control Circuitry

Each SCXI chassis includes control circuitry. This circuitry handles all signal routing on the SCXIbus. During high-speed analog input operations, it controls which input signals are connected to the bus and routed back to the DAQ device. It also ensures tight synchronization between the SCXI modules and the DAQ device.

INFO CODES

For more information, or to order products online visit *ni.com/info* and enter:

scxi1000
scxi1000dc
scxi1001

BUY ONLINE!

Expandability

If your initial system requires more SCXI modules than one chassis can hold, or your system requirements change, simply add another chassis. With the SCXI expandable architecture, you can daisy-chain up to eight chassis to a single multifunction DAQ device. Whether you are using a single-chassis or multichassis system, you can still acquire data at rates up to 333 kS/s.

Power Options

These SCXI chassis offer a number of standard AC power options. Simply choose the option for your country or a country compatible with your power specifications. If you move your system to another country, you can easily reconfigure the system for any of the other AC power configurations.

A16. SCXI-1100 and SCXI-1102C Modules Specification Sheet

SCXI 32-Channel Analog Input Modules

NI SCXI-1100, NI SCXI-1102B/C, NI SCXI-1104/C

- SCXI-1102 is recommended for thermocouple measurements (See page 259)
- 32 analog input channels
- Programmable gain settings
- Lowpass filtering
- NI-DAQ simplifies configuration and measurements

SCXI-1100

- 240 kS/s at full bandwidth, with gain up to 100
- 6.6 kS/s maximum10 kHz filter
- 3 S/s maximum 4 Hz filter

SCXI-1102B, SCXI-1102C

- Programmatic input range from ±100 mV to ±10 V (per channel)
- Per-channel lowpass filter
  - 200 Hz (SCXI-1102B)
  - 10 kHz (SCXI-1102C)

SCXI-1104, SCXI-1104C

- ±60 VDC input range 333 kS/s
- Per-channel lowpass filters
  - 2 Hz (SXCI-1104)
  - 10kHZ (SCXI-1104C)

Operating Systems

- Windows 2000/NT/XP/Me/9x
- Mac OS 9 (see ordering information)

Recommended Software

- LabVIEW
- LabWindows/CVI
- Measurement Studio for Visual Basic
- VI Logger

Driver Software

- NI-DAQ

Calibration Certificate Included
See page 21

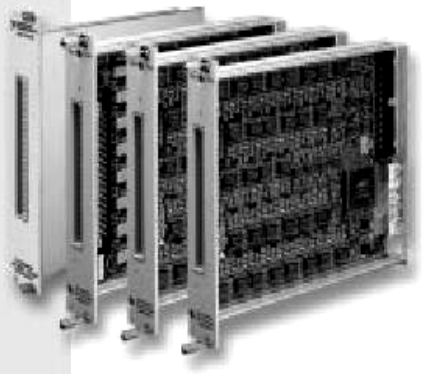

Module	Signal Compatibility		
	±100 mV to ±10 V	±60 V	0-20 mA
SCXI-1100	✔	–	✔
SCXI-1102B	✔	–	✔
SCXI-1102C	✔	–	✔
SCXI-1104	–	✔	–
SCXI-1104C	–	✔	–

Table 1. Module Compatibility

Overview

The National Instruments SCXI-1100, SCXI-1102B/C, and the NI SCXI-1104/C are a variety of 32-channel analog input modules. The programmable gain and filter settings are ideal for conditioning a variety of millivolt, volt, and current inputs. Each module multiplexes the 32 channels into a single channel of the DAQ device, and you can add modules to increase channel count.

Analog Input

SCXI-1100

The SCXI-1102 is an economical solution for millivolt, volt, and currnet outputs. The SCXI-1100 is an economical solution for millivolt, volt, and current inputs. All 32 channels are multiplexed into a single programmable gain instrumentation amplifier (PGIA) and jumper-selectable lowpass filter. Because each module multiplexes the 32 channels into a single channel of the DAQ device, you can add modules to increase channel count. For thermocouple measurements, the SCXI-1102 offers gain and filter settings on a per-channel basis and provides better performance and higher sampling rates.

SCXI-1102B, SCXI-1102C, SCXI-1104, SCXI-1104C

Each analog input channel passes through a PGIA and lowpass filter, before it is multiplexed. With this architecture, you program the input range of each channel independently. Filter settings are preset, and specific to each module (1102B – 200 Hz, 1102C – 10 kHz, 1104 – 2 Hz, 1104C – 10 kHz). You can scan channels at full hardware rate (up to 3 µs per channel) at any gain setting. Each channel includes input protection circuitry for up to ±42 V for the SCXI-1102B/C, and ±60 V for the SCXI-1104/C.

INFO CODES
For more information or to order products online, visit *ni.com/info* and enter:

scxi1100
scxi1102b
scxi1102c
scxi1104
scxi1104c

BUY ONLINE!

A17. SCXI-1100 and SCXI-1102C Modules Schematics

SCXI 32-Channel Analog Input Modules

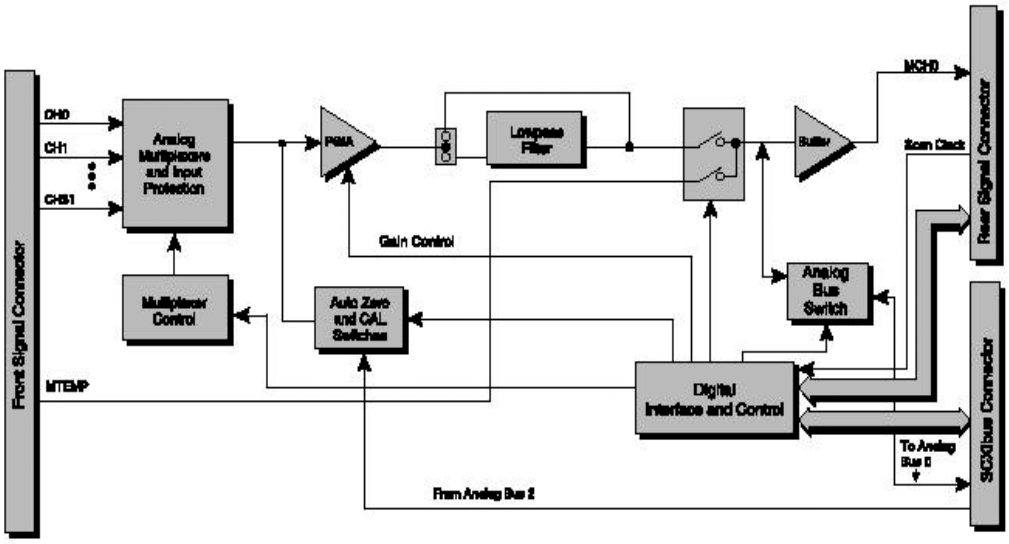

Figure 1. SCXI-1100 Block Diagram

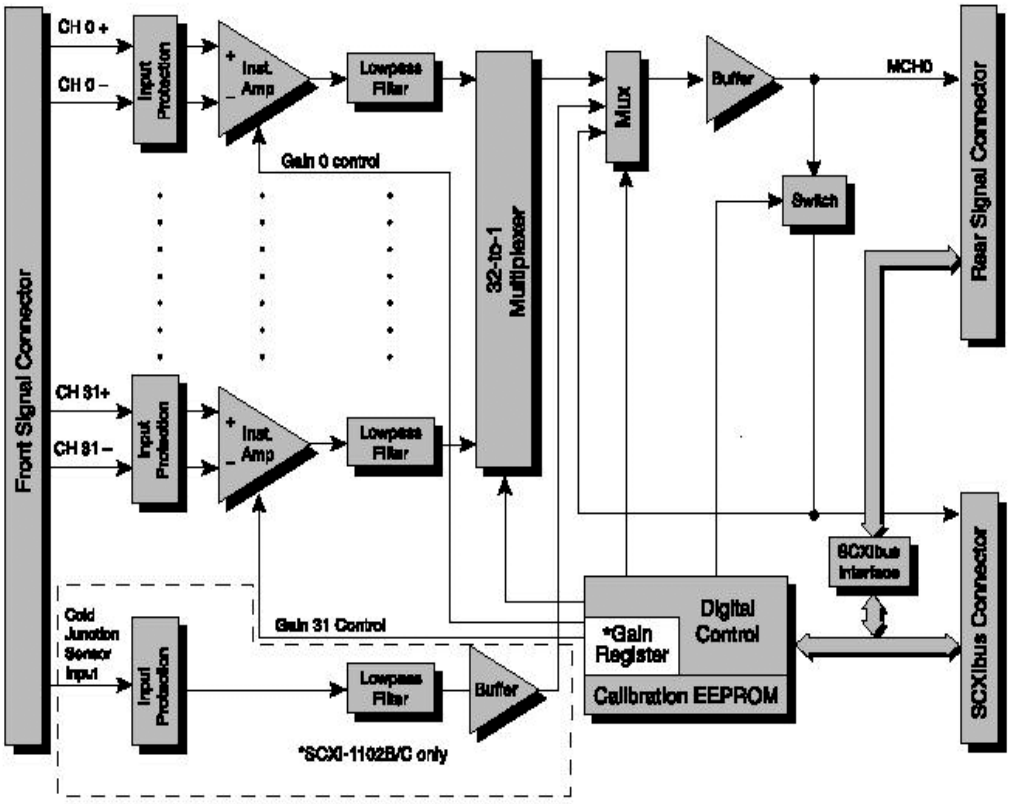

A18. SCXI-1163R Module Specification Sheets

32-Channel Solid-State Relay

NI SCXI-1163R

- 32 optically isolated solid-state relays
- Relays arranged in 8 banks of 4x1 multiplexers
- 750 operations/s
- 200 mA at 240 VDC/V_{rms} capacity
- Fully software programmable

Operating Systems
- Windows 2000/NT/XP/Me/9x

Recommended Software
- LabVIEW
- LabWindows/CVI
- Measurement Studio for Visual C++
- NI Switch Executive

Other Compatible Software
- Visual Basic
- C/C++

Driver Software (included)
- NI-SWITCH

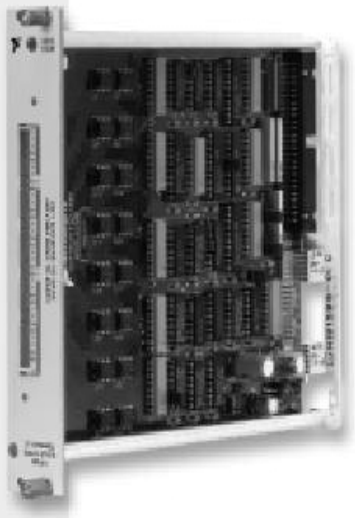

Module	Function	Description	Switching Specifications
SCXI-1163R	Multiplexer	8 banks of 4x1 SSR multiplexer	240 VAC/ VDC

Table 1. SCXI-1163R Switch Specifications

Overview

The National Instruments SCXI-1163R includes 32 normally open, or Form A, optically isolated solid-state relays, arranged into eight banks of four relays with one common pole for each bank. You can use the NI SCXI-1163R to switch high-voltage loads, up to 240 VAC/VDC and up to 200 mA.

The SCXI-1163R is programmed serially over the SCXIbus. You can therefore easily integrate SCXI-1163R modules into existing SCXI systems without additional DAQ devices or cabling. The modules can also operate in parallel mode when cabled directly to a plug-in DIO device.

Applications

You can use an SCXI system equipped with the SCXI-1163R in a variety of industrial and laboratory applications. The SCXI-1163R safely isolates the computer from large common-mode voltages, ground loops, and voltage spikes that often occur in industrial and research environments. You can use the solid-state relay channels to switch a wide range of AC and DC voltage and power signals to control field devices.

SCXI Relay Control

Every SCXI switch system requires an external switch controller. The switch controller uses the digital communications bus on the SCXI chassis to control the switch circuitry. The NI PXI-4070 FlexDMM and NI 4021 switch controller are common examples of SCXI switch controllers. Refer to page 507 for more information on choosing the correct switch controller.

INFO CODES
For more information, or to order products online visit *ni.com/info* and enter:

scxi1163r

BUY ONLINE!

Ordering Information

NI SCXI-1163R 776572-63R
Includes switch module and NI-SWITCH driver software.

Accessories

SCXI-1326 terminal block 777687-26
PCI- 4021 switch controller 778277-01
PXI- 4021 switch controller 778278-01

For information on extended warranty and value added services, see page 16.

See page 507 for accessory and cable information.

32-Channel Solid-State Relay

Signal Connection

Field digital signals connect to screw terminals located in the SCXI-1326 terminal block, which plugs directly into the front of the SCXI module, or the TBX-1326, a DIN-rail mountable terminal block that you connect to the SCXI-1163R using the SH48-48-B shielded cable.

Software

All National Instruments PXI and SCXI switch modules are shipped with NI-SWITCH, an IVI-compliant driver offering complete functionality for all switch modules. For additional assistance in configuring, programming, and managing higher channel count switching systems, NI Switch Executive software offers an easy-to-use intelligent switch management and visual routing environment. See page 112 to learn more about the features of NI Switch Executive.

Specifications

Typical for 25 °C unless otherwise stated.

Input Characteristics

Number of relays	32 organized as 8 optically isolated banks of 4 relays each
Relay type	Normally open (Form A), solid-state relays
Maximum switching voltage	
AC	240 VAC
DC	240 VDC
Maximum switching capacity	200 mA
Commonmode isolation	250 V_{rms} between banks, and bank to ground
On resistance	6 Ω
Output capacitance	110 pF at 50 V, 1 MHz
Leakage current	1 µA maximum
Transfer rate in serial mode[1]	
(1 word = 32 bits)	750 words/s
Relay set time	0.6 ms
Relay reset time	0.1 ms
Power-on state	Relays open

Physical

Dimensions	17.2 by 20.3 by 3.0 cm (6.8 by 8.0 by 1.2 in.)

Environment

Operating temperature	0 to 50 °C
Storage temperature	-20 to 70 °C
Relative humidity	5 to 90% noncondensing

[1]Transfer rate depends largely on the computer and software. These tests were made using an AT-MIO-16E-2 installed in a 450 MHz Pentium III computer running LabVIEW and Windows NT.

APPENDIX B

DETAILED CALCULATIONS

B1. Test Section Pressure Drop Calculations

Inside tube geometries to be tested:

$$\text{TubeGeometries} := \begin{pmatrix} .616 & .015 & 25 & 10 \\ .615 & .015 & 25 & 30 \\ .615 & .015 & 48 & 30 \\ .613 & .015 & 25 & 45 \\ .614 & .012 & 35 & 45 \\ .613 & .015 & 35 & 45 \\ .614 & .020 & 35 & 45 \\ .613 & .015 & 48 & 45 \end{pmatrix}$$

Inside diameter:

$$D_i := \text{TubeGeometries}^{\langle 0 \rangle} \cdot \text{in}$$

Fin height:

$$e := \text{TubeGeometries}^{\langle 1 \rangle} \cdot \text{in}$$

Helix angle:

$$\alpha := \text{TubeGeometries}^{\langle 2 \rangle}$$

Number of starts:

$$n_s := \text{TubeGeometries}^{\langle 3 \rangle}$$

Physical properties of water: assumed temperature of 70 F

$$\mu := .578 \cdot 10^{-3} \cdot \frac{\text{lb}}{\text{ft} \cdot \text{s}}$$

$$\rho := 62.4 \cdot \frac{\text{lb}}{\text{ft}^3}$$

Water velocities to be tested

$$v_{high} := 8 \cdot \frac{\text{ft}}{\text{s}}$$

$$v_{average} := 5 \cdot \frac{ft}{s}$$

$$v_{low} := 2 \cdot \frac{ft}{s}$$

Cross sectional area of the tube:

$$A_c := \overrightarrow{\frac{\pi \cdot D_i^2}{4}}$$

Mass flow rates of water:

$$m_{dothigh} := v_{high} \cdot \rho \cdot A_c$$

$$m_{dotavg} := v_{average} \cdot \rho \cdot A_c$$

$$m_{dotlow} := v_{low} \cdot \rho \cdot A_c$$

Mass velocities for given flows:

$$G_{high} := \overrightarrow{\frac{m_{dothigh}}{A_c}}$$

$$G_{avg} := \overrightarrow{\frac{m_{dotavg}}{A_c}}$$

$$G_{low} := \overrightarrow{\frac{m_{dotlow}}{A_c}}$$

Reynolds numbers for given flow velocities:

$$Re_{high} := \overrightarrow{\frac{D_i \cdot G_{high}}{\mu}}$$

$$Re_{avg} := \overrightarrow{\frac{D_i \cdot G_{avg}}{\mu}}$$

$$Re_{low} := \overrightarrow{\frac{D_i \cdot G_{low}}{\mu}}$$

Friction factors for each tube geometry at the given flow velocities:

$$f_{high} := \left[\overrightarrow{.108 \cdot Re_{high}^{-.283} \cdot n_s^{.221} \cdot \left(\frac{e}{D_i} \right)^{.785} \cdot \alpha^{.78}} \right]$$

$$f_{high} = \begin{pmatrix} 5.797 \times 10^{-3} \\ 7.403 \times 10^{-3} \\ 0.012 \\ 8.125 \times 10^{-3} \\ 8.851 \times 10^{-3} \\ 0.011 \\ 0.013 \\ 0.014 \end{pmatrix}$$

$$f_{avg} := \left[\overrightarrow{.108 \cdot Re_{avg}^{-.283} \cdot n_s^{.221} \cdot \left(\frac{e}{D_i} \right)^{.785} \cdot \alpha^{.78}} \right]$$

$$f_{avg} = \begin{pmatrix} 6.622 \times 10^{-3} \\ 8.456 \times 10^{-3} \\ 0.014 \\ 9.281 \times 10^{-3} \\ 0.01 \\ 0.012 \\ 0.015 \\ 0.015 \end{pmatrix}$$

$$f_{low} := \left[\overrightarrow{.108 \cdot Re_{low}^{-.283} \cdot n_s^{.221} \cdot \left(\frac{e}{D_i} \right)^{.785} \cdot \alpha^{.78}} \right]$$

$$f_{low} = \begin{pmatrix} 8.582 \times 10^{-3} \\ 0.011 \\ 0.018 \\ 0.012 \\ 0.013 \\ 0.016 \\ 0.02 \\ 0.02 \end{pmatrix}$$

Calculations for High Test Tube Water Velocity.

Entrance head loss:

For a tee, used as an elbow entering the branch

$K_i := 1.5$

$H_i := K_i \cdot \frac{v_{high}^2}{2}$

$H_i = 1.492 \frac{lbf \cdot ft}{lb}$

Head loss due to globe valve upstream of the test section:

Globe valve half Open

$K_{gv} := 4.5$

$H_{gv} := K_{gv} \cdot \frac{v_{high}^2}{2}$

$H_{gv} = 4.476 ft \cdot \frac{lbf}{lb}$

Head loss due to union:

$K_u := .04$

$H_u := K_u \cdot \frac{v_{high}^2}{2}$

$$H_u = 0.04 \frac{ft \cdot lbf}{lb}$$

Head loss due to friction over the test section:

Length of the test section:

$$L := 10 \cdot ft$$

$$H_{TS} := \overrightarrow{\left(4 \cdot f_{high} \cdot \frac{L}{D_i} \cdot \frac{v_{high}^2}{2} \right)}$$

$$H_{TS} = \begin{pmatrix} 4.493 \\ 5.747 \\ 9.558 \\ 6.328 \\ 6.882 \\ 8.227 \\ 10.276 \\ 10.525 \end{pmatrix} ft \cdot \frac{lbf}{lb}$$

Head loss from flow meter:

For a rotary-type flow meter with a star-shaped disk

$$K_{fm} := 10$$

$$H_{fm} := K_{fm} \cdot \frac{v_{high}^2}{2}$$

$$H_{fm} = 9.946 ft \cdot \frac{lbf}{lb}$$

Head loss over thermocouple mounting:

For a tee with the branch blanked off

$$K_{th} := .4$$

$$H_{th} := K_{th} \cdot \frac{v_{high}^2}{2}$$

$$H_{th} = 0.398\text{ft}\cdot\frac{\text{lbf}}{\text{lb}}$$

Head loss through downstream globe valve:

Fully-open globe valve

$$K_{GVO} := .17$$

$$H_{GVO} := K_{GVO}\cdot\frac{v_{high}^{2}}{2}$$

$$H_{GVO} = 0.169\text{ft}\cdot\frac{\text{lbf}}{\text{lb}}$$

Head loss at exit (tee branching flow):

$$K_{exit} := 1$$

$$H_{exit} := K_{exit}\cdot\frac{v_{high}^{2}}{2}$$

$$H_{exit} = 0.995\text{ft}\cdot\frac{\text{lbf}}{\text{lb}}$$

Head loss for connecting tubing:

Relative roughness for drawn tubing

$$\varepsilon := .000005\cdot\text{ft}$$

$$f := \frac{.25}{\left(\log\left(\frac{\varepsilon}{3.7\cdot D_i} + \frac{5.74}{Re_{high}^{.9}}\right)\right)^{2}}$$

Approximate total length of tubing connecting the instruments

$$L_{ct} := 1.5\cdot\text{ft}$$

$$H_{ct} := \left(f\cdot\frac{L_{ct}}{D_i}\cdot\frac{v_{high}^{2}}{2}\right)$$

Total head loss:

$$H_{Total} := \overrightarrow{\left(H_i + H_{gv} + H_u + H_{TS} + H_u + H_{fm} + H_{th} + H_{GVO} + H_{ct} + H_{exit}\right)}$$

$$H_{Total} = \begin{pmatrix} 22.678 \\ 23.933 \\ 27.745 \\ 24.517 \\ 25.069 \\ 26.416 \\ 28.464 \\ 28.714 \end{pmatrix} ft \cdot \frac{lbf}{lb}$$

Calculations for Average Test Tube Water Velocity.

Entrance head loss:

For a tee, used as an elbow entering the branch

$$K_i := 1.5$$

$$H_i := K_i \cdot \frac{v_{average}^2}{2 \cdot g}$$

$$H_i = 0.583 ft$$

Head loss due to globe valve upstream of the test section:

Globe valve half open

$$K_{gv} := 4.5$$

$$H_{gv} := K_{gv} \cdot \frac{v_{average}^2}{2 \cdot g}$$

$$H_{gv} = 1.748 \text{ ft}$$

Head loss due to union:

$$K_u := .04$$

$$H_u := K_u \cdot \frac{v_{average}^2}{2 \cdot g}$$

$$H_u = 0.016 \text{ ft}$$

Head loss due to friction over the test section:

Length of the test section

$$L = 10 \text{ ft}$$

$$H_{TS} := \overrightarrow{\left(4 \cdot f_{avg} \cdot \frac{L}{D_i} \cdot \frac{v_{average}^2}{2 \cdot g} \right)}$$

$$H_{TS} = \begin{pmatrix} 2.005 \\ 2.564 \\ 4.265 \\ 2.823 \\ 3.071 \\ 3.671 \\ 4.585 \\ 4.696 \end{pmatrix} \text{ ft}$$

Head loss from flow meter:

For a rotary-type flow meter with a star-shaped disk

$$K_{fm} := 10$$

$$H_{fm} := K_{fm} \cdot \frac{v_{average}^2}{2 \cdot g}$$

$$H_{fm} = 3.885 \text{ ft}$$

Head loss over thermocouple mounting:

For a tee with the branch blanked off

$$K_{th} := .4$$

$$H_{th} := K_{th} \cdot \frac{v_{average}^{2}}{2 \cdot g}$$

$$H_{th} = 0.155 \text{ ft}$$

Head loss through downstream globe valve:

Fully-open globe valve

$$K_{GVO} := .17$$

$$H_{GVO} := K_{GVO} \cdot \frac{v_{average}^{2}}{2 \cdot g}$$

$$H_{GVO} = 0.066 \text{ ft}$$

Head loss at exit:

$$K_{exit} := 1$$

$$H_{exit} := K_{exit} \cdot \frac{v_{average}^{2}}{2 \cdot g}$$

$$H_{exit} = 0.389 \text{ ft}$$

Head loss for connecting tubing:

Relative roughness for drawn tubing

$$\varepsilon := .000005 \cdot \text{ft}$$

$$f := \frac{\overrightarrow{\qquad\qquad\qquad\qquad}}{\left(\log\left(\frac{\varepsilon}{3.7 \cdot D_i} + \frac{5.74}{Re_{avg}^{.9}} \right) \right)^{2}}$$

Approximate total length of tubing connecting the instruments

$$L_{ct} := 1.5 \cdot \text{ft}$$

$$H_{ct} := \overrightarrow{\left(f \cdot \frac{L_{ct}}{D_i} \cdot \frac{v_{average}^{2}}{2 \cdot g} \right)}$$

Total head loss:

$$H_{Total} := \overrightarrow{(H_i + H_{gv} + H_u + H_{TS} + H_u + H_{fm} + H_{th} + H_{GVO} + H_{ct} + H_{exit})}$$

$$H_{Total} = \begin{pmatrix} 9.136 \\ 9.696 \\ 11.396 \\ 9.956 \\ 10.203 \\ 10.803 \\ 11.717 \\ 11.829 \end{pmatrix} \text{ ft}$$

Calculations for Low Test Tube Water Velocity.

Entrance head loss:

For a tee, used as an elbow entering the branch

$K_i := 1.5$

$$H_i := K_i \cdot \frac{v_{low}^{2}}{2 \cdot g}$$

$H_i = 0.093$ ft

Head loss due to globe valve upstream of the test section:

Globe valve half open

$K_{gv} := 4.5$

$$H_{gv} := K_{gv} \cdot \frac{v_{low}^{2}}{2 \cdot g}$$

$H_{gv} = 0.28$ ft

Head loss due to union:

$K_u := .04$

$H_u := K_u \cdot \frac{v_{low}^2}{2 \cdot g}$

$H_u = 2.486 \times 10^{-3}\ ft$

Head loss due to friction over the test section:

Length of the test section

$L = 10\ ft$

$H_{TS} := \overrightarrow{\left(4 \cdot f_{low} \cdot \frac{L}{D_i} \cdot \frac{v_{low}^2}{2 \cdot g} \right)}$

$$H_{TS} = \begin{pmatrix} 0.416 \\ 0.532 \\ 0.884 \\ 0.585 \\ 0.637 \\ 0.761 \\ 0.951 \\ 0.974 \end{pmatrix} ft$$

Head loss from flow meter:

For a rotary-type flow meter with a star-shaped disk

$K_{fm} := 10$

$H_{fm} := K_{fm} \cdot \frac{v_{low}^2}{2 \cdot g}$

$H_{fm} = 0.622\ ft$

Head loss over thermocouple mounting:

For a tee with the branch blanked off

$K_{th} := .4$

$H_{th} := K_{th} \cdot \frac{(v_{low})^2}{2 \cdot g}$

$H_{th} = 0.025 \text{ ft}$

Head loss through downstream globe valve:

$K_{GVO} := .17$

Fully-open globe valve

$H_{GVO} := K_{GVO} \cdot \frac{v_{low}^2}{2 \cdot g}$

$H_{GVO} = 0.011 \text{ ft}$

Head loss at exit:

$K_{exit} := 1$

$H_{exit} := K_{exit} \cdot \frac{v_{low}^2}{2 \cdot g}$

$H_{exit} = 0.062 \text{ ft}$

Head loss for connecting tubing:

Relative roughness for drawn tubing

$\varepsilon := .000005 \cdot \text{ft}$

$$f := \frac{\overrightarrow{.25}}{\left(\log\left(\frac{\varepsilon}{3.7 \cdot D_i} + \frac{5.74}{Re_{low}^{.9}} \right) \right)^2}$$

Approximate total length of tubing connecting the instruments

$$L_{ct} := 1.5 \cdot ft$$

$$H_{ct} := \overrightarrow{\left(f \cdot \frac{L_{ct}}{D_i} \cdot \frac{v_{low}^{2}}{2 \cdot g} \right)}$$

Total head loss:

$$H_{Total} := \overrightarrow{(H_i + H_{gv} + H_u + H_{TS} + H_u + H_{fm} + H_{th} + H_{GVO} + H_{ct} + H_{exit})}$$

$$H_{Total} = \begin{pmatrix} 1.568 \\ 1.684 \\ 2.037 \\ 1.738 \\ 1.789 \\ 1.914 \\ 2.103 \\ 2.126 \end{pmatrix} ft$$

B2. Apparatus Pressure Drop Calculations

Calculation for a Water Test Velocity of 2 ft/s

Constants

P1(lb/ft^2)	2117.664				initial pressure
P2(lb/ft^2)	2116.8				final pressure
V1(ft/s)	0				initial velocity
V2(ft/s)	0				final velocity
Z1(ft)	2				initial elevation
z2(ft)	5				final elevation
Q(ft^3/s)	0.036771	=	16.5039	gpm	flow rate
rho(lb/ft^3)	62.2				density
mu(lb/ft*s)	0.000578				viscosity
Gc	32.174				

Piping and HX Pressure Drop

	Di(ft)	L(ft)	eps(ft)	K	V(ft/s)	Re	f	H(ft)	dP(psi)
1.375 in Tubing	0.105417	75	5E-06	26.95	4.21303	4.779E+04	0.0212	11.587	5.00495
Heat Exchanger 4 Pipes in Parallel	0.065417	23.5	5E-06	2	2.73512	1.925E+04	0.0262	1.32879	0.573964
								12.9158	5.578914

Loss Coefficients Applied

Description	K	Amount	Total
Elbow	0.75	11	8.25
Tee, Branch Closed	0.4	1	0.4
Tee	1	2	2
Globe valve	6.4	2	12.8
Sudden Enlargement	1	1	1
Sudden Contraction	1	1	1
Entrance	0.5	1	0.5
Exit	1	1	1
			26.95

Continued

Manifold Pressure Drop (2.625 in tubing)

	D(ft)	Q(ft^3/s)	V(ft/s)	Re	f	H(ft)	dP(psi)
Section 1	0.205417	0.032685	0.98625	2.180E+04	0.02533	0.0188439	0.0081
Section 2	0.205417	0.028599	0.86297	1.908E+04	0.02618	0.0145237	0.0063
Section 3	0.205417	0.024514	0.73969	1.635E+04	0.02723	0.0107569	0.0046
Section 4	0.205417	0.020428	0.61641	1.363E+04	0.02855	0.0075458	0.0033
Section 5	0.205417	0.016343	0.49313	1.090E+04	0.03029	0.0048937	0.0021
Section 6	0.205417	0.012257	0.36985	8.176E+03	0.0328	0.0028046	0.0012
Section 7	0.205417	0.008171	0.24656	5.450E+03	0.0369	0.0012842	0.0006
Section 8	0.205417	0.004086	0.12328	2.725E+03	0.04596	0.0003419	0.0001
						0.0609947	0.0263
Test Section Pressure Drop (Calculated by Ian Tubman)						(ft)	(psi)
Maximum at 2 ft/s						2.126	0.9183
						(ft)	(psi)
Total Pressure Drop:						15.10	6.5236

W/m	18.08892	lbf*ft/lbm			
Power	41.37193	lbf*ft/s	=	0.07522168	hp

Calculation for a Water Test Velocity of 5 ft/s

Constants

P1(lb/ft^2)	2117.664				initial pressure
P2(lb/ft^2)	2116.8				final pressure
V1(ft/s)	0				initial velocity
V2(ft/s)	0				final velocity
z1(ft)	2				initial elevation
z2(ft)	5				final elevation
Q(ft^3/s)	0.091927	=	41.2597	gpm	flow rate
rho(lb/ft^3)	62.2				density
mu(lb/ft*s)	0.000578				viscosity
Gc	32.174				

Piping and HX Pressure Drop

	Di(ft)	L(ft)	eps(ft)	K	V(ft/s)	Re	f	H(ft)	dP(psi)
1.375 in Tubing	0.105417	75	5E-06	26.95	10.5326	1.195E+05	0.0175	67.9666	29.3578
Heat Exchanger 4 Pipes in Parallel	0.065417	23.5	5E-06	2	6.83779	4.814E+04	0.0212	6.99841	3.022923
							Total	74.965	32.38072

Loss Coefficients Applied

Description	K	Amount	Total
Elbow	0.75	11	8.25
Tee, Branch Closed	0.4	1	0.4
Tee	1	2	2
Globe Valve	6.4	2	12.8
Sudden Enlargement	1	1	1
Sudden Contraction	1	1	1
Entrance	0.5	1	0.5
Exit	1	1	1
			26.95

Continued

Manifold Pressure Drop (2.625 in tubing)

	D(ft)	Q(ft^3/s)	V(ft/s)	Re	f	H(ft)	dP(psi)
Section 1	0.205417	0.081713	2.46564	5.450E+04	0.02047	0.1133041	0.0489
Section 2	0.205417	0.071499	2.15743	4.769E+04	0.02108	0.0871801	0.0377
Section 3	0.205417	0.061285	1.84923	4.088E+04	0.02183	0.0644358	0.0278
Section 4	0.205417	0.051071	1.54102	3.406E+04	0.02276	0.0450829	0.0195
Section 5	0.205417	0.040856	1.23282	2.725E+04	0.02399	0.0291361	0.0126
Section 6	0.205417	0.030642	0.92461	2.044E+04	0.02574	0.0166148	0.0072
Section 7	0.205417	0.020428	0.61641	1.363E+04	0.02855	0.0075458	0.0033
Section 8	0.205417	0.010214	0.3082	6.813E+03	0.03456	0.0019729	0.0009
					Total	0.3652725	0.1578
Test Section Pressure Drop (Calculated by Ian Tubman)						(ft)	(psi)
Maximum at 5 ft/s						11.829	5.1095
						(ft)	(psi)
Total Pressure Drop:						87.16	37.648

W/m	90.14541	lbf*ft/lbm			
Power	515.4383	lbf*ft/s	=	0.93716063	hp

Calculation for a Water Test Velocity of 8 ft/s

Constants

P1(lb/ft^2)	2117.664				initial pressure
P2(lb/ft^2)	2116.8				final pressure
V1(ft/s)	0				initial velocity
V2(ft/s)	0				final velocity
z1(ft)	2				initial elevation
z2(ft)	5				final elevation
Q(ft^3/s)	0.147083	=	66.0155	gpm	flow rate
rho(lb/ft^3)	62.2				density
mu(lb/ft*s)	0.000578				viscosity
Gc	32.174				

Piping and HX Pressure Drop

	Di(ft)	L(ft)	eps(ft)	K	V(ft/s)	Re	f	H(ft)	dP(psi)
1.375 in Tubing	0.105417	75	5E-06	26.95	16.8521	1.912E+05	0.0161	169.442	73.18935
Heat Exchanger 4 Pipes in Parallel	0.065417	23.5	5E-06	2	10.9405	7.702E+04	0.0193	16.5987	7.169716
								186.04	80.35906

Loss Coefficients Applied

Description	K	Amount	Total
Elbow	0.75	11	8.25
Tee, Branch Closed	0.4	1	0.4
Tee	1	2	2
Globe Valve	6.4	2	12.8
Sudden Enlargement	1	1	1
Sudden Contraction	1	1	1
Entrance	0.5	1	0.5
Exit	1	1	1
			26.95

Continued

Manifold Pressure Drop (2.625 in tubing)

	D(ft)	Q(ft^3/s)	V(ft/s)	Re	f	H(ft)	dP(psi)
Section 1	0.205417	0.130741	3.94502	8.721E+04	0.01852	0.2854754	0.1233
Section 2	0.205417	0.114398	3.45189	7.631E+04	0.01904	0.2195075	0.0948
Section 3	0.205417	0.098055	2.95876	6.540E+04	0.01968	0.1621084	0.07
Section 4	0.205417	0.081713	2.46564	5.450E+04	0.02047	0.1133041	0.0489
Section 5	0.205417	0.06537	1.97251	4.360E+04	0.02151	0.0731273	0.0316
Section 6	0.205417	0.049028	1.47938	3.270E+04	0.02298	0.0416205	0.018
Section 7	0.205417	0.032685	0.98625	2.180E+04	0.02533	0.0188439	0.0081
Section 8	0.205417	0.016343	0.49313	1.090E+04	0.03029	0.0048937	0.0021
						0.9188808	0.3969
Test Section Pressure Drop						(ft)	(psi)
Maximum at 8 ft/s						28.76	12.423
						(ft)	(psi)
Total Pressure Drop:						215.72	93.179

W/m	218.7053	lbf*ft/lbm			
Power	2000.84	lbf*ft/s	=	3.63789085	hp

B3. Calculations of Refrigerant Heat Loads

Fluid properties and tank dimensions:

Outside diameter:

$OD_{tank} := 8.625\ in$

Tank thickness:

$t_{tank} := 0.188\ in$

Tank height:

$h_{tank} := 18\,in$

Internal Diameter

$ID_{tank} := OD_{tank} - t_{tank}$

Specific volume of R-134a saturated liquid:

$v_{fR134a} := 0.0136 \frac{ft^3}{lb}$

Specific internal energy of R-134a saturated liquid:

$u_{fR134a} := 40.61 \frac{BTU}{lb}$

Specific internal energy of R-134a saturated vapor:

$u_{gR134a} := 105.6 \frac{BTU}{lb}$

Density of water

$\rho_{H2O} := 62.4 \frac{lb}{ft^3}$

Specific heat of water

$$c_{pH2O} := 4181 \frac{J}{kg \cdot K}$$

Volume of the tank:

$$V_{tank} := \pi \cdot \left(\frac{ID_{tank}}{2} \right)^2 \cdot h_{tank}$$

$$V_{tank} = 4.356 \text{ gal}$$

Mass of the refrigerant contained in the tank:

$$M_{R134a} := \frac{V_{tank}}{v_{fR134a}}$$

$$M_{R134a} = 42.821 \text{ lb}$$

Water inlet and outlet temperatures:

$$T_{H2Oin} := (70 + 460)R$$

$$T_{H2Oout} := T_{H2Oin} + 3R$$

Water velocity and mass flowrate:

$$velocity_{H2O} := \begin{pmatrix} 2 \\ 5 \\ 8 \end{pmatrix} \frac{ft}{s}$$

Cross-sectional area of the tube:

$$Ac_{tube} := \pi \cdot \left(\frac{0.614 \text{ in}}{2} \right)^2$$

Mass flow rate of water:

$$mdot_{H2O} := Ac_{tube} \cdot \rho_{H2O} \cdot velocity_{H2O}$$

$$mdot_{H2O} = \begin{pmatrix} 0.257 \\ 0.642 \\ 1.026 \end{pmatrix} \frac{lb}{s}$$

Heat load:

$$Qdot := mdot_{H2O} \cdot c_{pH2O} \cdot \left(T_{H2Oout} - T_{H2Oin}\right)$$

$$Qdot = \begin{pmatrix} 811.1 \\ 2027.7 \\ 3244.4 \end{pmatrix} W$$

Energy required to boil the refrigerant:

$$U_{fgR134a} := M_{R134a} \cdot \left(u_{gR134a} - u_{fR134a}\right)$$

$$U_{fgR134a} = 2.936 \times 10^{6} J$$

Refrigerant boiling time required:

$$Boiling\_time := \frac{U_{fgR134a}}{Qdot}$$

$$Boiling\_time = \begin{pmatrix} 60.333 \\ 24.133 \\ 15.083 \end{pmatrix} min$$

B4. Flow Meter Calibration Curve

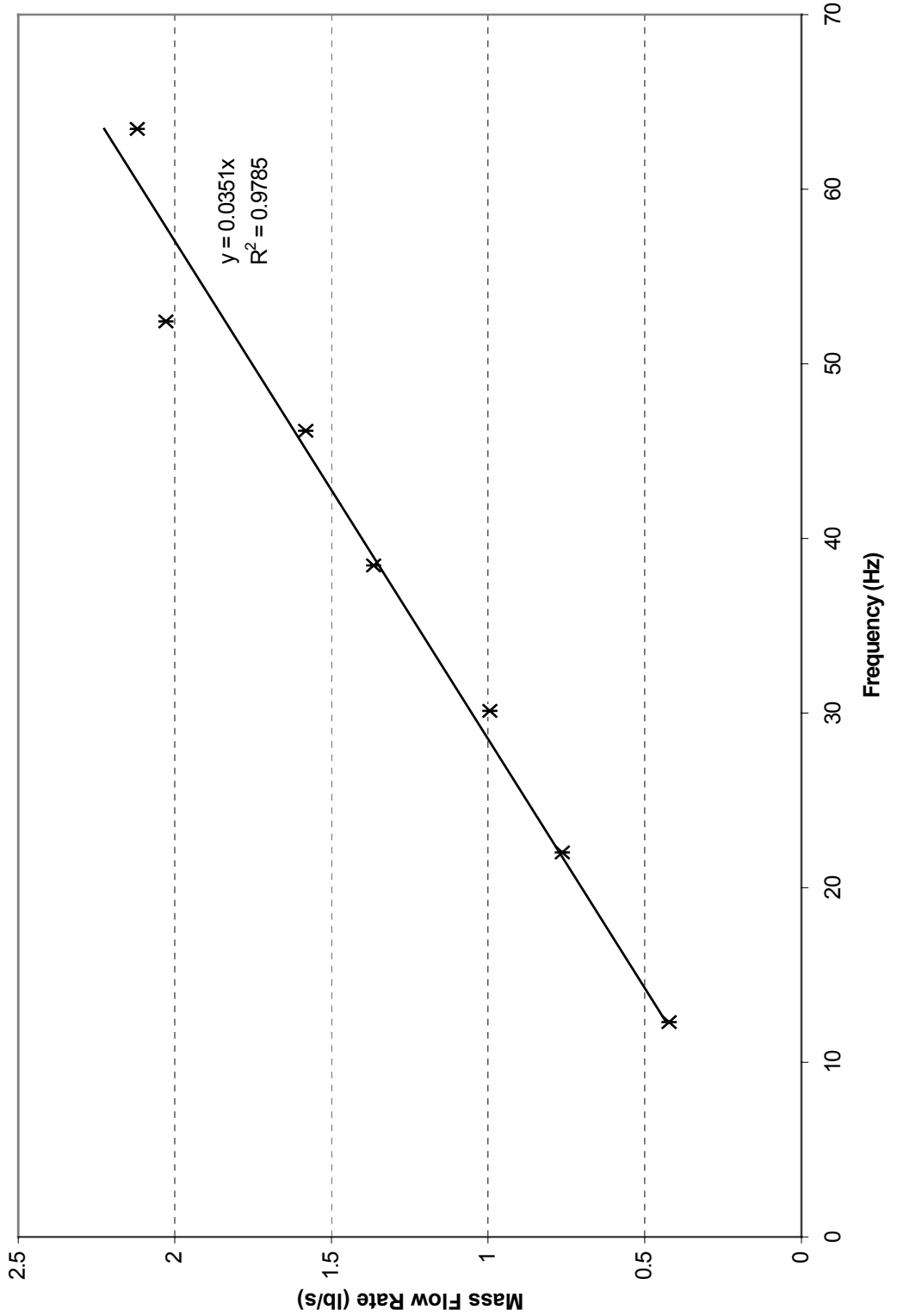

B5. Pressure Transducer Calibration Curve

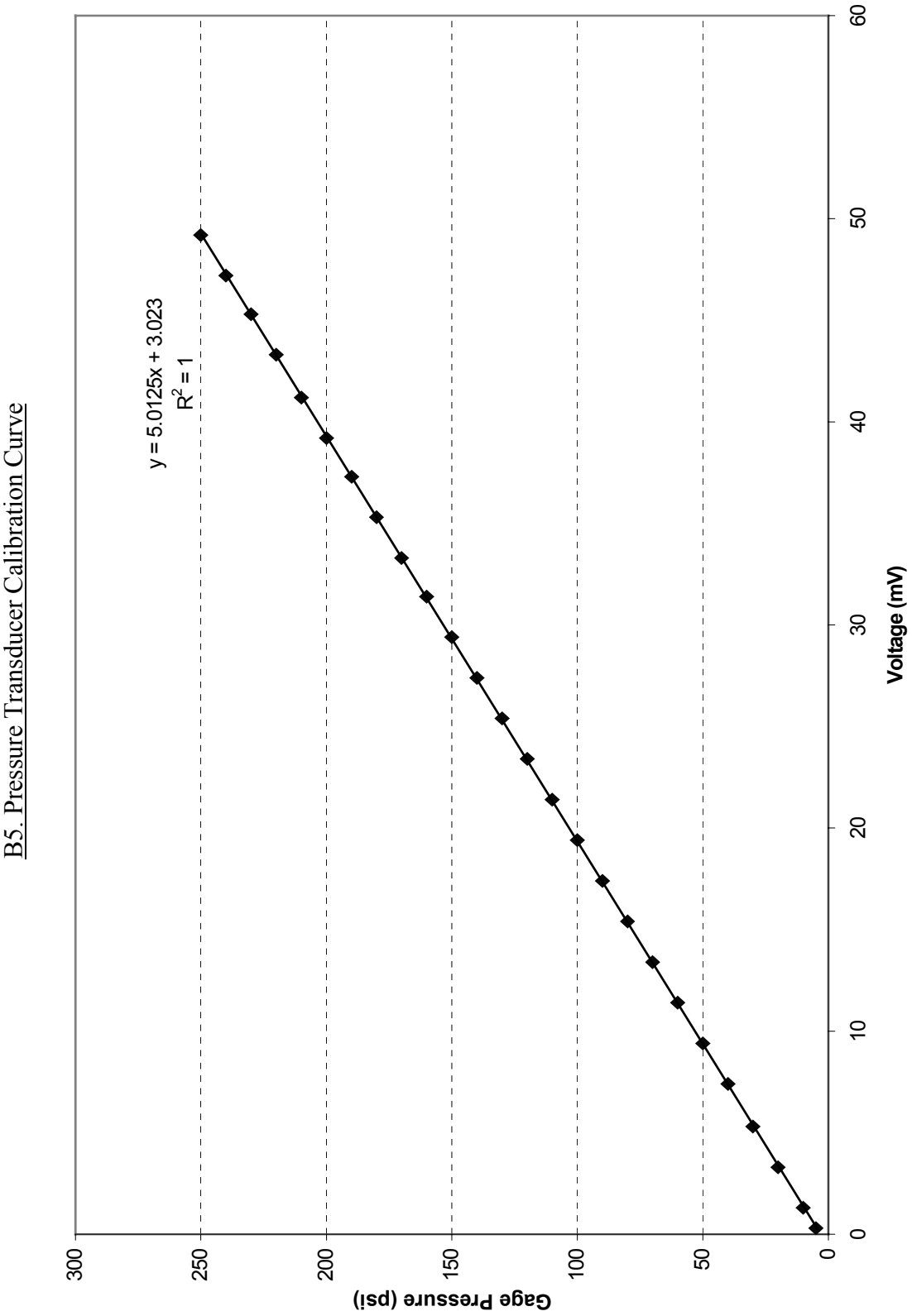

B6. A Mathcad Worksheet for the Calculation of the Uncertainty in the Fouling Factor.

PART 1. Calculation of the uncertainty in the mass flow rate calibration plot.

The mass (lbs) and time (sec) values measured in the calibration process were:

$M_1 := 78.2$ $M_2 := 92$ $M_3 := 107.2$ $M_4 := 86.3$ $M_5 := 104.1$ $M_6 := 102$ $M_7 := 107.5$

$t_1 := 185.1$ $t_2 := 120.5$ $t_3 := 107.8$ $t_4 := 63.2$ $t_5 := 65.8$ $t_6 := 50.3$ $t_7 := 50.7$

The resulting mass flow rates are calculated and stored in an array:

$mdot_1 := \frac{M_1}{t_1}$ $mdot_2 := \frac{M_2}{t_2}$ $mdot_3 := \frac{M_3}{t_3}$ $mdot_4 := \frac{M_4}{t_4}$ $mdot_5 := \frac{M_5}{t_5}$ $mdot_6 := \frac{M_6}{t_6}$ $mdot_7 := \frac{M_7}{t_7}$

$$mdot := \begin{pmatrix} mdot_1 \\ mdot_2 \\ mdot_3 \\ mdot_4 \\ mdot_5 \\ mdot_6 \\ mdot_7 \end{pmatrix}$$

The systematic uncertainty in the mass flow rate is found using the propagation equation:

$$m_{dot}(M,t) := \frac{M}{t}$$

The systematic uncertainty of the mass measurement is:

$B_M := 0.5$

The systematic and random uncertainties in the time measurement are:

$B_t := 0.01 \qquad P_t := 0.5$

Finding the partial derivatives to be used in the propagation equation

$$\frac{\partial}{\partial M} m_{dot}(M,t) \rightarrow \frac{1}{t} \qquad \frac{\partial}{\partial t} m_{dot}(M,t) \rightarrow \frac{-M}{t^2}$$

Substituting the results in the propagation equation:

$$B_{mdot}(M,t) := \sqrt{\left(\frac{1}{t}\right)^2 \cdot B_M{}^2 + \left(\frac{-M}{t^2}\right)^2 \cdot \left(B_t{}^2 + P_t{}^2\right)}$$

The resulting uncertainties are now computed and stored in an array:

$B_{mdot1} := B_{mdot}(M_1, t_1) \qquad B_{mdot2} := B_{mdot}(M_2, t_2) \qquad B_{mdot3} := B_{mdot}(M_3, t_3)$

$B_{mdot4} := B_{mdot}(M_4, t_4) \qquad B_{mdot5} := B_{mdot}(M_5, t_5) \qquad B_{mdot6} := B_{mdot}(M_6, t_6)$

$B_{mdot7} := B_{mdot}(M_7, t_7)$

$$B_{mdot} := \begin{pmatrix} B_{mdot1} \\ B_{mdot2} \\ B_{mdot3} \\ B_{mdot4} \\ B_{mdot5} \\ B_{mdot6} \\ B_{mdot7} \end{pmatrix}$$

The measured frequencies during the calibration process are:

$f_1 := 12.31$ $f_2 := 22.02$ $f_3 := 30.12$ $f_4 := 38.46$ $f_5 := 46.16$ $f_6 := 52.43$ $f_7 := 63.45$

$$f := \begin{pmatrix} f_1 \\ f_2 \\ f_3 \\ f_4 \\ f_5 \\ f_6 \\ f_7 \end{pmatrix}$$

Performing a linear fit to obtain a calibration curve of the format y = m*x:

$F(X) := X$ $S := linfit(f, mdot, F)$

The resulting slope is:

$S = 0.035$ $\quad m := S$

Finding the standard error of regression:

$i := 0 .. 6$

$N := 7$

$$S_Y := \left[\frac{\sum_i \left(mdot_i - m \cdot f_i \right)^2}{N - 2} \right]^{0.5} \qquad S_Y = 0.102$$

$$S_{XX} := \sum_i \left(f_i \right)^2 - \frac{\left(\sum_i f_i \right)^2}{N} \qquad S_{XX} = 1.9 \times 10^3$$

$fbar := mean(f)$ $\quad fbar = 37.85$

The slope m can be rewritten as:

$$m := \frac{f_1 \cdot mdot_1 + f_2 \cdot mdot_2 + f_3 \cdot mdot_3 + f_4 \cdot mdot_4 + f_5 \cdot mdot_5 + f_6 \cdot mdot_6 + f_7 \cdot mdot_7}{f_1^2 + f_2^2 + f_3^2 + f_4^2 + f_5^2 + f_6^2 + f_7^2}$$

The calibration function for the mass flow rate can be therefore defined as:

$$m_{dot}(f_{new}, f_1, f_2, f_3, f_4, f_5, f_6, f_7, mdot_1, mdot_2, mdot_3, mdot_4, mdot_5, mdot_6, mdot_7) := \frac{f_1 \cdot mdot_1 + f_2 \cdot mdot_2 + f_3 \cdot mdot_3 + f_4 \cdot mdot_4 \ldots + f_5 \cdot mdot_5 + f_6 \cdot mdot_6 + f_7 \cdot mdot_7}{f_1^2 + f_2^2 + f_3^2 + f_4^2 + f_5^2 + f_6^2 + f_7^2} \cdot f_{new}$$

where f_{new} is the new measured frequency.

Defining the necessary variables needed for plotting the uncertainty of the measured mass flow rate:

$NPoints := 100$ $\quad$ $j := 0 .. NPoints$

$fnewSTART := f_1$ $\quad$ $fnewEND := f_7$

The array of frequencies needed for plotting can be defined as:

$$f_{new_j} := fnewSTART + (fnewEND - fnewSTART) \cdot \frac{j}{NPoints}$$

Finding the partial derivatives of the calibration function with respect to each variable for the defined range of plotting frequencies f_{new}:

$$\theta_{mdot1} := \left| \begin{array}{l} \text{for } j \in 0 .. NPoints \\ \quad \theta mdot1_j \leftarrow \frac{\partial}{\partial mdot_1} m_{dot}(f_{new_j}, f_1, f_2, f_3, f_4, f_5, f_6, f_7, mdot_1, mdot_2, mdot_3, mdot_4, mdot_5, mdot_6, mdot_7) \\ \text{return } \theta mdot1 \end{array} \right.$$

$$\theta_{mdot2} := \left| \begin{array}{l} \text{for } j \in 0..\,NPoints \\ \quad \theta mdot2_j \leftarrow \dfrac{\partial}{\partial mdot_2} m_{dot}\left(f_{new_j}, f_1, f_2, f_3, f_4, f_5, f_6, f_7, mdot_1, mdot_2, mdot_3, mdot_4, mdot_5, mdot_6, mdot_7\right) \\ \text{return } \theta mdot2 \end{array} \right.$$

$$\theta_{mdot3} := \left| \begin{array}{l} \text{for } j \in 0..\,NPoints \\ \quad \theta mdot3_j \leftarrow \dfrac{\partial}{\partial mdot_3} m_{dot}\left(f_{new_j}, f_1, f_2, f_3, f_4, f_5, f_6, f_7, mdot_1, mdot_2, mdot_3, mdot_4, mdot_5, mdot_6, mdot_7\right) \\ \text{return } \theta mdot3 \end{array} \right.$$

$$\theta_{mdot4} := \left| \begin{array}{l} \text{for } j \in 0..\,NPoints \\ \quad \theta mdot4_j \leftarrow \dfrac{\partial}{\partial mdot_4} m_{dot}\left(f_{new_j}, f_1, f_2, f_3, f_4, f_5, f_6, f_7, mdot_1, mdot_2, mdot_3, mdot_4, mdot_5, mdot_6, mdot_7\right) \\ \text{return } \theta mdot4 \end{array} \right.$$

$$\theta_{mdot5} := \left| \begin{array}{l} \text{for } j \in 0..\,NPoints \\ \quad \theta mdot5_j \leftarrow \dfrac{\partial}{\partial mdot_5} m_{dot}\left(f_{new_j}, f_1, f_2, f_3, f_4, f_5, f_6, f_7, mdot_1, mdot_2, mdot_3, mdot_4, mdot_5, mdot_6, mdot_7\right) \\ \text{return } \theta mdot5 \end{array} \right.$$

$$\theta_{mdot6} := \left| \begin{array}{l} \text{for } j \in 0..\,NPoints \\ \quad \theta mdot6_j \leftarrow \dfrac{\partial}{\partial mdot_6} m_{dot}\left(f_{new_j}, f_1, f_2, f_3, f_4, f_5, f_6, f_7, mdot_1, mdot_2, mdot_3, mdot_4, mdot_5, mdot_6, mdot_7\right) \\ \text{return } \theta mdot6 \end{array} \right.$$

$$\theta_{mdot7} := \left| \begin{array}{l} \text{for } j \in 0..\,NPoints \\ \quad \theta mdot7_j \leftarrow \dfrac{\partial}{\partial mdot_7} m_{dot}\left(f_{new_j}, f_1, f_2, f_3, f_4, f_5, f_6, f_7, mdot_1, mdot_2, mdot_3, mdot_4, mdot_5, mdot_6, mdot_7\right) \\ \text{return } \theta mdot7 \end{array} \right.$$

$$\theta_{f1} := \left| \begin{array}{l} \text{for } j \in 0..\,NPoints \\ \quad \theta f1_j \leftarrow \dfrac{\partial}{\partial f_1} m_{dot}\left(f_{new_j}, f_1, f_2, f_3, f_4, f_5, f_6, f_7, mdot_1, mdot_2, mdot_3, mdot_4, mdot_5, mdot_6, mdot_7\right) \\ \text{return } \theta f1 \end{array} \right.$$

$$\theta_{f2} := \left| \begin{array}{l} \text{for } j \in 0..\,NPoints \\ \quad \theta f2_j \leftarrow \dfrac{\partial}{\partial f_2} m_{dot}\left(f_{new_j}, f_1, f_2, f_3, f_4, f_5, f_6, f_7, mdot_1, mdot_2, mdot_3, mdot_4, mdot_5, mdot_6, mdot_7\right) \\ \text{return } \theta f2 \end{array} \right.$$

$$\theta_{f3} := \left| \begin{array}{l} \text{for } j \in 0..\,NPoints \\ \quad \theta f3_j \leftarrow \dfrac{\partial}{\partial f_3} m_{dot}\left(f_{new_j}, f_1, f_2, f_3, f_4, f_5, f_6, f_7, mdot_1, mdot_2, mdot_3, mdot_4, mdot_5, mdot_6, mdot_7\right) \\ \text{return } \theta f3 \end{array} \right.$$

$$\theta_{f4} := \left| \begin{array}{l} \text{for } j \in 0..\text{NPoints} \\ \quad \theta f4_j \leftarrow \frac{\partial}{\partial f_4} m_{dot}\left(f_{new_j}, f_1, f_2, f_3, f_4, f_5, f_6, f_7, mdot_1, mdot_2, mdot_3, mdot_4, mdot_5, mdot_6, mdot_7\right) \\ \text{return } \theta f4 \end{array} \right.$$

$$\theta_{f5} := \left| \begin{array}{l} \text{for } j \in 0..\text{NPoints} \\ \quad \theta f5_j \leftarrow \frac{\partial}{\partial f_5} m_{dot}\left(f_{new_j}, f_1, f_2, f_3, f_4, f_5, f_6, f_7, mdot_1, mdot_2, mdot_3, mdot_4, mdot_5, mdot_6, mdot_7\right) \\ \text{return } \theta f5 \end{array} \right.$$

$$\theta_{f6} := \left| \begin{array}{l} \text{for } j \in 0..\text{NPoints} \\ \quad \theta f6_j \leftarrow \frac{\partial}{\partial f_6} m_{dot}\left(f_{new_j}, f_1, f_2, f_3, f_4, f_5, f_6, f_7, mdot_1, mdot_2, mdot_3, mdot_4, mdot_5, mdot_6, mdot_7\right) \\ \text{return } \theta f6 \end{array} \right.$$

$$\theta_{f7} := \left| \begin{array}{l} \text{for } j \in 0..\text{NPoints} \\ \quad \theta f7_j \leftarrow \frac{\partial}{\partial f_7} m_{dot}\left(f_{new_j}, f_1, f_2, f_3, f_4, f_5, f_6, f_7, mdot_1, mdot_2, mdot_3, mdot_4, mdot_5, mdot_6, mdot_7\right) \\ \text{return } \theta f7 \end{array} \right.$$

$$\theta_{fnew} := m$$

This last derivative is independent of f_{new}.

The systematic and random uncertainties in the frequency measurements are:

$B_f := 0.5 \qquad P_f := 0.5$

The systematic uncertainty of the frequency measured by the data acquisition program is:

$B_{fnew} := 0.25$

After substituting everything into the uncertainty propagation equation, a plot for the uncertainty in the mass flow rate can be obtained.

The propagation equation becomes:

$$U_{mdot} := \sqrt{\begin{aligned}
&4\cdot S_Y^{\,2}\cdot\left[\frac{1}{N}+\frac{\left(f_{new}-fbar\right)^2}{S_{XX}}\right]+\theta_{mdot1}^{\,2}\cdot B_{mdot1}^{\,2}+\theta_{mdot2}^{\,2}\cdot B_{mdot2}^{\,2}+\theta_{mdot3}^{\,2}\cdot B_{mdot3}^{\,2}+\theta_{mdot4}^{\,2}\cdot B_{mdot4}^{\,2}\ \cdots\\
&+\theta_{mdot5}^{\,2}\cdot B_{mdot5}^{\,2}+\theta_{mdot6}^{\,2}\cdot B_{mdot6}^{\,2}+\theta_{mdot7}^{\,2}\cdot B_{mdot7}^{\,2}\ \cdots\\
&+2\cdot\theta_{mdot1}\cdot\theta_{mdot2}\cdot B_{mdot1}\cdot B_{mdot2}+2\cdot\theta_{mdot1}\cdot\theta_{mdot3}\cdot B_{mdot1}\cdot B_{mdot3}+2\cdot\theta_{mdot1}\cdot\theta_{mdot4}\cdot B_{mdot1}\cdot B_{mdot4}\ \cdots\\
&+2\cdot\theta_{mdot1}\cdot\theta_{mdot5}\cdot B_{mdot1}\cdot B_{mdot5}+2\cdot\theta_{mdot1}\cdot\theta_{mdot6}\cdot B_{mdot1}\cdot B_{mdot6}+2\cdot\theta_{mdot1}\cdot\theta_{mdot7}\cdot B_{mdot1}\cdot B_{mdot7}\ \cdots\\
&+2\cdot\theta_{mdot2}\cdot\theta_{mdot3}\cdot B_{mdot2}\cdot B_{mdot3}+2\cdot\theta_{mdot2}\cdot\theta_{mdot4}\cdot B_{mdot2}\cdot B_{mdot4}+2\cdot\theta_{mdot2}\cdot\theta_{mdot5}\cdot B_{mdot2}\cdot B_{mdot5}\ \cdots\\
&+2\cdot\theta_{mdot2}\cdot\theta_{mdot6}\cdot B_{mdot2}\cdot B_{mdot6}+2\cdot\theta_{mdot2}\cdot\theta_{mdot7}\cdot B_{mdot2}\cdot B_{mdot7}+2\cdot\theta_{mdot3}\cdot\theta_{mdot4}\cdot B_{mdot3}\cdot B_{mdot4}\ \cdots\\
&+2\cdot\theta_{mdot3}\cdot\theta_{mdot5}\cdot B_{mdot3}\cdot B_{mdot5}+2\cdot\theta_{mdot3}\cdot\theta_{mdot6}\cdot B_{mdot3}\cdot B_{mdot6}+2\cdot\theta_{mdot3}\cdot\theta_{mdot7}\cdot B_{mdot3}\cdot B_{mdot7}\ \cdots\\
&+2\cdot\theta_{mdot4}\cdot\theta_{mdot5}\cdot B_{mdot4}\cdot B_{mdot5}+2\cdot\theta_{mdot4}\cdot\theta_{mdot6}\cdot B_{mdot4}\cdot B_{mdot6}+2\cdot\theta_{mdot4}\cdot\theta_{mdot7}\cdot B_{mdot4}\cdot B_{mdot7}\ \cdots\\
&+2\cdot\theta_{mdot5}\cdot\theta_{mdot6}\cdot B_{mdot5}\cdot B_{mdot6}+2\cdot\theta_{mdot5}\cdot\theta_{mdot7}\cdot B_{mdot5}\cdot B_{mdot7}+2\cdot\theta_{mdot6}\cdot\theta_{mdot7}\cdot B_{mdot6}\cdot B_{mdot7}\ \cdots\\
&+\left(B_f^{\,2}+P_f^{\,2}\right)\cdot\left(\theta_{f1}^{\,2}+\theta_{f2}^{\,2}+\theta_{f3}^{\,2}+\theta_{f4}^{\,2}+\theta_{f5}^{\,2}+\theta_{f6}^{\,2}+\theta_{f7}^{\,2}\right)+2\cdot\theta_{f1}\cdot\theta_{f2}\cdot B_f^{\,2}\ \cdots\\
&+2\cdot\theta_{f1}\cdot\theta_{f3}\cdot B_f^{\,2}+2\cdot\theta_{f1}\cdot\theta_{f4}\cdot B_f^{\,2}+2\cdot\theta_{f1}\cdot\theta_{f5}\cdot B_f^{\,2}+2\cdot\theta_{f1}\cdot\theta_{f6}\cdot B_f^{\,2}+2\cdot\theta_{f1}\cdot\theta_{f7}\cdot B_f^{\,2}+2\cdot\theta_{f2}\cdot\theta_{f3}\cdot B_f^{\,2}\ \cdots\\
&+2\cdot\theta_{f2}\cdot\theta_{f4}\cdot B_f^{\,2}+2\cdot\theta_{f2}\cdot\theta_{f5}\cdot B_f^{\,2}+2\cdot\theta_{f2}\cdot\theta_{f6}\cdot B_f^{\,2}+2\cdot\theta_{f2}\cdot\theta_{f7}\cdot B_f^{\,2}+2\cdot\theta_{f3}\cdot\theta_{f4}\cdot B_f^{\,2}+2\cdot\theta_{f3}\cdot\theta_{f5}\cdot B_f^{\,2}\ \cdots\\
&+2\cdot\theta_{f3}\cdot\theta_{f6}\cdot B_f^{\,2}+2\cdot\theta_{f3}\cdot\theta_{f7}\cdot B_f^{\,2}+2\cdot\theta_{f4}\cdot\theta_{f5}\cdot B_f^{\,2}+2\cdot\theta_{f4}\cdot\theta_{f6}\cdot B_f^{\,2}+2\cdot\theta_{f4}\cdot\theta_{f7}\cdot B_f^{\,2}+2\cdot\theta_{f5}\cdot\theta_{f6}\cdot B_f^{\,2}\ \cdots\\
&+2\cdot\theta_{f5}\cdot\theta_{f7}\cdot B_f^{\,2}+2\cdot\theta_{f6}\cdot\theta_{f7}\cdot B_f^{\,2}+\theta_{fnew}^{\,2}\cdot\left(B_{fnew}\right)^2
\end{aligned}}$$

The uncertainty in mass flow rate can now be plotted as a function of the new measured frequency:

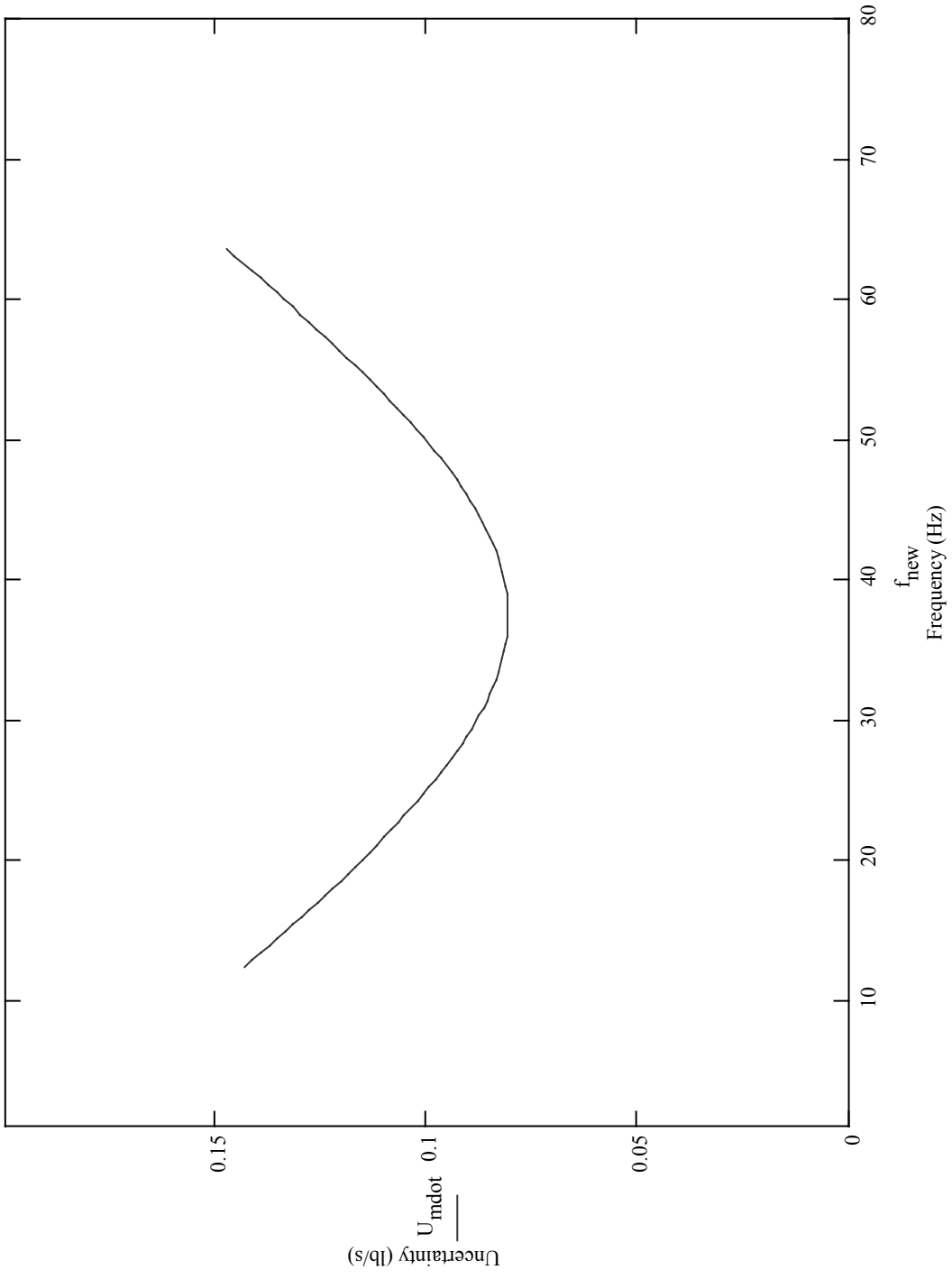
0.15
0.1
0.05
0
10
20
30
40
50
60
70
80
Uncertainty (lb/s)
U_{mdot}
f_{new}
Frequency (Hz)

Performing a quadratic least squares regression of the uncertainty curve:

$$F(X) := \begin{pmatrix} X^2 \\ X \\ 1 \end{pmatrix} \qquad S := \text{linfit}(f_{new}, U_{mdot}, F)$$

$$S = \begin{pmatrix} 1.013 \times 10^{-4} \\ -7.577 \times 10^{-3} \\ 0.224 \end{pmatrix}$$

The uncertainty in mass flow rate can be defined as the following function:

$$U_{mdot}(f) := F(f) \cdot S$$

Recall that:

$$mdot = f \cdot m$$

Therefore:

$$U_{mdot}(mdot) := F\left(\frac{mdot}{m}\right) \cdot S$$

For example, if the measurement is 1.36 lb/s, the uncertainty associated with that measurement is:

$$U_{mdot}(1.36) = 0.083$$

PART 2. Calculation of the uncertainty in the fouling resistance with values obtained during the test run.

The data reduction equation for the experiment is:

$$R_f = \frac{1}{U_f} - \frac{1}{U_c}$$

where

$$U = \frac{Q}{A \cdot LMTD}$$

Substituting in the equations for the internal area and the log mean temperature difference yields:

$$R_f = \frac{1}{\frac{mdot2_w \cdot c_{pw} \cdot \left(T2_{wout} - T2_{win}\right)}{\pi \cdot D_i \cdot L \cdot \frac{\left(T2_{win} - T2_{wout}\right)}{\ln\left(\frac{T2_{ref} - T2_{wout}}{T2_{ref} - T2_{win}}\right)}}} - \frac{1}{\frac{mdot1_w \cdot c_{pw} \cdot \left(T1_{wout} - T1_{win}\right)}{\pi \cdot D_i \cdot L \cdot \frac{\left(T1_{win} - T1_{wout}\right)}{\ln\left(\frac{T1_{ref} - T1_{wout}}{T1_{ref} - T1_{win}}\right)}}}$$

where

$$c_{pw} := 4182 \frac{J}{kg \cdot K}$$

Simplifying the equation yields:

$$R_f = \frac{-\pi \cdot D_i \cdot L}{mdot2_w \cdot c_{pw} \cdot \ln\left(\frac{T2_{ref} - T2_{wout}}{T2_{ref} - T2_{win}}\right)} - \frac{-\pi \cdot D_i \cdot L}{mdot1_w \cdot c_{pw} \cdot \ln\left(\frac{T1_{ref} - T1_{wout}}{T1_{ref} - T1_{win}}\right)}$$

We can define this equation as a function:

$$R_f\left(D_i, L, mdot1_w, T1_{ref}, T1_{win}, T1_{wout}, mdot2_w, T2_{ref}, T2_{win}, T2_{wout}\right) := \frac{\pi \cdot D_i \cdot L}{c_{pw}} \cdot \left(\frac{1}{mdot1_w \cdot \ln\left(\frac{T1_{ref} - T1_{wout}}{T1_{ref} - T1_{win}}\right)} - \frac{1}{mdot2_w \cdot \ln\left(\frac{T2_{ref} - T2_{wout}}{T2_{ref} - T2_{win}}\right)}\right)$$

The sample readings of the test run are:

$L := 9\,ft$

$T1_{win} := 99.0\,F$

$T2_{win} := 100.2\,F$

$T1_{wout} := 100.6\,F$

$T2_{wout} := 101.9\,F$

$mdot1_w := 0.99\,\frac{lb}{s}$

$mdot2_w := 0.98\,\frac{lb}{s}$

$T1_{ref} := 102.0\,F$

$T2_{ref} := 103.9\,F$

$D_i := 0.65\,in$

From the uncertainty analysis of the mass flow rate (Part 1):

$B_{mdot1.w} := U_{mdot}\left(mdot1_w \cdot \frac{s}{lb}\right) \cdot \frac{lb}{s}$ $\qquad$ $B_{mdot2.w} := U_{mdot}\left(mdot2_w \cdot \frac{s}{lb}\right) \cdot \frac{lb}{s}$

$\frac{B_{mdot1.w}}{mdot1_w} = 9.201\%$ $\qquad$ $\frac{B_{mdot2.w}}{mdot2_w} = 9.35\%$

The systematic uncertainty of the thermocouple reading is:

$B_T := 0.8$

The uncertainties in length and diameter measurements are negligible:

$B_{D.i} := 0$ $\qquad$ $B_L := 0$

Finding the partial derivatives of the data reduction equation.

$\theta_{D.i} := \frac{\partial}{\partial D_i} R_f(D_i, L, mdot1_w, T1_{ref}, T1_{win}, T1_{wout}, mdot2_w, T2_{ref}, T2_{win}, T2_{wout})$

$$\theta_L := \frac{\partial}{\partial L} R_f\left(D_i, L, mdot1_w, T1_{ref}, T1_{win}, T1_{wout}, mdot2_w, T2_{ref}, T2_{win}, T2_{wout}\right)$$

$$\theta_{mdot1.w} := \frac{\partial}{\partial mdot1_w} R_f\left(D_i, L, mdot1_w, T1_{ref}, T1_{win}, T1_{wout}, mdot2_w, T2_{ref}, T2_{win}, T2_{wout}\right)$$

$$\theta_{mdot2.w} := \frac{\partial}{\partial mdot2_w} R_f\left(D_i, L, mdot1_w, T1_{ref}, T1_{win}, T1_{wout}, mdot2_w, T2_{ref}, T2_{win}, T2_{wout}\right)$$

$$\theta_{T1.win} := \frac{\partial}{\partial T1_{win}} R_f\left(D_i, L, mdot1_w, T1_{ref}, T1_{win}, T1_{wout}, mdot2_w, T2_{ref}, T2_{win}, T2_{wout}\right)$$

$$\theta_{T2.win} := \frac{\partial}{\partial T2_{win}} R_f\left(D_i, L, mdot1_w, T1_{ref}, T1_{win}, T1_{wout}, mdot2_w, T2_{ref}, T2_{win}, T2_{wout}\right)$$

$$\theta_{T1.wout} := \frac{\partial}{\partial T1_{wout}} R_f\left(D_i, L, mdot1_w, T1_{ref}, T1_{win}, T1_{wout}, mdot2_w, T2_{ref}, T2_{win}, T2_{wout}\right)$$

$$\theta_{T2.wout} := \frac{\partial}{\partial T2_{wout}} R_f\left(D_i, L, mdot1_w, T1_{ref}, T1_{win}, T1_{wout}, mdot2_w, T2_{ref}, T2_{win}, T2_{wout}\right)$$

$$\theta_{T1.ref} := \frac{\partial}{\partial T1_{ref}} R_f\left(D_i, L, mdot1_w, T1_{ref}, T1_{win}, T1_{wout}, mdot2_w, T2_{ref}, T2_{win}, T2_{wout}\right)$$

$$\theta_{T2.ref} := \frac{\partial}{\partial T2_{ref}} R_f\left(D_i, L, mdot1_w, T1_{ref}, T1_{win}, T1_{wout}, mdot2_w, T2_{ref}, T2_{win}, T2_{wout}\right)$$

The correlated systematic uncertainties are:

$mdot1_w, mdot2_w$ $\quad$ $T1_{ref}, T2_{ref}$ $\quad$ $T1_{win}, T2_{win}$ $\quad$ $T1_{wout}, T2_{wout}$

Substituting the calculated values in the propagation equation:

$$B_{R.f} := \sqrt{\begin{aligned}&\theta_{D.i}^{2}\cdot B_{D.i}^{2} + \theta_{L}^{2}\cdot B_{L}^{2} + \theta_{mdot1.w}^{2}\cdot B_{mdot1.w}^{2} + \theta_{mdot2.w}^{2}\cdot B_{mdot2.w}^{2} + \theta_{T1.ref}^{2}\cdot B_{T}^{2} + \theta_{T2.ref}^{2}\cdot B_{T}^{2} + \theta_{T1.win}^{2}\cdot B_{T}^{2} \ldots \\ &+ \theta_{T2.win}^{2}\cdot B_{T}^{2} + \theta_{T1.wout}^{2}\cdot B_{T}^{2} + \theta_{T2.wout}^{2}\cdot B_{T}^{2} + 2\cdot\theta_{T1.wout}\cdot\theta_{T2.wout}\cdot B_{T}^{2} + 2\cdot\theta_{T1.win}\cdot\theta_{T2.win}\cdot B_{T}^{2} + 2\cdot\theta_{T1.ref}\theta_{T2.ref}B_{T}^{2} \ldots \\ &+ 2\cdot\theta_{mdot1.w}\cdot\theta_{mdot2.w}\cdot B_{mdot1.w}\cdot B_{mdot2.w}\end{aligned}}$$

Finally, the systematic uncertainty of the fouling resistance is:

$$B_{R.f} = 6.556\times 10^{-5}\ \text{hr*ft}^2\text{*R/BTU}$$

The random uncertainty P is taken as 2 times the standard deviation of the fouling resistance readings at constant conditions.

$$P_{R.f} := 2\cdot 1.1\cdot 10^{-5}\ \text{hr*ft}^2\text{*R/BTU}$$

The total uncertainty in the fouling resistance is then:

$$U_{R.f} := \sqrt{B_{R.f}^{2} + P_{R.f}^{2}}\cdot\frac{hr\cdot ft^{2}\cdot R}{BTU} \qquad \boxed{U_{R.f} = 6.915\times 10^{-5}\ \frac{hr\cdot ft^{2}\cdot R}{BTU}}$$

The resulting uncertainty can be expressed as a percentage:

$$\frac{U_{R.f}}{R_f\left(D_i, L, mdot1_w, T1_{ref}, T1_{win}, T1_{wout}, mdot2_w, T2_{ref}, T2_{win}, T2_{wout}\right)\cdot\frac{hr\cdot ft^2\cdot R}{BTU}} = 48.708\%$$

APPENDIX C

APPARATUS PHOTOGRAPHS

C1. Supporting Structure

C2. Test Sections Lay Out

C3. Outlet Manifold

C4. Installed Test Sections

C5. Mixing Tank and Pump

C6. Water-Loop Heat Exchangers

C7. Rupture Disc

C8. Control Panel

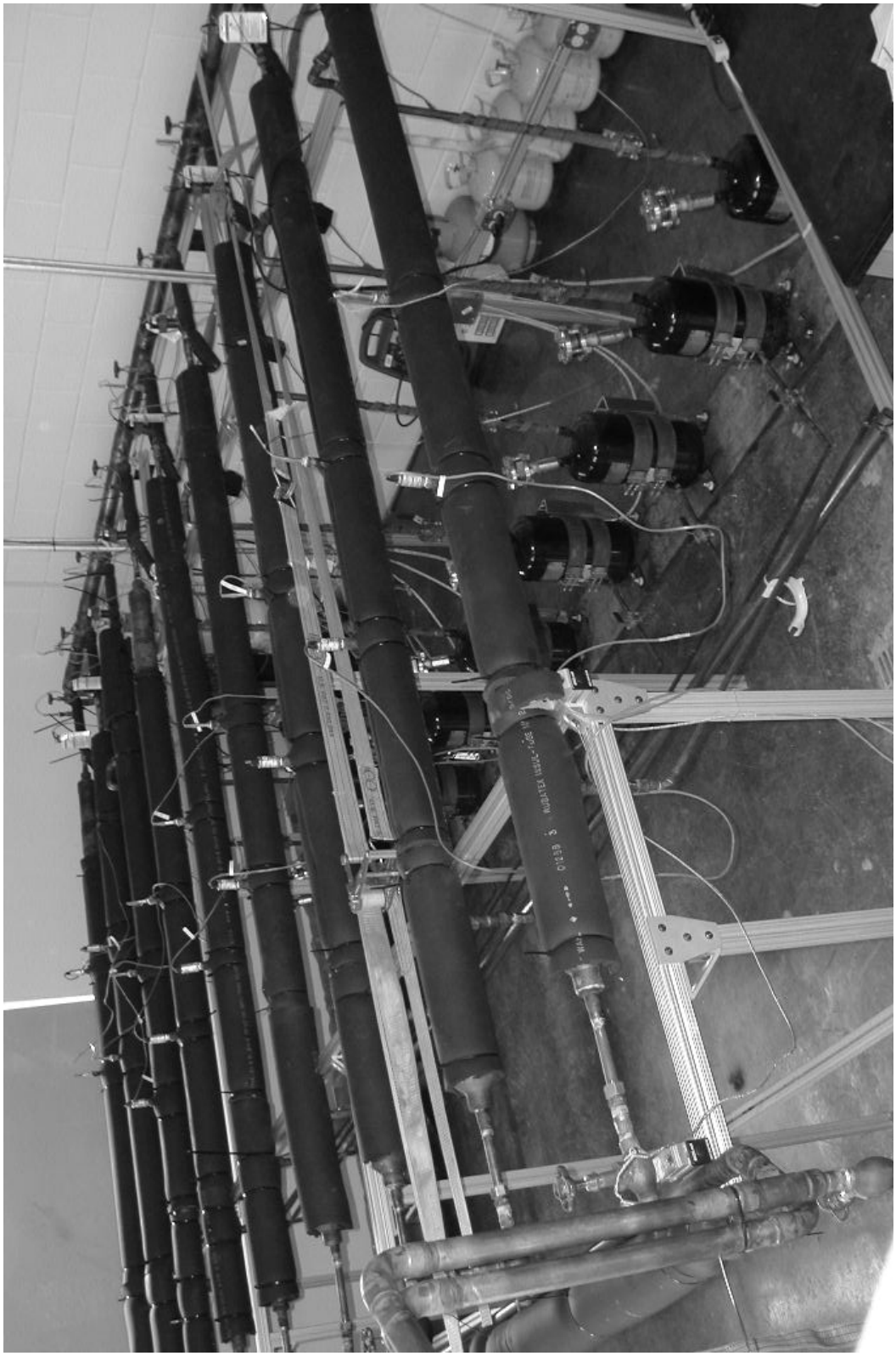

C9. Completed Experimental Apparatus